UNIVERSITE YAHIA FARES DE MEDEA

2018-UYFM-LBMPT

Doctorat

T H ÈS E

Pour obtenir le grade de docteur délivré par

L'Université Yahia Farès de Médéa
Faculté de technologie
Spécialité : Génie des Procédés

BENNIA Ayoub

ECOULEMENT SOUS MHD D'UN NANOFLUIDE DANS UN CYLINDRE HORIZONTAL

Directeur de thèse : **Mohamed Najib BOUAZIZ**

Jury

M. Salah HANINI	Professeur, Université Y.F Médéa	Président
M. Mohamed Najib BOUAZIZ	Professeur, Université Y.F Médéa	Directeur de Thèse
M. MAZOUZI Rédha	Maitre de Conférences A, Université D.B.Khemis	Examinateur
M. ZIRARI Mounir	Maitre de Conférences A, Université Y.F Médéa	Examinateur

Laboratoire de Biomatériaux
et Phénomènes de Transport

THÈSE

Acknowledgement

*In the name of **ALLAH**, the Most Gracious and the Most Merciful*

*Alhamdulillah, all praises to **ALLAH** for the strengths and His blessing in completing this thesis.*

*Now, I would like to say thanks to my supervisor, **Prof. M.N. BOUAZIZ**, for his supervision and encouragement during this research. His inspiring comments and suggestions motivated me to continue my research work. From his remarkable support and advice during my PhD studies, I gained a lot of experience and knowledge which will help me in future. I would have never been able to reach the goal without his support.*

I would like to thank the members of the jury who accepted to judge this thesis work

President of the jury,

First Examiner,

Second Examiner,

Finally, I thank all those who have helped me directly or indirectly in the successful completion of my thesis.

الملخص

في هذه الأطروحة قمنا ببحث رقمي حول التدفق الحمل الحراري لسائل النانو (نانوفلويد) في أنبوب، وقد تم إجراء دراسة عميقة لفهم تأثير تركيز حجم الجسيمات النانو ورقم رينولدز على تدفق السائل و نقل الحرارة. كما تم إجراء دراسة خاصة لتأثير المجال المغناطيسي على نقل الحرارة نانوفلويد و الأخذ بعين الاعتبار نظام التدفق مضطربا.

كما تم الاستعانة ببرنامج للمحاكت لدراسة هذا المشكل و حله و قيد بينت النتائج المتحصلة انه هناك اتفاق جيد مع نتائج سابقة لباحثين. كما تبين النتائج انه هناك زيادة في نقل الحرارة و عامل الاحتكاك عند زيادة عدد الجزيات النانوية و عدد رينولدز . و أيضا عند عدد رينولدز ثابت هناك زيادة في نقل الحرارة و عامل الاحتكاك عند زيادة التدفق المغنطيسي.

الكلمات المفتاحية نقل الحرارة ، نانوفلويد، عامل الاحتكاك, تدفق مغنطيسي

Resumé

Dans cette thèse, nous avons étudié numériquement le transfert de chaleur par convection mixte et forcée pour un nanofluide dans un tube, une étude a été réalisée pour comprendre l'effet de la concentration volumique des nanoparticules et du nombre de Reynolds sur le transfert de chaleur.

Une étude particulière a également été réalisée pour examiner l'effet du champ magnétique sur le transfert de chaleur de nanofluide (Fe3O4-eau) et le régime d'écoulement considéré comme turbulent.

Le logiciel de Dynamique des fluides computationnelle (CFD) FLUENT a été utilisé pour résoudre ce problème, les résultats obtenus de la simulation monte un bon accord avec la littérature.

Les résultats indiquent que le nombre de Nusselt et le facteur de friction augmentent avec l'augmentation de la concentration volumique et nombre de Reynolds. Aussi pour un nombre de Reynolds fixe, Nu et le facteur de frottement sont proportionnels au champ magnétique.

***Mots clés**: Transfert de chaleur par convection, Magnétique, CFD, Nanofluide, facteur de frottement*

Abstract

In this thesis we investigated numerically the mixed and forced convection flow for a nanofluid in pipe, a depth study has been done to understand the effect of nanoparticules volume concentration and Reynolds number on heat transfer fluid flow. Also a particular study has been done to examine the effect of magnetic field on nanofluid turbulent flow (Fe3O4–water) and heat transfer.

Computational fluid dynamics (CFD) tool was used to solve this problem, the simulation output data compared with an experimental literature data from other study and found a matching. The result shows that Nu and friction factor increase with increase of volume concentration and Reynolds number. Also for fixed Reynolds number the Nu and friction factor are proportional to the magnetic field.

***Keywords**: Convective heat transfer, Magnetic, CFD, Nanofluid, friction factor*

Nomenclature

List of symbols

a	Acceleration	(m/s2)
Cp	Specific heat of the fluid	(J/kgK)
D	Hydraulic diameter.	(m)
d	Particles diameter	(m)
fdrag	Drag function	
h	Heat transfer coefficient.	(W/m2K)
L	Channel length	(m)
Nu	Nusselt number	
f	friction factor	
K	Thermal conductivity of the fluid	(W/mK)
k	Turbulent kinetic energy	(m2/s2)
P	Pressure	(pas)
q	Wall heat flux	(W/m2)
Re	Reynolds number	
T	temperature	(K)
v	velocity	(m/s)
j	electrical current density	(A/m2)
B	magnetic field	(Tesla)
Ur	nanoparticule zeta potential	(mv)
R	universal gas constant	(8.31 j/mol .k)
A	Avogadro constant	(6.023.1023 mol-1)
r	nanoparticle radius	(nm)
x	Axial coordinate	(m)
g	Gravitational acceleration	(m/s2)
I	Turbulent intensity	
Cμ	Turbulent viscosity	(pas)
SP	Single phase model	
MP	Multi phase model (Mixture).	
RANS	Reynolds Average Navier Stokes	

Greek Letters

β	Thermal expansion coefficient	(1/K)
ε	Dissipation of turbulent kinetic energy	(m2/s3)
εr	relatively dielectric constant of base fluid	
φ	scalar potential	(V)
μ	Fluid dynamic viscosity	(kg/ms)
$\varepsilon 0$	dielectric constant of vacuum	
$\mu 0$	magnetic permeability in vacuum	(N/A2)
ρ	Fluid density	(Kg/m3)
τ	Wall shear stress	(pa)
σe	electrical conductivity	(s/m)
ϕ	Particle volume concentration	(1]

Subscripts

b	Bulk value
M	Mixture
bf	base-fluid
nf	nanofluid
p	nanoparticle
r	Refers to “nanofluid/base-fluid” ratio
w	wall

List of Figures

Figure 1.1 Represent carbon nanotube and spherical nanoparticules 5

Figure I.2 Two-step preparation process of nanofluids 7

Figure I.3 Al2O3-water nanofluid 7

Figure I.4 Stable (left) and unstable (right) nanofluids 8

Figure 1.5 Zalman's Reserator 3 Max nanoliquid cooler 10

Figure 1.6 Transformer Cooling 11

Figure 1.7 A smart fluid developed in labs at the Michigan Institute of Technology 12

Figure 1.8 The MR Fluid is liquid on the left, and as a solid in magnetics field on the right 13

Figure 1.9 Nuclear Reactor Plant 14

Figure 1.10 Binary Cycle Power Plan 15

Figure 1.11 a solar collector using nanofluid 16

Figure 1.12 Ferrofluid with external magnetic field 18

Figure 3.1 the steps of the simulation on gambit software and FLUENT 36

Figure 4.1 Schema of the configuration under investigation 38

Figure 4.2 Nusselt number as a function of Re for (a) φ=1% 40

Figure 4.3 Nusselt number as a function of Re for φ=4% 40

Figure 4.4 wall temperature along tube axis for volume concentrations 1% and for different Reynolds number 41

Figure 4.5 wall temperature along tube axis for volume concentrations 4% and for different Reynolds number 41

Figure 4.6 heat transfer coefficient along tube length for Re=250 and φ=1%, 4% 42

Figure 4.7 Simulation results for friction factor as function of Reynolds number 42

Figure 4.8 Nusselt number as a function of Re for φ=1% 43

Figure 4.9 Nusselt number as a function of Re for φ=4% 44

Figure 4.10 Profiles of bulk temperature along tube axis for volume concentrations

1%..... 44

Figure 4.11 Profiles of bulk temperature along tube axis for volume concentrations 4%..... 45

Figure 4.12 Heat flux for several concentration and Reynolds number..... 45

Figure 4.13 Simulation results for friction factor as function of Reynolds number..... 46

Figure 5.1 Pipe schema 49

Figure 5.2 tested of three turbulence models..... 50

Figure 5.3 grid test with experimental (tested with water)..... 50

Figure 5.4 grid 14×340..... 51

Figure 5.5 Comparison of friction factor with literature (Ahsan [67] , Moody [68]) and computed values for water.)..... 52

Figure 5.6 Comparison of the average Nusselt using single phase approach with the experimental data of Sunder [51]..... 52

Figure 5.7 Comparison of the average Nusselt using mixture approach with the experimental data of Sunder [51]..... 53

Figure 5.8 Comparison of friction factor using single phase approach with the experimental data of Sunder [51]..... 54

Figure 5.9 Comparison of friction factor using mixture approach with the experimental data of Sunder [51]..... 54

Figure 5.10 fully developed velocity profile at outlet for turbulent flow (Re=7000, Ø=0.6%)..... 55

Figure 5.11 Effect of magnetic field on the velocity at the center of the pipe, Re =7000 and 0.6% (SP)..... 56

Figure 5.12 Effect of magnetic field (electrical potential) on the velocity at the center of the pipe Re 7000 and 0.6% (SP)..... 57

Figure 5.13 Effect of magnetic field (electrical potential) on the velocity at the center of the pipe Re 7000 and 0.6% (MP)..... 57

Figure 5.14 Effect of magnetic field on Nusselt number Re9800 and 0.3% (a-SP, b-MP)..... 59

Figure 5.15 Effect of magnetic field on Nusselt number Re 7000 and 0.6% (a-SP, b-MP)..... 60

Figure 5.16 Effect of magnetic field on Nusselt number, Re = 9500 and 0.6% (a-SP, b-MP)..... 61

Figure 5.17 Effect of magnetic field on friction factor Re 9800 and 0.3% (a-SP, b-MP)..... 62

Figure 5.18 Effect of magnetic field on friction factor Re7000 and 0.6% (a-SP, b-MP)..... 63

Figure 5.19 Effect of magnetic field on friction factor Re9500 and 0.6% (a-SP, b-MP)..... 64

Figure 5.20 Investigation of Nusselt number ratio in different volume fraction and field intensities (SP) for ferrofluid..... 65

Figure 5.21 Investigation of friction factor ratio in different volume fraction and field intensities (SP) for ferrofluid..... 65

Figure 5.22 velocity contour of ferrolfuid for volume fraction φ= 1% and B=0T (Re=15000)..... 66

Figure 5.23 velocity contour of ferrolfuid for volume fraction φ= 1% and B=1T (Re=15000)..... 66

Figure 5.24 velocity contour of ferrolfuid for volume fraction φ= 1% and B=2T (Re=15000)..... 66

Figure 5.25 velocity contour of ferrolfuid for volume fraction φ= 1% and B=3T (Re=15000)..... 67

Figure 5.26 velocity contour of nanofluid for volume fraction φ= 1% and B=4T (Re=15000) 67

Figure 5.27 temperature contour of nanofluid for volume fraction φ= 1% and B=0T (Re=15000)..... 68

Figure 5.28 temperature contour of nanofluid for volume fraction φ= 1% and B=1T (Re=15000) 68

Figure 5.29 temperature contour of nanofluid for volume fraction φ= 1% and B=2T (Re=15000)..... 68

Figure 5.30 temperature contour of nanofluid for volume fraction φ= 1% and B=3T (Re=15000)..... 69

Figure 5.31 temperature contour of nanofluid for volume fraction φ= 1% and B=4T (Re=15000)..... 69

Figure 5.32 The effect of magnetic field of nanolfuid (0.6%) pressure drop..... 70

Figure 6.1 Schematic diagram of the geometry under consideration..... 72

Figure 6.2 grid 80×800..... 74

Figure 6.3 Comparison of Nusselt number with literature Xuan..... 75

Figure 6.4 velocity profile at the outlet of pipe for two angle 0° (a) ; 30° (b) and Re=10000..... 76

Figure 6.5 velocity contour of pipe for angle 30° and Re=10000..... 77

Figure 6.6 velocity contour of pipe for angle 30° and Re=12000..... 77

Figure 6.7 temperature contour of pipe for angle 0° and Re=10000..... 78

Figure 6.8 temperature contour of pipe for angle 30° and Re=10000..... 79

Figure 6.9 local Nusselt number with different inclination and Re=10000..... 79

Figure 6.10 local Nusselt number with different inclination and Re=12000..... 80

Figure 6.11 local Darcy friction factor with different inclination and Re=10000..... 81

Figure 6.11 local Darcy friction factor with different inclination and Re=12000..... 81

Liste of tables

Table 5.1 Average error (%) of friction factor and Nusselt number for the two approaches..... 55

Contents

	Page
Acknowledgments	*i*
Nomenclature	*ii*
List of Figures	*v*
Liste of Tables	*viii*
Contents	*ix*
Introduction	1
Chapter 1: **Introduction to Nanofluids**	4
1.1 Introduction	4
1.2 Definition	4
1.3 Properties of nanofluids	4
1.3.1Particle Material and Base Fluid	5
1.3.2. Particle Size	5
1.3.3 Shapes of nanoparticles	6
1.4 Preparation Methods for Nanofluids	6
1.4.1 Two-step method	6
1.4.2 One-Step Method	7
1.4.3 Other Novel Method	8
1.5. The Stability of Nanofluid	8
1.6. Potential features of nanofluids	9
1.7 Application of nanofluids	9
1.7.1 Electronics Cooling	9
1.7.2 Vehicle Cooling	10
1.7.3 Transformer Cooling	10
1.7.4 Heating Buildings and Reducing Pollution	11
1.7.5 Smart fluid	11
1.7.6 Nuclear cooling systems	13
1.7.7 Geothermal Power Extraction	14
1.7.8 Space and Defence	15
1.7.9 Solar absorption	15
1.7.10 Biomedical Applications	16

1.8 Magnetohydrodynamics (MHD) 17
1.9 Ferrofluids 17
1.10 Conclusion 18
Chapter 2 : **Literature Review** 19
2.1 Introduction 19
2.2 Laminar 19
2.3 Turbulent 22
3.3 Objectif of thesis 24
Chapter 3: **Mathematical Modelling** 26
3.1 Introduction 26
3.2 Governing Equations 26
3.2.1. Single Phase Model 27
3.2.2. Mixture 28
3.3 Turbulence modelling 30
3.4 Thermophysical Properties for Nanofluids 31
3.4.1 Density 31
3.4.2 Specific Heat 32
3.4.3 Thermal Conductivity 32
3.4.5 Dynamic Viscosity 32
3.4.6 Electrical conductivity 32
3.4.7 Properties for Nanoparticles 33
3.5 Some Useful Definitions 34
3.6 Introduction to Computational fluid dynamics (CFD) 35
3.7 Advantages of CFD 35
3.8 Presentation of fluent 35
3.8.1 Pre-processor gambit 36
3.8.2 Solver FLUENT 36
3.8.3 Post processor 36
3.9 Summary of the Numerical Methods 37
Chapter 4: **Simulation of nanofluids (Al2O3-H2O) Flow in Heated Pipe** 38
4.1. Introduction 38
4.2 Geometry description 38
4.3 Boundary Conditions 39
4.4 Numerical method and the grid 39
4.5 Validation and results discussion 39
4.5.1 Laminar case 39

4.5.1.1 Average Nusselt number 40
4.5.1.2 Friction factor 42
4.5.2 Turbulent case 43
4.5.2.1 Average Nusselt number 43
4.5.2.2 Friction factor 46
4.6 Conclusion 47

Chapter 5: Simulation of Fe3O4 magnetic nanofluid with presence of magnetic field 48
5.1. Introduction 48
5.2 Choice of turbulence model 48
5.3 Boundary Conditions 49
5.4 Grid Sensitivity Test 49
5.5 Validation 51
5.6 Results and Discussion 55
5.6.1 Effect the magnetic field on velocity 54
5.6.2 Effect the magnetic field on Nusselt number 58
5.6.3 Effect the magnetic field on friction factor 61
5.6.4 Effect the magnetic field on pressure drop 69
5.7 Conclusion 70

Chapter 6: Simulation of nanofluids (Cu-H2O) Flow in an Inclined Heated Pipe 72
6.1. Introduction 72
6.2 Boundary condition 73
6.3 Selected Grid 73
6.4 Properties of nanofluid 74
6.5 Validation 74
6.6 Results and Discussions 75
6.6.1 Velocity Contours 76
6.6.2 Temperature Contours 78
6.6.3 Local Nusselt Number 79
6.6.4 Darcy Friction Factor 80
6. 7 Conclusion 81

Conclusion 82

References..... 85
Annex..... 92

INTRODUCTION

Heat transfer plays an important role in numerous applications. For example, in vehicles, heat generated by the prime mover needs to be removed for proper operation. Similarly, electronic equipments dissipate heat, which requires a cooling system. Heating, ventilating, and air conditioning systems also include various heat transfer processes. Heat transfer is the key process in thermal power stations. In addition to these, many production processes include heat transfer in various forms; it might be the cooling of a machine tool or the temperature adjustment for triggering a chemical process. In almost all industrial equipments heat should be added, removed or transferred from one part to another and this is a prominent task in industry.

Higher efficiency in heating and cooling saves energy and time and increases the lifetime of the equipments. Some processes are even affected qualitatively by higher efficiency of heat transfer. Nowadays systems with higher heat transfer efficiencies are popular. Some works have been done for better understanding of heat transfer and it's augmentation in practical applications. The emerge of processes with high heat have increased the demand for modern technologies in heat transfer.

There are several methods to increase the heat transfer rate. Some are based upon the increment of heat transfer surface and using microchannels. Moreover, heat transfer increases with an increase in thermal conductivity of the working fluid. Common working fluids in heat transfer industry such as water, ethylene glycol, and engine oil have low thermal conductivities compared to solids. So as we know that metals in solid form have orders-of-magnitude larger thermal conductivities than fluids at room temperature. For example, the thermal conductivity of copper at room temperature is 700 times greater than that of water and is 3000 times greater than that of engine oil. And, the thermal conductivity of metallic liquids is much greater than that of non-metallic liquids. Therefore, the thermal conductivities of fluids that contain suspended solid metallic particles are expected to be significantly more enhanced when compared with conventional heat transfer fluids.

Since the solid materials possess have higher thermal conductivities many studies have been focused on the usage of suspensions of solid particles with sizes on the order of millimetres or micrometres in conventional heat transfer fluids [1] [2].

Most of these early studies showing some promise but on the other hand a significant drawbacks were observed. These drawbacks are sedimentation of particles, clogging of channels and erosion in channel walls, which prevented the practical application of suspensions of solid particles in base fluids as advanced working fluids in heat transfer applications.

A decade ago, with the recent developments in nanotechnology, the production of particles with sizes on the order of nanometres (nanoparticles) can be achieved with relative ease. Which led to appear a new kind of heat transfer fluid called nanofluid. It was derived from stably suspending nanoparticles in conventional heat transfer fluids, usually liquids. Commonly used oxide nanoparticles are Aluminium (Al), Silicon (Si), Titanium (Ti), Copper (Cu), Zinc (Zn), Iron (Fe), Magnesium (Mg) and Silver (Ag); and base fluids are water, engine oil, kerosene, ethanol, methanol, ethylene glycol and mono ethylene glycol.

The term nanofluid was coined by Choi [3] at Argonne National Laboratory. He used a nanoparticles (1–100 nm) suspended in a conventional heat transfer fluid and proposed that the addition of nanometer size particles into the base fluid helped to increase the thermal conductivity, allowing for more heat transfer, higher heat conduction, minimal clogging and when it comes to the stability of the suspension, it was shown that sedimentation of particles can be prevented by utilizing proper dispersants. Hence, research is in progress to introduce nanofluids in many thermal applications where the conventional fluids are not capable of improving the rate of heat transfer any further and it can be considered as the next generation of the heat transfer fluids.

various applications of nanofluids were found in electronic cooling components, transportation, industrial cooling , heating buildings and reducing pollution, nuclear systems cooling , space and defence, energy storage , solar absorption , friction reduction , magnetic sealing , antibacterial activity , nanodrug delivery , intensify micro reactors and microbial fuel cells [4] and so on.

Our interest in this thesis is to study the forced and mixed convection heat transfer of nanofluids flowing through a pipe under turbulent flow regimes, to achieve that a particular investigation has been done using computational fluid dynamics software. It’s necessary to study the present problem to understand the behaviour of nanoparticules concentration, Reynolds number and magnetic field on the heat transfer and friction factor.

Outline of the thesis

Chapter 1, presents an introduction to new generation heat transfer fluid known as nanofluid and clarify different ways to production nanofluid. Also illustrate various useful application of nanofluid in electronic cooling components, transportation, heating buildings and nuclear systems….etc.

Chapter 2, presents a literature review on the nanofluids flow in pipe under the laminar and turbulent flow regimes. The objective of the thesis is presented too.

Chapter 3, presents two mathematical models namely single phase and multiphase mixture models to govern the incompressible fluid flow and heat transfer in a pipe. In addition, thermophysical properties of water, nanofluids and nanoparticles are presented.

In Chapter 4, we have examined the effect of nanoparticles concentration of nanoparticles on the convective heat transfer of laminar and turbulent flow of Al2O3 -water nanofluids using a single-phase model.

In Chapter 5, a numerical investigation is performed on heat transfer and friction factor in forced convection for nanofluid (Fe3o4-water) flow in pipe. Here, the effect of magnetic field on velocity, heat transfer, friction factor and pressure drop are presented.

In Chapter 6, a numerical investigation is performed on heat transfer in mixed convection for a nanofluid Cu-H2O and inclined pipe. Here, the effect of inclination angles and Buoyancy force on heat transfer is also presented.

Introduction to Nanofluids

1.1 Introduction

Forced convection heat transfer is an important phenomenon in many engineering applications e.g. cooling of electronic components, nuclear energy, solar energy, transportation, building heating, lubrication technologies and so on. However, low thermal conductivity of conventional fluids such as water, engine oil and ethylene glycol is the primary limitation on the enhancement of heat transfer performance in such engineering applications. In order to achieve a better performance on the heat transfer, highly conductive nanoparticles are suspended in base fluid to form a nanofluid.

The Nanofluid becomes a promising alternative approach for thermal applications and engineering and research is underway to apply nanofluids in many applications where the conventional heat transfer fluids are not capable of improving the desired heat transfer rate.

1.2 Definition

The nanofluids are two phase mixtures engineered by dispersing nanometer sized particles with sizes ranging below 100 nm in base fluids (choi). The most commonly used base fluids are water, ethylene glycol or oil due to their use in conventional thermal systems. The commonly nanoparticles include are Aluminium (Al), Silicon (Si), Titanium (Ti), Copper (Cu), Zinc (Zn), Iron (Fe), Magnesium (Mg), Silver (Ag) and magnetic nanoparticles (Fe3O4).

1.3 Properties of nanofluids

It may be noted that particle size is an important physical parameter in nanofluids because it can be used to tailor the nanofluid, thermal properties as well as the suspension stability of nanoparticles. Researchers in nanofluids have been trying to exploit the unique properties of nanoparticles to develop stable as well as highly conducting heat transfer fluids.

Compared to micrometer sized particles, nanoparticles possess high surface area to volume ratio due to the occupancy of large number of atoms on the boundaries, which make them highly stable in suspensions. Thus the nano suspensions show high thermal conductivity possibly due to enhanced convection between the solid particle and liquid surfaces. Since the properties like the thermal conductivity of the nano sized materials are typically an order of

magnitude higher than those of the base fluids, nanofluids show enhancement in their effective thermal properties. Due to the lower dimensions, the dispersed nanoparticles can behave like a base fluid molecule in a suspension, which helps us to reduce problems like particle clogging, sedimentation etc. found with micro particle suspensions. [1]

1.3.1 Particle Material and Base Fluid

Many different particle materials are used for nanofluid preparation Al_2O_3, CuO , SiC, TiC, TiO_2, Ag, Au, Cu, and Fe nanoparticles are frequently used in nanofluid research. Carbon nanotubes are also utilized due to their extremely high thermal conductivity in the longitudinal (axial) direction.

Base fluids mostly used in the preparation of nanofluids are the common working fluids of heat transfer applications; such as, water, ethylene glycol and engine oil. In order to improve the stability of nanoparticles inside the base fluid, some additives are added to the mixture in small amounts.

1.3.2 Particle Size

Nanoparticles used in nanofluid preparation usually have diameters below 100 nm. Particles 10 nm has been used in nanofluid research [2]. When particles are not spherical but rod or tube-shaped (carbon nanotube), the diameter is still below 100 nm, but the length of the particles may be on the order of micrometers. It should also be noted that due to the clustering phenomenon, particles may form clusters with sizes on the order of micrometers.

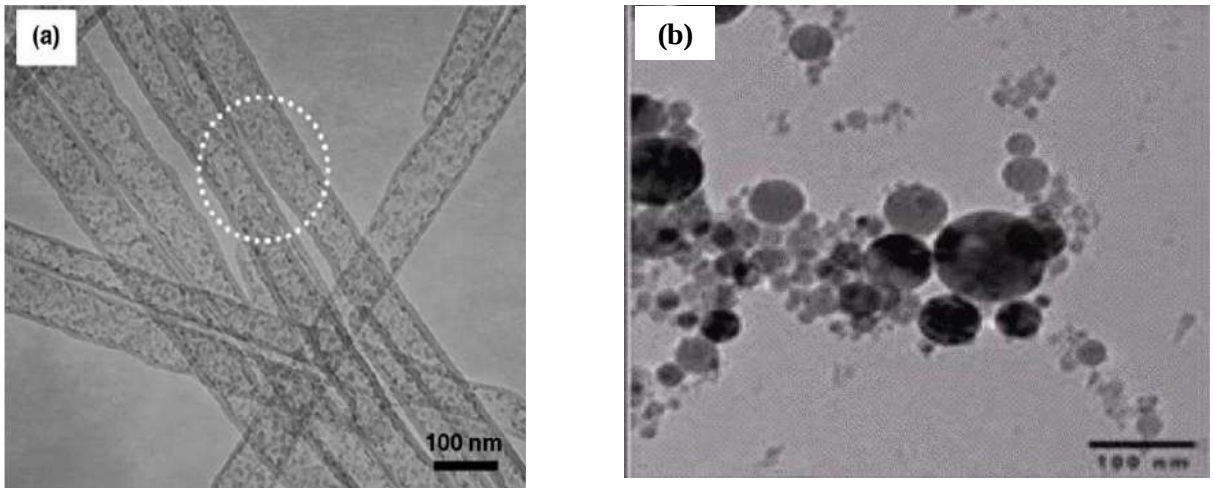


Fig 1.1: represent carbon nanotube and spherical nanoparticules

1.3.3 Shapes of nanoparticles

For experimentation, spherical as well as cylindrical shaped nanoparticles are commonly used for nanofluid synthesis. The cylindrical particles have larger aspect ratio (length to diameter ratio) than spherical particles. The wide differences in the dimensions of these particles do influence the enhancement in effective thermal properties of nanofluids. However, disk shaped and tube shaped nanoparticles are also used. On the other hand, the clusters formed by nanoparticles may have fractal-like shapes.[3]

1.4. Preparation Methods for Nanofluids

There are mainly two methods of nanofluid production, namely, two-step method and one step method. Both the methods to manufacture nanofluids are discussed as follows:

1.4.1 Two-step method

The two step method is the most suitable and simple method for production of nanofluid. Nanoparticles, nanofibers or other nanomaterials used in this method are first produced as dry powders by chemical or physical methods.

Then, the nanosized powder will be dispersed into a fluid in the second processing step with the help of intensive magnetic force agitation, ultrasonic agitation, high-shear mixing, homogenizing, and ball milling. Two-step method is the most economic method to produce nanofluids in large scale, because nanopowder synthesis techniques have already been scaled up to industrial production levels.[4]

The main disadvantage of the two-step technique is that the nanoparticles form clusters during the preparation of the nanofluid which prevents the proper dispersion of nanoparticles inside the base fluid [5].

Due to the difficulty in preparing stable nanofluids by two-step method, several advanced techniques are developed to produce nanofluids, including one-step method. In the following part, we will introduce one-step method in detail.

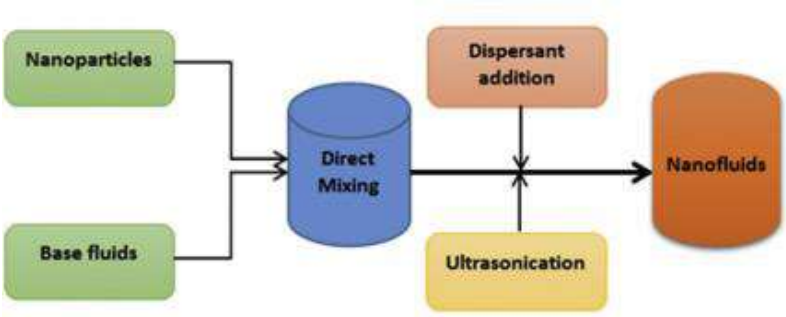


Fig. 1.2. Two-step preparation process of nanofluids

1.4.2 One-Step Method

One-step technique combines the production of nanoparticles and dispersion of nanoparticles in the base fluid into a single step. There are some variations of this technique. In one of the common methods, named direct evaporation one-step method, which was first developed by Yatsuya and coworkers [6] and later improved by Wagener and Günther [7]

During this process, the nanofluid is produced by the solidification of the nanoparticles, which are initially gas phase, inside the base fluid.

The single-step method can significantly reduce the agglomeration and improve the stability of nanofluid [8]. However, at present the quantities of nanofluids that can be produced via this method are much more limited than two-step techniques, although, if desired, it is likely that those single-step techniques could also be scaled to an affordable cost range for the mass production of nanofluids.

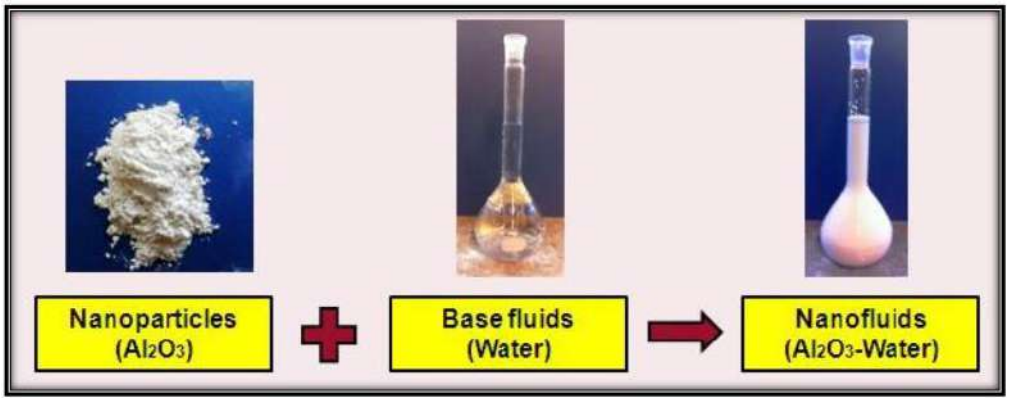


Fig 1.3: Al2O3-water nanofluid

1.4.3 Other Novel Method

Wei et al. developed a continuous low microfluidic microreactor to synthesize copper nanofluids. By this method, CuO nanofluid was synthesized by transforming an unstable Cu(OH)2 precursor to CuO in water under an ultrasonic vibration, followed by microwave irradiation. [9]

1.5. The Stability of Nanofluid

The main challenge in preparing nanofluids is their poor stability caused by the formation of agglomerates. The stability of nanofluids is essential in practical applications because the thermo-physical properties of unstable fluids change through time.

Gravitational force causes particles to separate from the liquid and settle on the bottom. Fig1.4 shows nanofluid samples where one is visually stable, while the other shows that particles are visibly separated from the liquid.

Surfactants enhance nanoparticle stability in fluids. However, surfactant functionality under high temperatures is a major concern, especially for high-temperature applications. The sedimentation method, also called the settling bed, is the most decisive and extensively used technique for evaluating the stability of a nanofluid [10]. In this method, light absorbance is measured or the bed height is visually monitored over a certain period of time.

The main drawback of using this method on fairly slow settling suspension is the long observation time; a faster technique involves the time-resolved measurement of the zeta potential of the sample. Another disadvantage of this method is that it restricts the viscosity and particle concentration of samples.



Fig. 1.4. Stable (left) and unstable (right) nanofluids.

1.6. Potential features of nanofluids

Nanofluids have uncommon features that are essential for various engineering applications. These special qualities include:

- Ultrafast heat transfer ability
- Increased thermal conductivity and exceptional theoretical predictions
- Decreased pumping power
- Enhanced stability over other colloids
- Superior lubrication
- Decreased friction coefficient
- Decreased erosion and clogging in microchannels [11]

1.7 Application of nanofluids

1.7.1 Electronics Cooling

Due to high heat generations in chips electronic circuitry components with compact designs and geometry suffering from thermal management. To extract such a high heat from these compact devices has become difficult.

Heat can be removed by two methods: by optimizing the design of cooling system and other by using high heat dissipating capacity fluids. Here nanofluids play the role of higher heat carrying capacity fluids than conventional coolants. Nanofluids have higher thermal conductivity compared to those of base fluids, as proved by many researchers. [4]

Some high-end desktop computers use small water cooling systems to move the heat from the CPU to the case. High-power-density devices such as power electronics have used cooling nanofluid. [12]

The Reserator 3 Max nanofluid cooler was developed by Zalman's company with the features of nanofluid technology and created the first commercial CPU cooler which is shown in figure 4. This cooler system achieved cooling of loads up to 400W of heat through a single CPU water block by using a dual pure-copper radial radiator design. An integrated high-performance pump was provided and the liquid through the system can withstand 90 litres per hour flow rate. In this system, the added nanoparticles increase the thermal conductivity of the

liquid coolant. The Zalman Reserator 3 Max is the world's first nanofluids applied cooler and it won an award at CES 2013.

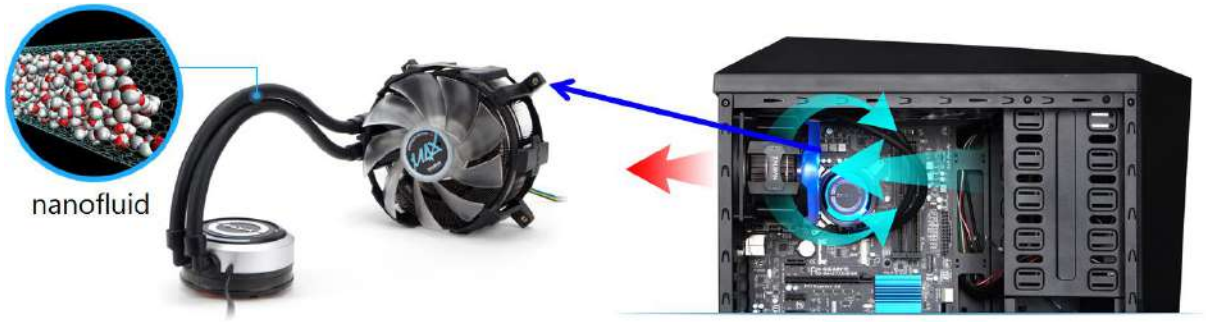


Fig 1.5. Zalman's Reserator 3 Max nanoliquid cooler.

1.7.2 Vehicle Cooling

Nanofluids are been used in automobile for applications such as coolant, fuel additives, lubricant, shock absorber and refrigerant. The current engine oils, automatic transmission fluids, coolants, lubricants, and other synthetic high-temperature heat transfer fluids found in conventional truck thermal systems radiators, engines, heating, ventilation and air-conditioning have inherently poor heat transfer properties. These could benefit from the high thermal conductivity offered by nanofluids. Nanofluids are commonly used in cooling radiators for automobiles and trucks, and power electronics for hybrid electric vehicles.

These nanofluids provide better insight into thermal management system and better lubrication. Tzeng et al. [13] applied nanofluids to the cooling of automatic transmissions. The experimental platform was the transmission of a four-wheel drive vehicle. The used nanofluids were prepared by dispersing CuO and Al2O3 nanoparticles into engine transmission oil. The results showed that CuO nanofluids produced the lower transmission temperatures both at high and low rotating speeds. This work is vital since it shows real world application of nanofluids representing a greater step forward for industrial applications of nanofluids.

1.7.3 Transformer Cooling

The power generation industry is greatly interested in transformer cooling application with the usage of nanofluids for reducing size and weight of the transformer. The ever increasing demand for greater electricity production, especially in our nation will require upgrades of most

transformers at some point in the near future at a potential cost of millions of dollars in hardware retrofits.

Yu et al. [14] and Xuan and Li [15] examined that the heat transfer properties of transformer oils could be significantly improved by using additives of nanoparticles. Specifically, nanofluid based transformer oil is likely to be the next generation cooling fluid in transformers.

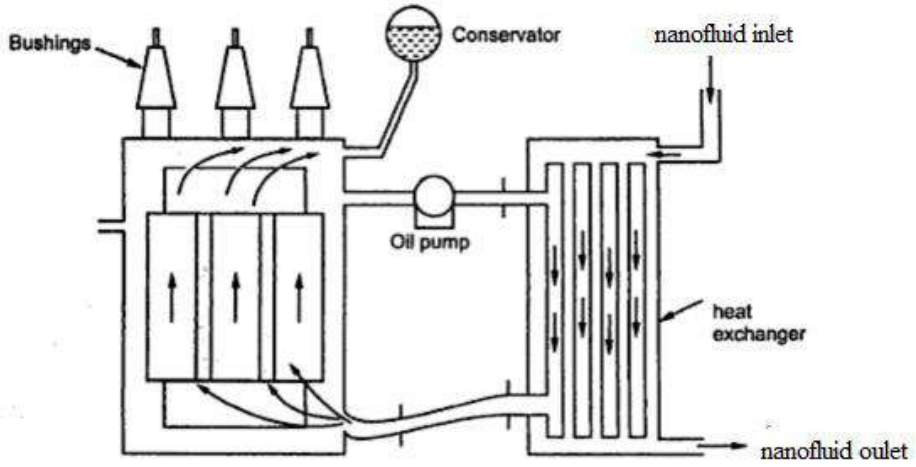


Fig 1.6: Transformer Cooling

1.7.4 Heating Buildings and Reducing Pollution

Nanofluids can be applied in the building heating systems. Kulkarni et al. evaluated how they perform heating buildings in cold regions [16]. In cold regions, it is a common practice to use ethylene or propylene glycol mixed with water in different proportions as a heat transfer fluid. So, 60: 40 ethylene glcol/water (by weight) was selected as the base fluid. The results showed that using nanofluids in heat exchangers could reduce volumetric and mass flow rates, resulting in an overall pumping power savings. Nanofluids necessitate smaller heating systems,

Which are capable of delivering the same amount of thermal energy as larger heating systems but are less expensive. This lowers the initial equipment cost excluding nanofluid cost. This will also reduce environmental pollutants, because smaller heating units use less power, and the heat transfer unit has less liquid and material waste to discard at the end of its life cycle.

1.7.5 Smart fluid

In this era of energy saving and the widespread use of battery operated devices, such as cellphones and laptops, have accented the necessity for a smart technological handling of

energetic resources. Smart materials have one or more properties that can be dramatically altered, eg, smart material with variable viscosity may turn from a fluid which flows easily to a solid. Nanofluids have been demonstrated to be able to handle this role in some instances as a smart fluid.



Fig 1.7: A smart fluid developed in labs at the Michigan Institute of Technology

Nanofluids can be used as a smart material working as a heat valve to control the flow of heat, where heat transfer can be reduced or enhanced at will [17].

The nanofluid can be readily configured either in a low state, where it conducts heat poorly, or in a high state, where the dissipation is more efficient. This shows that nanofluids can be used as a double edged sword to provide heating or cooling technologies as required. In particular, Magnetorheostatic (MR) materials is a nanofluid, which consists of tiny iron particles suspended in oil. It changes from a thick fluid (similar to motor oil) to nearly a solid substance within the span of a millisecond when exposed to a magnetic field, and the effect is completely reversed when the field is removed.



Fig 1.8: The MR Fluid is liquid on the left, and as a solid in magnetics field on the right

1.7.6 Nuclear cooling systems

A nuclear reactor is a system that contains and controls sustained nuclear chain reactions. Reactors are used for generating electricity, moving aircraft carriers and submarines, producing medical isotopes for imaging and cancer treatment, and for conducting research. Fuel with heavy atoms are placed in a reactor vessel with neutrons. The neutrons start a chain reaction where each atom splits releasing more neutrons that cause other atoms to split. This produces large amounts of energy in form of heat. The heat is carried to coolants, which heat up and go off to a turbine to spin a generator, thus producing electricity. This provided clean energy alternative that frees us from the shackles of fossil fuel dependence [18].

At the Nuclear Science and Engineering Department of the Massachusetts Institute of Technology (MIT), carried feasibility studies on the use of nanofluids in nuclear energy industry as an alternative to improving the performance of water-cooled nuclear system for heat removal. The studies have shown possible applications in pressurized water reactor (PWR) primary coolant [19].

Nanofluids can be used as the main reactor coolant for PWRs, thus enabling significant power uprates the PWRs and enhancing their economic performance. The experiments demonstrated that, the use of nanofluids with at least 32% higher critical heat flux (CHF)

enabled a 20% power density uprate in current plants without changing the fuel assembly design.

Nanofluids can also be used as a coolant for the emergency core cooling systems (ECCSs) of both PWRs and boiling water reactors, where they could cool down overheat surfaces more quickly leading to an improvement in power plant safety.

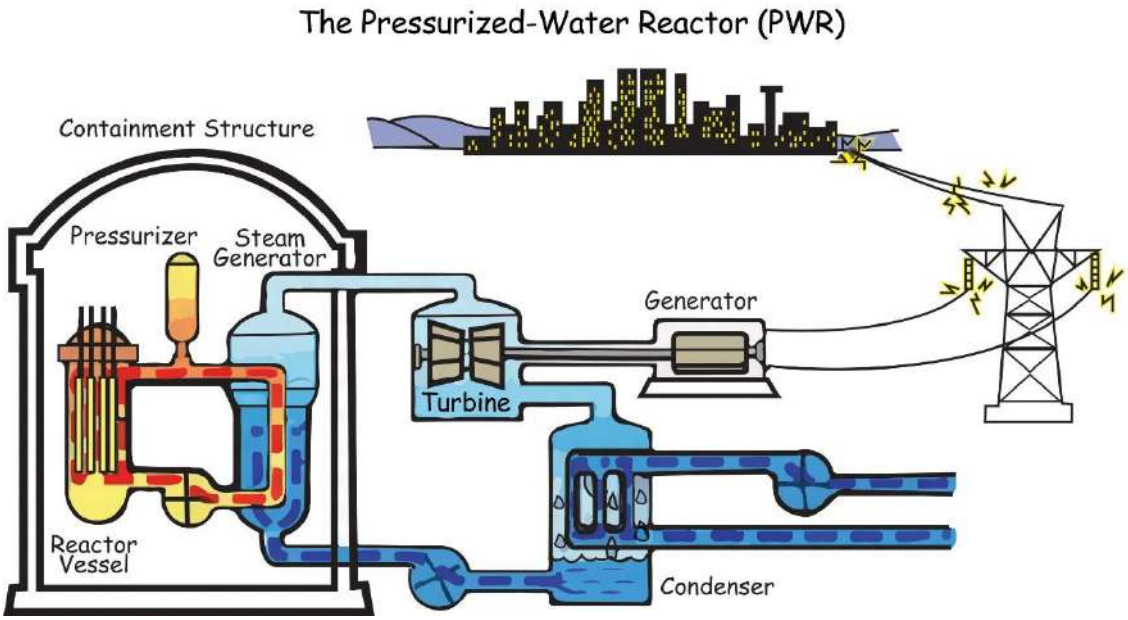


Fig 1.9: Nuclear Reactor Plant

1.7.7 Geothermal Power Extraction

When extracting energy from the earth‘s crust that varies in length between 5 to 10 km and temperature between 500oC and 1000oC, nanofluids can be employed to cool the pipes exposed to such high temperatures. When drilling, nanofluids can serve in cooling the machinery and equipment working in high friction and high temperature environment. Also a nanofluids could be used as a working fluid to extract energy from the earth core and processed in a pressurized water reactor (PWR) power plant system.

In drilling technology, which in vital in geothermal power, the use of nanofluids can ensure improved sensors and electronics capable of operating at higher temperature. Such improvements will enable access to deeper and hotter regions. Nanofluids can be used as a highly specialized drilling fluid that has superior performance in high temperature drilling. [4]

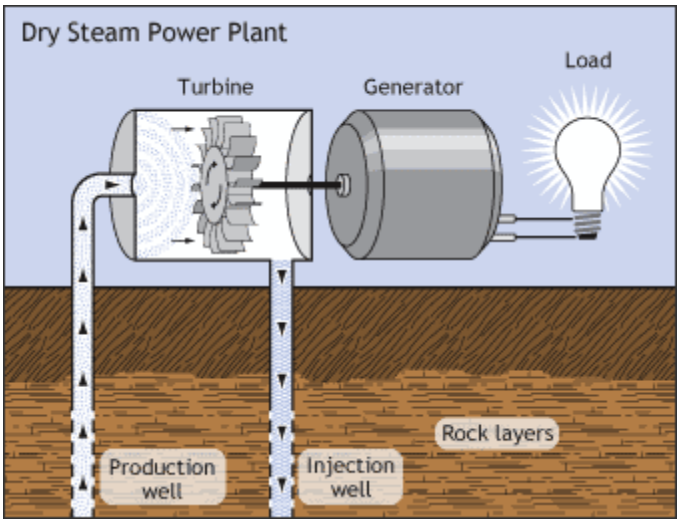


Fig 1.10: Binary Cycle Power Plan

1.7.8 Space and Defence

The restriction of space, energy and weight at space stations and in aircraft generates the need for highly efficient cooling system which has high heat flux capacity. This presenting a vision for lighter weight of cooling systems due to compact and simple designs of heat exchangers, which further makes space travel cheaper than present. The high critical heat flux capacity make nanofluids capable of being used in military devices and systems such as high powered military electronics, military vehicle components, radars, and lasers, require high-heat-flux cooling, to the level of thousands of W/cm2. At this level, cooling with conventional heat transfer fluids is difficult. Some specific examples of potential military applications include power electronics and directed-energy weapons cooling. Since directed-energy weapons involve heat sources with high heat fluxes (> 500 to 1000 W/cm2), cooling of the direct-energy weapon and associated power electronics is critical and is further complicated by the limited capability of current heat transfer fluids. Nanofluids also provide advanced cooling technology for military vehicles, submarines, and high-power laser diodes. It appears that nanofluid research for defense applications considers multifunctional nanofluids with added thermal energy storage or energy harvesting through chemical reactions. [12]

1.7.9 Solar absorption

Is one of the best sources of renewable energy with minimal environmental impact. The conventional direct absorption solar collector is a well-established technology, and it has been proposed for a variety of applications such as water heating; however, the efficiency of these

collectors is limited by the absorption properties of the working fluid, which is very poor for typical fluids used in solar collectors. Recently, this technology has been combined with the emerging technologies of nanofluids and liquid-nanoparticle suspensions to create a new class of nanofluid-based solar collectors. Otanicar et al [20] performed experiments on direct absorption solar collector with nanofluids as working fluid and reported 5% increase in efficiency of solar thermal collectors.

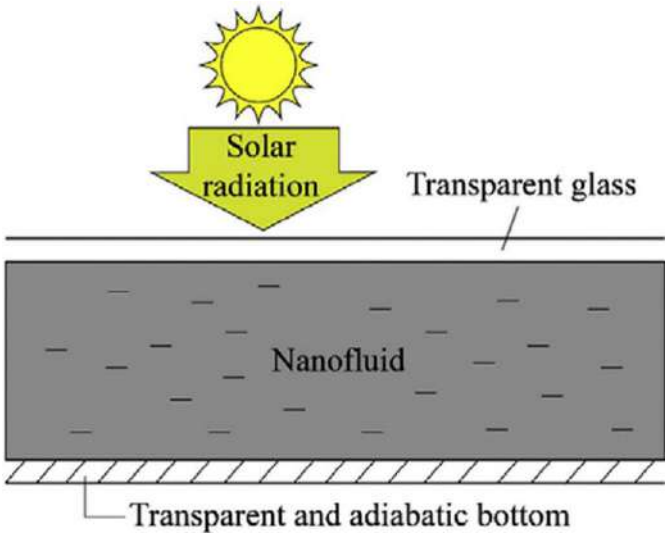


Fig 1.11 a solar collector using nanofluid

1.7.10 Biomedical Applications

Nanofluids was originally developed primarily for thermal management applications such as engine, microelectronics, and photonics. However, nanofluids can be formulated for a variety of other uses for faster cooling.

Nanofluids are now being developed for medical applications, including cancer therapy. Traditional cancer treatment methods have significant side effects. Iron-based nanoparticles can be used as delivery vehicles for drugs or radiation without damaging nearby healthy tissue by guiding the particles up the bloodstream to a tumor with magnets. Nanofluids could also be used for safer surgery by cooling around the surgical region, thereby enhancing a patient's chance of survival and reducing the risk of organ damage. In contrast to cooling, nanofluids could be used to produce higher temperatures around tumors, to kill cancerous cells without affecting nearby healthy cells [21].

1.8 Magnetohydrodynamics (MHD)

Magnetohydrodynamics (MHD) is the academic discipline concerned with the dynamics of electrically conducting fluids in a magnetic field. These fluids include salt water, liquid metals (such as Mercury, gallium, molten Iron) and ionized gases or plasmas (such as solar atmosphere). The term MHD is comprised of the words magneto – meaning magnetic, hydro – meaning fluids, and dynamics – meaning movement. Synonyms of MHD that are less frequently used are the terms magneto fluid dynamics and hydromagnetics. The field of MHD was initiated by the Swedish Physicist Hannes Alfvén (1908-1995), who received the Nobel Prize in Physics in 1970 for fundamental work and discoveries in magnetohydrodynamics with fruitful applications in different parts of plasma physics.

MHD covers those phenomena, where, in an electrically conducting fluid, the velocity field V and the magnetic field B are coupled. The magnetic field induces an electric current of density j in the moving conductive fluid (electromagnetism). The induced current creates forces on the liquid and also changes the magnetic field. Each unit volume of the fluid having magnetic field B experiences an MHD force j x B known as Lorentz force. The set of equations which describe MHD flows are a combination of Navier-Stokes equation of fluid dynamics and Maxwell‘s equation of electromagnetism (see chapter 3). These differential equations are solved simultaneously either analytically or numerically.

1.9 Ferrofluids

Magnetic nanofluid, popularly known as ferrofluid, is a magnetic colloidal suspension consisting of base liquid and magnetic nanoparticles with a size range of 5 to 30nm in diameter coated with a surfactant layer. The nanoparticles are suspended by Brownian motion and generally will not settle under normal conditions. The most often used magnetic particle materials are magnetite, iron or cobalt; and the base liquids are water or kerosene. The advantage of the ferrofluids is that the fluid flow and heat transfer may be controlled by an external magnetic field which makes it applicable in various fields such as electronic packing, mechanical engineering, smart fluids, thermal engineering and aerospace. [22]

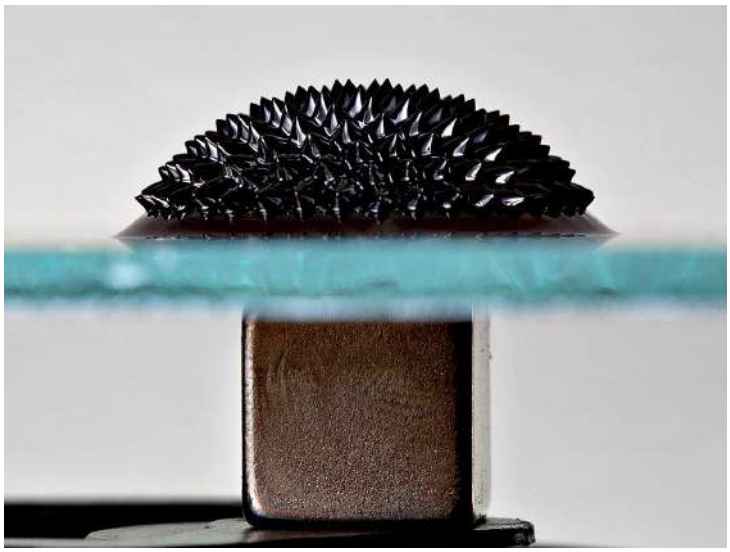


Fig 1.12: Ferrofluid with external magnetic field

1.10 Conclusion

In this chapter we focused on different properties of nanofluid and the two method of preparation one-step and two-steps, also we presented a different applications of nanofluid in many fields such as Electronics Cooling, Vehicle Cooling, Transformer Cooling, Heating Buildings and Reducing Pollution, Nuclear cooling systems, Space and Defence, Solar absorption and Biomedical Applications.

Literature Review

2.1 Introduction

In this chapter, several experimental and numerical research works related to nanofluids flow in pipe or tube have been presented and discussed, for laminar and turbulent nanofluids flow with single phase and Eulerian-Eulerian mixture model. This chapter also illustrates the studies on laminar and turbulent flows. Finally, the objective of the thesis is presented

2.2 Laminar

Experimental results for the convective heat transfer of Al2O3 (27–56 nm) / water based nanofluids flowing through a copper tube in laminar regime was reported by Wen and Ding [23]. It was observed that the improvement of the heat transfer coefficient is particularly large at the entrance region, and it decreases with axial distance. Also it shown that the enhancement increases with the Reynolds number as well as the volume concentration of nanoparticle.

Jung et al. [24] did experiments for Al2O3–water nanofluids in rectangular microchannels. The particle diameter in their experiments was 170 nm. With only 1.8% of volume concentration they reported a 32% increase of the heat transfer coefficient in comparison to single distilled water. Also, experiments on nanofluid heat transfer in trapezoidal silicon microchannels have been performed by Wu et al. [25]. For channels with a hydraulic diameter of 194.5 um and an Al2O3–water nanofluid, they reported an increase in the Nusselt number with increasing particle concentration, Reynolds and Prandtl numbers, while the pressure drop increased slightly when compared to pure water.

Yang et al., reported experimental investigation of convective heat transfer of graphite/Water nanofluid in a horizontal tube heat exchanger [26]. In this study effect of Reynolds number, volume fraction, temperature and nanoparticle source on heat transfer coefficient have been studied. The results illustrated that heat transfer coefficient increases with the Reynolds number and particle volume fraction.

Experimental studies on convective heat transfer of Cu/Water, CuO/Water and Al2O3/Water nanofluids are reported by Heris et al. [27], [28]. The experimental set-up consisted of a one-meter annular tube, which was constructed of 6 mm diameter inner cupper tube 0.5 mm thick, and 32 mm diameter outer stainless steel tube. The nanofluid flows inside the inner tube while

saturated steam entered the annular section, which created constant wall temperature condition the effect of Peclet number and nanoparticle volume fraction on heat transfer of different nanofluids has been studied. The augmentation of heat transfer using nanofluids was found to be much higher than the predictions of existing correlations.

Many numerical studies have investigated heat transfer of nanofluids. Maiga et al. [29], Bajestan et al. [30] and Bayat and Nikseresht [31] numerically investigated the heat transfer characteristics of Al_2O_3 nanoparticles with different base fluids such as water, Ethylene Glycol (EG) or mixture of Ethylene Glycol (EG) and water inside a circular tube under laminar flow regime. After their investigation, it was reported that the water based nanofluids had showed inferior heat transfer enhancement than the other base fluids.

Moraveji et al studied numerically [32] forced convection heat transfer with laminar and developed flow for water-Al2O3 nanofluid inside a circular tube under constant heat flux from the wall was numerically investigated using computational fluid dynamics method. Both single and two-phase models are accomplished for either constant or temperature dependent properties. For this study nanofluids with size particles equal to 100 nm and particle concentrations of 1 and 4 % were used. It is observed that the nanoparticles when dispersed in base fluid such as water enhance the convective heat transfer coefficient. The Nusselt number and heat transfer coefficient of nanofluids were obtained for different nanoparticle concentrations and various Reynolds numbers. Heat transfer was enhanced by increasing the concentration of nanoparticles in nanofluid and Reynolds number.

V. Bianco [33] investigated numerically laminar forced convection flow of a water–Al2O3 nanofluid in a circular tube, submitted to a constant and uniform heat flux at the wall. A single and two-phase model (discrete particles model) is employed with either constant or temperature dependent properties. The investigation is accomplished for size particles equal to 100 nm. The maximum difference in the average heat transfer coefficient between single and two phase models results is about 11%. Convective heat transfer coefficient for nanofluids is greater than that of the base liquid. Heat transfer enhancement increases with the particle volume concentration and Reynolds number increases.

Akbarnia and Behzadmehr reported a CFD model based on single phase model for investigation of laminar convection of Water/Al2O3 nanofluid in a horizontal curved tube. In their study, effects of buoyancy force, centrifugal force and nanoparticle concentration have been discussed [34].

Fard, M et H. Esfahany [35] studied numerically a laminar convective heat transfer of nanofluids in a circular tube under constant wall temperature using a CFD software, a single-phase and two-phase models have been used for prediction of heat transfer coefficient. Has been shown that the two-phase model is more precise than the single-phase model. The effects of some important parameters such as Peclet number, particle volume fraction and nanofluid type on heat transfer rate have been investigated under laminar conditions. Heat transfer coefficient of nanofluids increases with an increase in the volume fraction of nanofluids and Peclet number. At the fixed Peclet number of 6500, the heat transfer coefficient for 3% CuO/Water nanofluid increases by 1.54 times over the base fluid. Increasing the nanofluid volume fraction from 0.2% to 3%, results in 27.8% increase in the heat transfer coefficient.

R. Lotfi [36] investigated numerically forced convective of a nanofluid that consists of water and Al2O3 in horizontal tubes. Computed results were validated with existing established correlation. A single-phase model and two phase mixture model formulations were used for comparison. The comparison of calculated results with experimental values shows that the mixture model is more precise. It is clear from the results that the rate of thermal enhancement decreases with the increase of nanoparticles volume concentration.

Kalteh, M [37] studied experimentally and numerically laminar convective heat transfer of an alumina-water nanofluid flow inside a wide rectangular microchannel heat sink. For the numerical study, a two-phase Euleriane Eulerian method using the finite volume approach is adopted in this study. Comparing the experimental and numerical results show that two-phase results are in better agreement with experimental results than the single-phase approaches. The maximum deviation from experimental results is 12.61% and 7.42% for single and two-phase approaches, respectively. Moreover, the average Nusselt number increases with an increase in Reynolds number and volume concentration as well as with a decrease in the nanoparticle size

Lajvardi [38], investigated experimentally the convective heat transfer of ferrofluid flowing through a heated copper tube in the laminar regime in the presence of magnetic field, he observed that the heat transfer coefficient h enhanced significantly under the influence of an applied magnetic field and magnetic nanoparticle volume fraction.

Azizian et al. [39] studied the effect of a constant magnetic field on the laminar convective heat transfer and pressure drop of magnetite nanofluid in a vertical tube and reported large enhancement in the local heat transfer coefficient against only a 7.5% increase of pressure drop.

They also showed that the convective heat transfer enhancement increases with the magnetic field intensity and gradient.

Goharkhah [40], studied experimentally the convective heat transfer of nanofluid (Fe_3O_4-water) under external magnetic field. He investigated the effect of magnetic field intensity and frequency of the convective heat transfer under different flow rates (Re 200, 1200) and concentrations (1, 1.5, and 2 Vol. %). He observed that at a constant Reynolds number the heat transfer increased with the magnetic field intensity. Their results showed a maximum heat transfer enhancement of 16.4% by the use of (Fe_3O_4-water) in the absence of a magnetic field. This value is increased up to 24.9% and 37.3% by application of constant and alternating magnetic field.

2.3 Turbulent

Numerous experiments and numerical investigations have been carried out by researchers on pipes or tubes under turbulent flow regime. In some numerical research, the single phase and mixture approaches have been used.

Pak and cho [41], proposed the first experimental study for the turbulent convection of nanofluids. They proposed correlation experiment for the Nusselt number.

Behzadmehr, Saffar-Avval [42], were the first to apply the mixture model to the simulation of nanofluid-convection, the comparison of calculated results with experimental values shows that the mixture model is more precise than the single phase model.

Bianco, Manca [43], numerically investigated on nanofluids turbulent convection heat transfer inside a circular tube, and they used both single-phase and multi-phase approaches, and they found that the accuracy of the multi-phase mixture model was better than the single-phase model.

Azmi, Sharma [44], investigated experimentally the turbulent heat transfer and friction factor with SiO_2 nanofluid in a circular tube under a constant heat flux, they reported that the convective heat transfer coefficients in the Reynolds number range of 5000 and 27,000 increased with volume concentration up to 3.0% and decreased thereafter, as result the friction factor decreases with increase in Reynolds number.

Chen, Li [45], numerically examined the turbulent and laminar forced convection heat transfer in a circular tube, using CuO and γAl_2O_3 nanoparticles with the two-phase mixture and Eulerian models, their investigations showed that the mixture model was more accurate than the Eulerian model.

Fotukian and Esfahany [46], investigated experimentally the turbulent convective heat transfer of dilute γAl_2O_3/water nanofluid inside a circular tube, the results indicated that the maximum value of heat transfer coefficient was 48% compared to base fluid for volume fraction 0.054% at Reynolds number of 10000.

Namburu, Das [47], studied numerically the turbulent flow and heat transfer of three different nanofluids (CuO, Al_2O_3 and SiO_2) in a circular pipe under constant heat flux using single phase approach with thermo physical variable properties, they found the heat transfer coefficient increased if the volume concentration of nanofluids and Reynolds number increase, and for the same concentration of three nanofluids CuO, Al_2O_3 and SiO_2 at a particular Reynolds number, the CuO nanofluid had the higher heat transfer.

Experiments undertook by Azmi, Sharma [48] for the determination of forced convection heat transfer coefficient and friction factor at various nanofluids TiO_2 and SiO_2 with particles of 50 nm to 22 nm size respectively dispersed in base liquid water in tube under turbulent flow, the friction factor increased with the heat transfer coefficient of 26% at 1.0% volume concentration, and increased by 33% at 3.0% volume concentration for TiO_2 and SiO_2 nanofluids.

Hanafizadeh, Ashjaee [49], considered a horizontal tube under constant heat flux to study forced convection of a water–Fe_3O_4 nanofluid, two-phase (Eulerian, VOF and mixture) and single phase approaches have been used, the comparison with experimental results revealed that the mixture model had less error than other two methods, and it was closer to the experimental data.

Hejazian, Moraveji [50], made a comparison of Euler with mixture model for the turbulent convective flow of Al_2O_3/Water nanofluid in horizontal tube, they realized that the heat transfer coefficient enhanced with increasing of the particle volume concentration and Reynolds number, they concluded that both models predicted heat transfer with almost the same accuracy, but the mixture model was slightly more accurate than the Euler model in predicting of the Nusselt number, the maximum error was 9.91% for the mixture model and 11% for Euler model.

Hussein, Bakar [51], analysed numerically the turbulent forced convective in heated tube nanofluid TiO_2-water using single phase approach, the results showed that the heat transfer coefficient of nanofluid was higher than the base liquid, and increased with increasing of the Reynolds number and volume concentration.

Sundar, Naik [52], did an experimental work on Fe_3O_4 nanofluid flow in circular tube with turbulent condition, and they concluded increasing in thermal conductivity by 30.9% and increasing in friction factor by 10.01% at volume concentration of 0.6% and temperature range of 20–60 ℃, and they also developed Nusselt number and friction factor correlations.

Recently, a numerical study based on computational fluid dynamics method with a single phase approach has been done by Moraveji [53] to determine the effect of nanoparticle concentration and flow rate on the convective heat transfer and friction factor of Fe_3O_4, the results showed that the modeling data was in very good agreement with the experimental data, Nusselt number and friction factor increased with the volume fraction and Reynolds number, two correlations were developed for Nusselt number and friction factor with the maximum error around 10%.

Xuan and Li [54] studied the single-phase flow and heat transfer performance of nanofluids under turbulent flow in tubes. Their experimental results showed that the convective heat transfer coefficient and the Nusselt number of nanofluids increase with the Reynolds number and the volume fraction of nanoparticles under turbulent flow. Compared with water, the Nusselt number of the nanofluids with a 2.0 vol. % of Cu nanoparticles is more increased than 39%.

Davarnejad, R [55] investigated numerically The MgO-water nanofluid convective heat transfer in turbulent regime inside a tube. Friction factor and Nusselt number were studied in various nanoparticles concentrations and Reynolds numbers. Three models including single phase, mixture and VOF were applied to predict the modified heat transfer properties in the turbulent flow. The results indicated that nanofluid heat transfer and pressure drop (friction factor) increased with the nanoparticle volume fraction enhancement.

3.3 Objectif of thesis

As we can see above, numerous experimental and numerical investigations of nanofluids have been carried out by the researchers on different geometries and nanoparticules properties. They have conducted researches under laminar to turbulent flow regimes using both single and multi-phase approaches. A few papers research focused their work on forced convection heat transfer inside a tube with a magnetic field in laminar flow. In our knowledge, the turbulent flow with magnetic field has not investigated yet and this was the motivation for this work. Hence, the aim of our present investigation is to examine the effect of flow rate and nanofluid (Fe_3O_4–

water) concentration on the Nusselt number and friction factor in a system with the influence of magnetic field.

Additionally, an in-depth investigation is carried out to understand the nanofluids flow and heat transfer in an inclined and horizontal pipe under turbulent flow regime.

Mathematical Modelling

3.1 Introduction

Usually three different approaches have been used by the researchers to investigate the effect of heat transfer of nanofluid. The first approach is single phase model in which both the fluid phase and the nanoparticles are in thermal equilibrium and flow with the same velocity. The second approach is multi-phase model. And the third one is discrete phase model where a simple fluid solid mixture principle is considered instead of nanofluid.

Firstly, the details of the Reynolds-averaged Navier-Stokes (RANS) based governing equations for fluid continuity, momentum equation, energy equations and MHD equation of the two models are described in this chapter. Secondly, the turbulent Standard k-ε models, are presented. Thirdly, the thermo physical properties of nanofluids and nanoparticles and other useful definitions are described. Finally a summary of numerical method with definition of CFD and different steps using to solve a problem in FLUENT.

3.2 Governing Equations

Different models have been proposed to describe the governing equations in order to simulate nanofluid convection; particularly, they are as follows:

- Single-phase model
- Discrete-phase model
- Mixture model

For the main objective of thesis we only used the single phase and mixture approaches. In the single-phase model, the basic hypothesis is that the nanofluid behaves like a single-phase fluid with enhanced thermo physical properties; and in the mixture model, the fluid is considered to be a single fluid with two phases, and the coupling between them is strong. In the following section, the Reynolds-averaged Navier-Stokes equations for single phase and multi-phase approaches are presented.

3.2.1. Single Phase Model

The nanofluid as a single phase fluid with different physical properties such as density, thermal conductivity and viscosity was used. The fluid phase was assumed to be as continues phase and the following assumptions are considered:

1- Fluid flow is incompressible

2- Newtonian and turbulent.

3- The Boussinesq approximation is negligible as the pipe is placed horizontally.

4- Nanoparticles are spherical and uniform in size and shape.

5- Radiation effects are negligible.

The governing equations (continuity, momentum and energy) are written as follows:

Continuity equation:

$$\nabla(\rho_{nf}.V_m) = 0 \tag{3.1}$$

Momentum equation:

The MHD coupling is achieved by introducing additional source terms to the fluid momentum equation and energy equation. For the fluid momentum equation, the additional source term is the Lorentz force given by $\vec{F} = \vec{j} \times \vec{B}$ so the momentum equation written as:

$$\nabla(\rho_{nf}.V_m.VM) = -\nabla P + \nabla(\mu_{nf} \cdot V_m) + [j \times B] \tag{3.2}$$

$$\vec{j} = \sigma_{nf}\left(\vec{E} + \vec{V} \times \vec{B}\right) \tag{3.3}$$

For electrical potential the current density $\vec{j}$ can be written as:

$$\vec{j} = \sigma_{nf}\left(-\nabla\phi + \vec{V} \times \vec{B}\right) \tag{3.4}$$

Energy equation:

$$\nabla(\rho_{nf}.V_m.Cp.T) = k_{nf} + \nabla T + \frac{j^2}{\sigma_{nf}} \tag{3.5}$$

MHD model equations:

The magnetic induction equation can be derived from Ohm's law and Maxwell's equation as:

$$(\vec{V}.\nabla)\vec{B} = \frac{1}{\mu_0 \sigma}\nabla^2 \vec{B} + (\vec{B}.\nabla)\vec{V} \tag{3.6}$$

Where μ_0 and σ are the magnetic permeability and the electrical conductivity of the media. The electric potential equation is therefore given by:

$$\nabla^2 \varphi = \nabla(V \times B) \tag{3.7}$$

Where φ is the scalar potential.

3.2.2. Mixture

The mixture approach, based on a single fluid two-phase approach, is employed in the simulation by assuming that the coupling between phases is strong, and particles closely follow the flow. Each phase has its own velocity vector field, and use the governing equations of each phase separately.

It is also assumed that fluid and nanoparticles phases are in local thermal equilibrium in multi-phase mixture model. It means, mean temperature of the fluid phase and the nanoparticles phase are same. Under the above assumptions, the governing equations for the multi-phase mixture model can be expressed as:

Continuity equation:

$$\nabla(\rho_m . V_m) = 0 \tag{3.8}$$

Momentum equation:

$$\nabla(\rho_m . \vec{V}_m \vec{V}_m) = -\nabla\ \ p + \nabla \cdot \left[\mu_m (\nabla \vec{V_m} + \nabla \vec{V}_m^T) + \nabla \cdot (\sum_{k=1}^{n} \phi_k \rho_k \vec{V}_{dr,k}\ \vec{V}_{dr,k}) \right] + (\vec{j} \times \vec{B}) \tag{3.9}$$

Volume fraction:

$$\nabla(\phi_p \rho_p . \vec{V}_m) = -\nabla \cdot (\phi_p \rho_p \vec{V}_{dr,p}) \tag{3.10}$$

Energy equation:

$$\nabla(\phi_k V_k (\rho_k h_k + p) = \nabla \cdot (k_{eff} \nabla T - C_p \rho_m \vec{vt}) + \frac{j^2}{\sigma_m} \tag{3.11}$$

While considering ϕ is the volume fraction of phase k and $\vec{V}m$ the mass-average velocity, ρ_m mixture density, μ_m viscosity of the mixture, k_m mixture thermal conductivity coefficient and σ_m mixture electrical conductivity respectively and defined as:

$$\vec{V}_m = \sum_{k=1}^{n} \frac{\phi_k \rho_k \vec{V}_k}{\rho_m} \tag{3.12}$$

$$\rho_m = \sum_{k=1}^{n} \phi_k \rho_k \tag{3.13}$$

$$\mu_m = \sum_{k=1}^{n} \phi_k \mu_k \tag{3.14}$$

$$k_m = \sum_{k=1}^{n} \phi_k k_k \tag{3.15}$$

$$\sigma_m = \sum_{k=1}^{n} \phi_k \sigma_k \tag{3.16}$$

In the equation of conservation momentum $\vec{V}_{dr,k}$is the drift velocity for the secondary phase (the nanoparticles in the present study):

$$\vec{V}dr, k = \vec{V}_k k - \vec{V}_m \tag{3.17}$$

The slip velocity (relative velocity) is defined as the velocity of secondary phase (*p*) relative to the velocity of the primary phase (*f*)

$$\vec{V}_{pf} = \vec{V}_p - \vec{V}f \tag{3.18}$$

The drift velocity is related to the relative velocity

$$\vec{V}_{dr,p} = \vec{V}_{pf} - \sum_{k=1}^{n} \frac{\phi_k \rho_k}{\rho_m} \vec{V}_{fk} \tag{3.19}$$

In this study, the relative velocity is determined from Eq. (17) proposed by Manninen, Taivassalo [56] while Eq.(20) By Schiller and Naumann [57] is used to calculate the drag function f_{drag}.

$$\vec{V}_{pf} = \frac{\rho_p d_p}{18\mu_f f_{drag}} \frac{(\rho_p - \rho_m)}{\rho_p} \vec{a} \tag{3.20}$$

$$f_{drag} = \begin{pmatrix} 1 + 0.15\mathrm{Re}_p^{0.687} & \mathrm{Re}_p \leq 1000 \\ 0.0183\mathrm{Re}_p & \mathrm{Re}_p \succ 1000 \end{pmatrix} \tag{3.21}$$

Where the acceleration $\vec{a}$ is determined by:

$$\vec{a} = (\vec{V}m \cdot \nabla)\vec{V}_m \tag{3.22}$$

And d_p is the diameter of the nanoparticles of secondary phase, $\vec{a}$ is the secondary phase particle's acceleration, and p is the pressure.

Also, the buoyancy term in the momentum equations (3.2) and (3.9) is approximated (Fluent [58]) by

$$\rho(\rho - \rho_0)g \approx -\rho_0 \beta(T - T_0)g \tag{3.23}$$

Which is considered when Boussinesq approximation is taken into account for mixed convection case. Here this the thermal expansion coefficient of the fluid, ρ_0 and T_0 are the reference density and temperature respectively.

3.3 Turbulence modelling

In reality, no turbulence model which can be considered for all kinds of problems in the area of computational fluid dynamics exists. Hence, several factors can be considered in order to find a suitable turbulence model. Some of them are physics behind the flow field, the level of computational time and cost as well as accuracy.

Therefore, it's very important to understand the nature of turbulence models to be used in real-life applications. One of the objectives of this work is to assess the suitability of the various RANS based turbulence models in predicting the turbulent features of the nanofluids flowing through pipe.

Therefore, three different turbulent models called Realizable k-ε Standard k-ε and RNG k-ε models are considered and their performances are compared in this thesis. And it's shown the standard k-ε model with enhanced wall functions, it gave more accurate results for high Reynolds numbers than the other two k-ε turbulent models.

The standard k-ε model proposed by Launder and Spalding [59] introduces two new equations, one for the turbulent kinetic energy and the other for the rate of dissipation. The two equations can be expressed in the following form:

$$\nabla \cdot (\rho \vec{V} k) = \nabla (\frac{\mu_t}{\sigma_k} \nabla k) + G_k - \rho_\varepsilon \tag{3.24}$$

$$\nabla \cdot (\rho \vec{V} k) = \nabla (\frac{\mu_t}{\sigma_k} \nabla \varepsilon) + \frac{\varepsilon}{k} (C_1 G_k - C_2 \rho_\varepsilon) \tag{3.25}$$

Where0pp

$$\mu_t = \rho C_\mu \frac{k^2}{\varepsilon} \mu_t \tag{3.26}$$

$$G_k = \mu_t (\nabla V + (\nabla V)^T) \tag{3.27}$$

With C_1=1.44, C_2=1.92, C_μ=0.09, σ_k=1, σ_ε=1.3

3.4 Thermophysical Properties for Nanofluids

It is not easy to evaluate the thermophysical properties in nanofluids because we do not know which models might give us the most reliable results. We are often unaware of the ways the solutions are strongly affected by the thermophysical properties too. However, different types of models for nanofluids thermophysical properties are presented and published by many researchers. Nevertheless, categorisation of thermophysical properties of nanofluids still remains a matter of debate. Hence, no conclusion is drawn regarding the flow and heat transport applications because of its wide variety and intricacy. In this present analysis, thermophysical properties of density and heat capacitance of the nanofluids are calculated by using the following formulas which are considered as classical relationships between the base fluid and the nanoparticle.

3.4.1 Density

The density of the nanofluid is defined as:

$$\rho_{nf} = (1-\varphi)\rho_f + \varphi \rho_p \tag{3.28}$$

Where φ is the nanoparticles volume concentration, ρ_f and ρ_p are the density of the base fluid and nanoparticles respectively.

3.4.2 Specific Heat

For the heat capacitance of the nanofluid is defined as:

$$C_{nf} = (1-\varphi)C_f + \varphi C_p \tag{3.29}$$

Where Cf and Cp are the heat capacitance of the base fluid and the nanoparticles respectively.

3.4.3 Thermal Conductivity

among several proposition for the thermal conductivity of the nanofluid, a model proposed by Wasp, Kenny [60] is retained for case Fe3O4-H2O and Cu-H2O.

$$k_{nf} = k_f \left[\frac{k_p + 2k_f - 2\varphi(k_f - k_p)}{k_p + 2k_f + \varphi(k_f + k_p)} \right] \tag{3.30}$$

And for thermal conductivity of nanofluid Al_2O_3-H_2O a model given by Maiga et al [61]

$$k_{nf} = k_f((4.97\varphi^2) + (2.72\varphi) + 1 \tag{3.31}$$

Where k_f and k_p are the thermal conductivity of the base fluid and nanoparticles respectively.

3.4.5 Dynamic Viscosity

Brinkman [62], presented viscosity correlation for nanofluid defined as below:

$$\mu_{nf} = \mu_f \left(\frac{1}{(1-\varphi)^{2.5}} \right) \tag{3.32}$$

For dynamic viscosity of Al_2O_3-H_2O nanofluids is given by Maiga et al [61]

$$\mu_{nf} = \mu_f((123\varphi^2) + (7.3\varphi) + 1 \tag{3.33}$$

3.4.6 Electrical conductivity

For the electrical conductivity Shen, Wang [63] proposed a new model to describe the electrical conductivity of nanofluids based on the Maxwell model and considering the Brownian motion of particles and electrophoresis, can be written as the following:

$$\sigma_s = \sigma_M + \sigma_E + \sigma_B \tag{3.34}$$

Maxwell model for $\sigma_p \gg \sigma_0$ (highly conducting particles)

$$\sigma_M = \sigma_0(1+3\varphi) \tag{3.35}$$

- electrophoretic conductivity

$$\sigma_E = \frac{2\varphi\varepsilon_r^2\varepsilon_0^2U_0^2}{\mu r^2} \tag{3.36}$$

Here ε_r the relatively dielectric constant of the base fluid, ε_0 the dielectric constant of the vacuum $U_0$the nanoparticle Zeta potential, and r the nanoparticles radius.

- Brownian motion of particles

$$\sigma_B = \frac{3\varphi\varepsilon_r\varepsilon_0U_0^2}{r^{3/2}}\left(\frac{RT}{L\,3\pi\mu}\right)^{1/2} \tag{3.37}$$

The nanoparticle Zeta potential U0 = −40 mV, the average nanoparticles radius r = 18 nm and the dielectric constant of the fluid $\varepsilon_r = 80$ [64].

3.4.7 Properties for Nanoparticles

Three different nanoparticules have been used in the thesis, the Al_2O_3, Fe3O4 and copper nanoparticules.

The density, heat capacitance and thermal conductivity of Al_2O_3 are considered as [31]:

$$\rho_p = 3880\frac{Kg}{m^3}\ ;\ C_p = 733\frac{J}{KgK}\ ;\ K_p = 36\frac{w}{mK}$$

For iron oxide Fe3O4 are considered as [65]:

$$\rho_p = 5180\frac{Kg}{m^3}\ ;\ C_p = 670\frac{KJ}{KgK}\ ;\ K_p = 80.4\frac{w}{mK}$$

And for the copper nanoparticle (Cu) are considered as [10]:

$$\rho_p = 8954\frac{Kg}{m^3}\ ;\ C_p = 383.1\frac{J}{KgK}\ ;\ K_p = 401\frac{w}{mK}$$

3.5 Some Useful Definitions

In this section, Reynolds number, Darcy friction factor, local Nusselt number and heat transfer coefficient, average Nusselt number and turbulent intensity are defined and presented.

For the prediction of flow in a circular pipe, the Reynolds number is defined as:

$$\mathrm{Re} = \frac{\rho.v.D}{\mu} \tag{3.38}$$

Here, ρ is density of nanofluid, v is the mean fluid velocity, D is diameter of the pipe and μ is dynamic viscosity.

The Darcy friction factor and local Nusselt number are evaluated according to the following relations:

Darcy friction factor for turbulent flows in a circular pipe is defined as:

$$f = \frac{2\Delta P D}{L\rho\upsilon^2} \tag{3.39}$$

After balancing the pressure and shear forces the same expression takes the form:

$$f = \frac{8\tau_w}{\rho\upsilon^2} \tag{3.40}$$

Heat transfer coefficient and Nusselt number are defined as:

$$\bar{h} = \frac{q''}{T_w - T_b} \qquad \overline{Nu} = \frac{\bar{h}\cdot D}{k} \qquad Nu_{(x)} = \frac{h_{(x)}\cdot D}{k} \tag{3.41}$$

Where τ_w, ρ, υ,q″, h, D, k, Tw and Tb are shear stress on the wall, density of the fluid, velocity, heat flux, convective heat transfer coefficient, tube diameter, thermal conductivity of the fluid, wall temperature and temperature of the bulk, respectively.

The turbulent intensity can be defined as:

$$I = 0.16 \times \mathrm{Re}^{-\frac{1}{8}} \tag{3.42}$$

3.6 Introduction to Computational fluid dynamics (CFD)

Over the last twenty years, CFD has become a standard industrial simulation tool for the design, analysis, performance determination, and investigation of engineering systems involving fluid flows. CFD is a branch of fluid mechanics that uses numerical methods and algorithms to solve and analyse problems that involve fluid flows. Computers are used to perform the calculations required to simulate the flow.

With the high speed supercomputers, better solutions can be achieved. The accuracy of the numerical solutions is dependent on the quality of discretization used. CFD is finding its way into process, chemical, civil, and environmental engineering. Some of the important commercial CFD codes are: FLUENT, ANSYSCFX, ANSYS ICEM, STARCD, STARCCM, COMSOL, Open FOAM, KIVA, etc.

3.7 Advantages of CFD

CFD gives an insight into flow patterns that are difficult, expensive, or impossible to study using the traditional (experimental) techniques. The five major advantages of CFD over experimental fluid dynamics are given below:

- Lead time in design and development is significantly reduced.
- CFD can simulate flow conditions that are not reproducible in experimental tests.
- CFD provides more detailed information.
- CFD is increasingly more cost effective than wind tunnel testing.
- CFD produces lower energy consumption.

3.8 Presentation of fluent

Fluent is a numerical simulation program of compressible, incompressible, stationary or unsteady fluid flows involving various physical phenomena such as heat transfer, turbulence, chemical reactions, flows in rotating machinery, thermal engines, and for very complex industrial geometries. It is written in the C ++ programming language, modeled by the finite volume method.

It is used in several fields: Aeronautics, automotive, energy, process engineering and heat transfer. Like all CFD software, Fluent is composed of 3 modules corresponding to the different stages of a numerical study:

3.8.1 Pre-processor gambit

It allows us to represent the geometry of the system, and discretize the domain built using two or three dimensional mesh algorithms. The GAMBIT mesh generation options offer flexibility of choice. The geometry can be decomposed into several parts to generate a structured mesh, otherwise GAMBIT automatically generates an unstructured mesh adapted to the type of geometry built. It is also used to set boundary conditions and the type of materials (fluid, solid) in the flow domain.

3.8.2 Solver FLUENT

FLUENT solves the equations modelling the physical problem. It is based on solving the Navier-Stokes equations. The software offers numerous physical models resolve all the problems of fluid mechanics. One of the advantages of Fluent is the ability to create subprograms in C ++ (UDF) "User define function".

3.8.3 Post processor

It allows to display the geometry and the mesh of the domain, and especially to display the results obtained such as; velocity vectors, pressure, temperature, and turbulence. The PLOT menu offers the possibility of drawing curves and exporting the results in other formats for a more appropriate treatment.

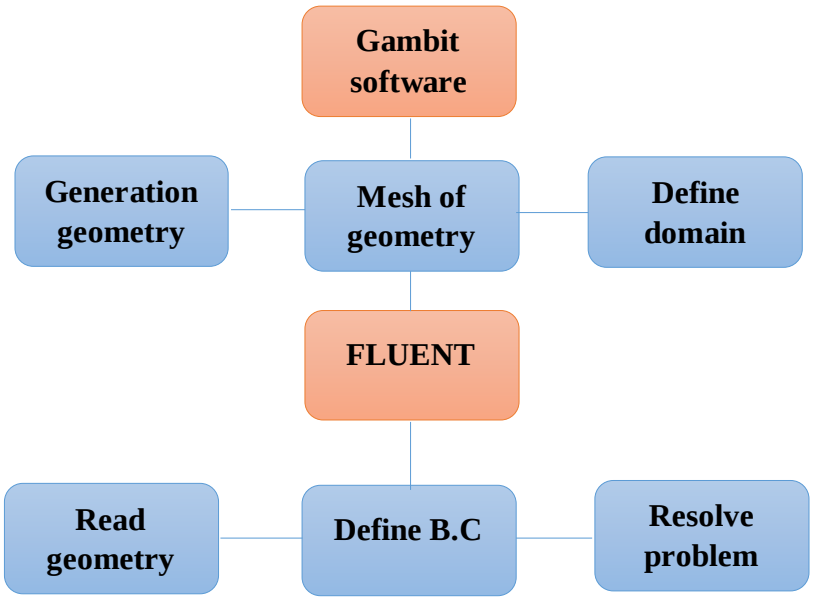


Figure 3.1 the steps of the simulation on gambit software and FLUENT

3.9 Summary of the Numerical Methods

The computational fluid dynamic code FLUENT was employed to solve the present problem. The Gambit preprocessor was used for creating geometry, meshing , define the boundary conditions and interpreted UDF, then the governing non-linear partial differential equations for the continuity, momentum, energy and other scalars such as turbulence and MHD, together with the suitable boundary conditions are discretized and hence solved by using the Finite volume solver Fluent 6.3.26. The pressure-based solver was used for the calculations.

The second order upwind scheme is used to obtain higher-order accuracy. The SIMPLE algorithm was chosen for the pressure-velocity coupling. All these equations are solved sequentially and iteratively so as to obtain a converged numerical solution. Different types of models like single phase and multi-phase mixture have been used throughout the thesis.

Simulation of nanofluids (Al_2O_3-H_2O) Flow in Heated Pipe

4.1 Introduction

The determination of forced convection heat transfer coefficient for flow of liquids such as water, ethylene glycol and oils have gained importance due to their diverse applications in the transfer of thermal energy. The analysis of such systems with single phase fluids for the estimation of heat transfer coefficients has been undertaken for a wide range of parameters and operating conditions. However, the performance of these equipment with conventional fluids in transferring heat has reached extremes. Studies for developing new thermal fluids for enhanced heat transfer capability have been initiated like a “nanofluid”.

In this chapter, we investigated numerically a forced convection of heat transfer with laminar and turbulent flow for water-Al2O3 nanofluid inside a circular tube under constant heat flux for laminar case and constant temperature for turbulent case.

The single phase models is employed to evaluate the developing laminar and turbulent forced convection flow in pipe. For this study nanofluids with size particles equal to 100 nm and particle concentrations of 1 and 4 % were used.

4.2 Geometry description

The considered geometrical configuration for both cases laminar and turbulent. It consists of a tube with length (L) of 1.0 m and circular section with the diameter (D) equal to 0.01 m as shown in figure 4.1

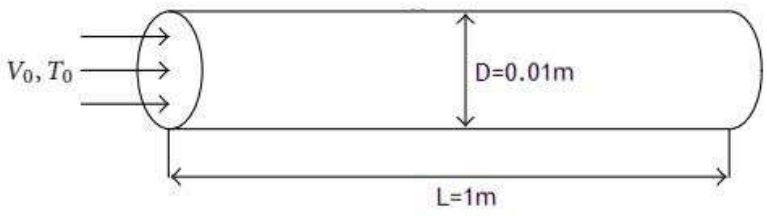


Fig 4.1: Schema of the configuration under investigation.

4.3 Boundary Conditions

The fluid has a uniform axial velocity v_0 as well as a uniform temperature (T_{in}= 293 K) at the pipe inlet section. At the exit section, a static gauge pressure, pgauge = 0, is specified.

On the pipe wall, a no-slip boundary condition is introduced with uniform heat flux, q" = 5000 W/m^2 for laminar case and for turbulent case a wall temperature have been stated at 350 K.

The calculations of thermo physical properties of nanofluids are taken at T_{in}. The specific details of these thermo physical properties of nanoparticle are given in Chapter 3.

4.4 Numerical method and the grid choices

The computational fluid dynamic is used to solve a laminar flow problem. The governing equations were discretized with the control volume technique. A first order upwind method was used while the SIMPLE procedure was introduced for solving iteratively the velocity–pressure coupling algebraic equations. The discretization grid is non-uniform in the radial and axial directions. The selected grid for the present calculations in all cases, consists of 400 and 10 nodes respectively in the axial and radial directions. The resolve numerical method for turbulent case was presented and detailed in chapter 3.

4.5 Validation and results discussion

Validation of the present numerical findings is done for nanofluid Al2o3-water against the existing data from literature for different Reynolds number and volume fraction. In the following, a numerical results of Nusselt number and friction factor are presented.

A numerical results of the average Nusselt number is compared with simulation data obtained by Moravej [31] and bianco [32] for laminar and turbulent flow respectively. It is observed that average Nusslet number results are in good agreement with the literature.

4.5.1 Laminar case

Results were obtained for the single-phase model and volume fraction (φ= 1, 4%), Reynolds number varied from Re 250 to 1050.

4.5.1.1 Average Nusselt number

In Figure 4.2, it shown the average Nusselt number behaviour for φ=1% and Reynlods number varied from 250 to 1050, a good accord is found with simulation result that given by Moravej [31] with average percentage error about 1.9%. The average Nusselt number for φ=4% is shown in Figure 4.3 and also in this case a good agreement with the data given by Moravej [31] with average percentage error 2.8%.

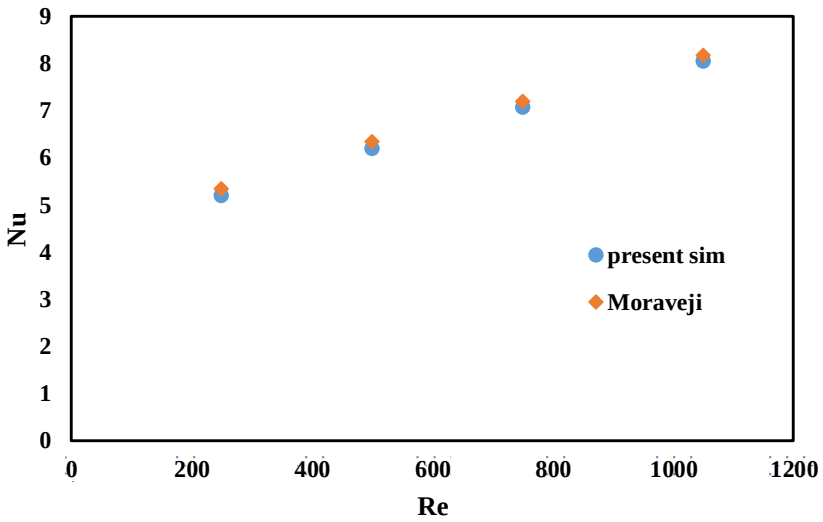


Fig 4.2. Nusselt number as a function of Re for φ=1%

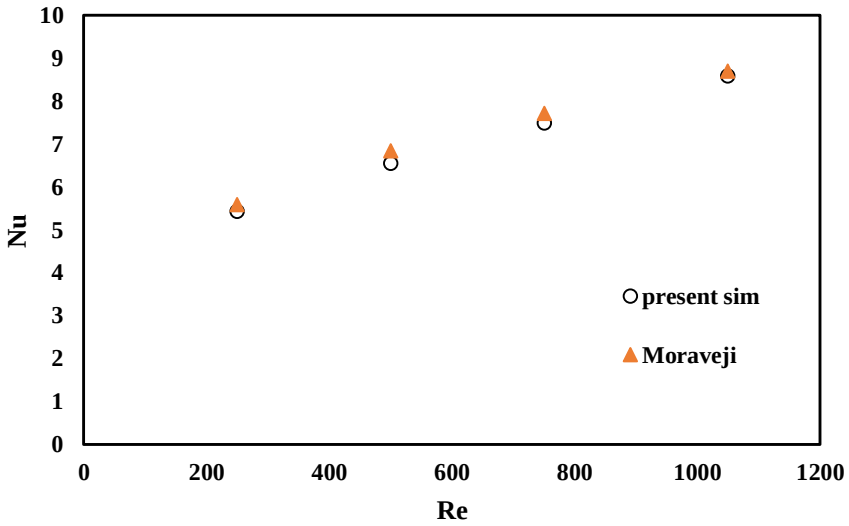


Fig 4.3. Nusselt number as a function of Re for φ=4%

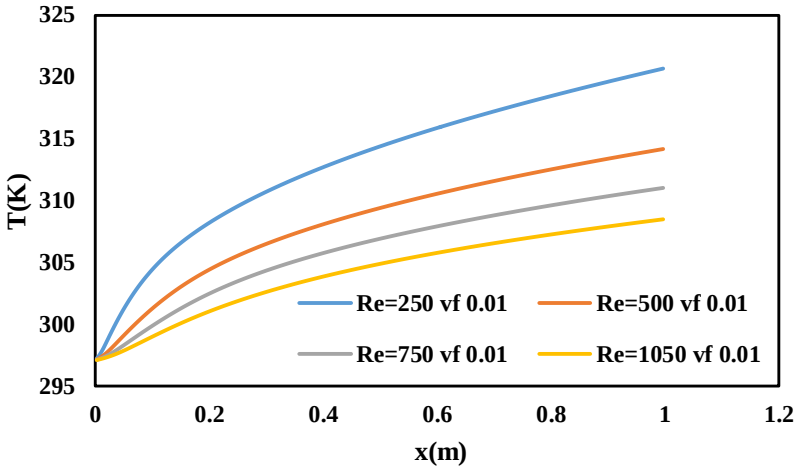


Fig 4.4 wall temperature along tube axis for volume concentrations 1% and for different Reynolds number

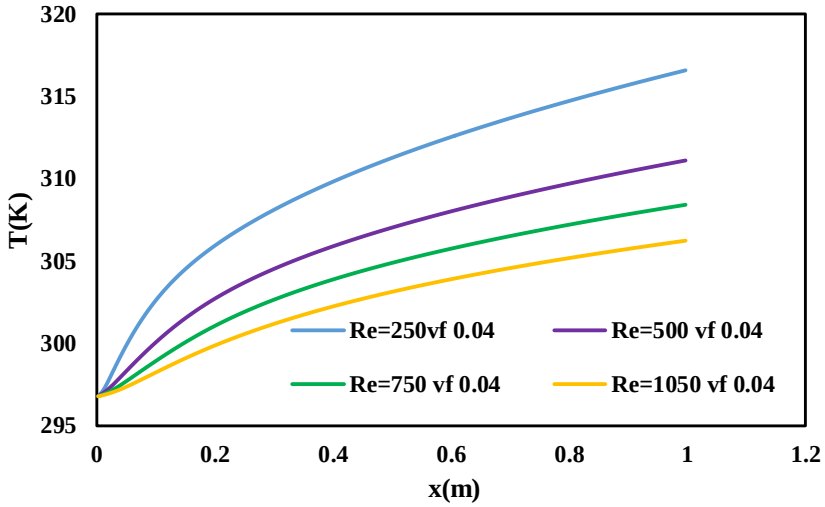


Fig 4.5 wall temperature along tube axis for volume concentrations 4% and for different Reynolds number

Figure 4.4 and 4.5 show the wall temperature along the tube length for different volume fraction and Reynolds number, it can be observed when volume fraction of nanoparticules increase the fluid temperature at the tube wall decrease. These results have obviously indicated the beneficial effect due to the nanoparticles, an effect that may be explained by the fact that with the presence of these particles, the thermal properties of the resulting mixture have been greatly improved.

Figure 4.6 show the effect of nanoparticules volume fraction on heat transfer coefficient along the pipe for Re=250. The heat transfer coefficient is always found maximum near the entrance

region. Then it starts to decrease rapidly with the axial distance until a minimum value. Also it observed that the increase of volume fraction of nanoparticles enhance the convective heat transfer coefficient. We can explain that increment of the heat transfer by increasing the thermal conductivity of the nanofluid, so the contact of the particles on the wall of the tubes leads to an increase in fluid temperature and heat transfer.

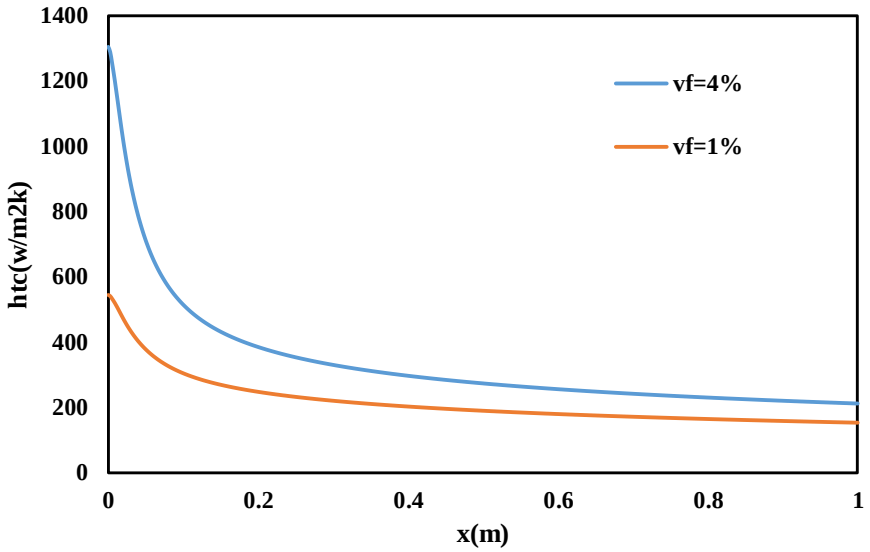


Fig 4.6 heat transfer coefficient along tube length for Re=250 and φ=1%, 4%.

4.5.1.2 Friction factor

Figure 4.7 shows the friction factor for nanofluid in tube versus Reynolds number. As shown in this figure, the friction factor decreased with increasing the Reynolds number. Also, in the same Reynolds number, the Friction factor of nanofluid enhanced slightly when the nanoparticle concentration increased. And therefore it has a poor effect on the quantity of pressure drop in the tube. We can explain that increment of the friction factor by the presence of nanoparticles may lead to create more viscous force on the walls of channel, which is due to increase in viscosity of nanofluid. Though the concentration of nanoparticle is less but some of the nanoparticles may get adhere to the walls of channel which may create more disturbance leading to increase the friction factor between the walls of channel and flowing fluid.

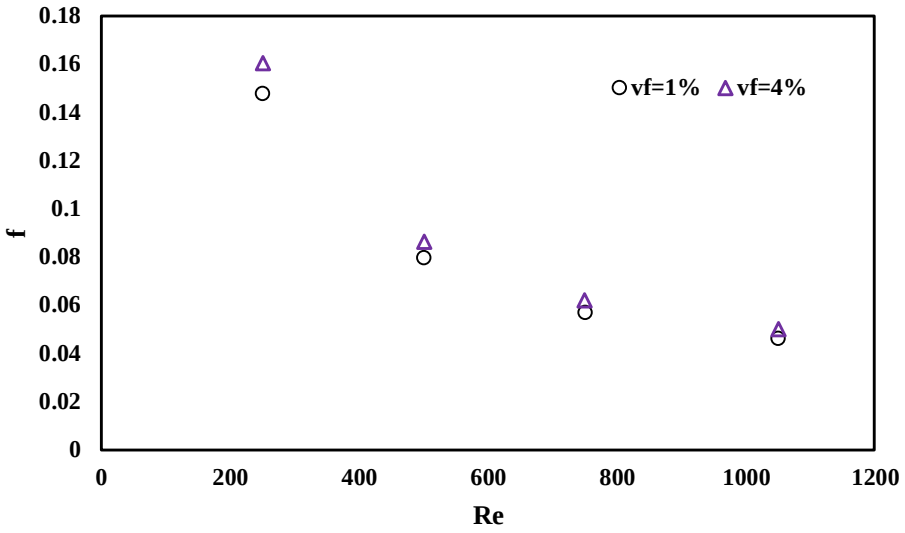


Fig 4.7 Simulation results for friction factor as function of Reynolds number.

4.5.2 Turbulent case

Results were carried out employing the single-phase model and volume fraction (φ= 1, 4%), Reynolds number varied from Re 20000 to 80000. From the comparisons presented in the section above, we can conclude that our computational model is producing the correct outcomes.

4.5.2.1 Average Nusselt number

In Figure 4.8, it shown the average Nusselt number behaviour for φ=1% and Reynlods number varied from 20000 to 80000. The obtained result from CFD simulations are in close agreement with the data presented by Pak [40] and Bianco [32], with average percentage error around 3%.

In figure 4.9 shows a comparison of the average Nusselt number obtained by numerical simulation with the values determined by Pak [40] and Bianco [32]. It can be detected a good agreement among the results with average percentage error about 1.4%. Also the results shows the increase of volume fraction lead to increase the Nusselt number.

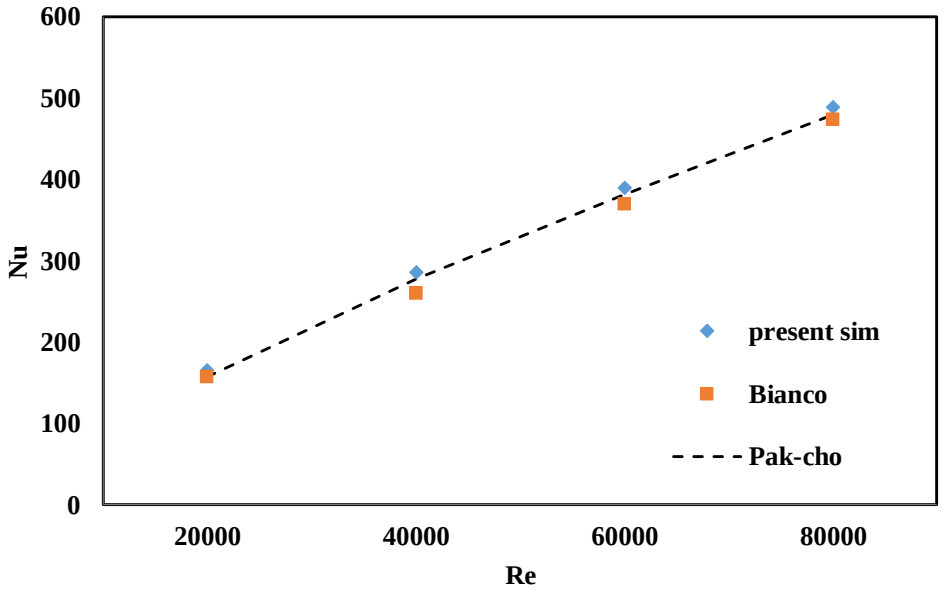


Fig 4.8. Nusselt number as a function of Re for φ=1%

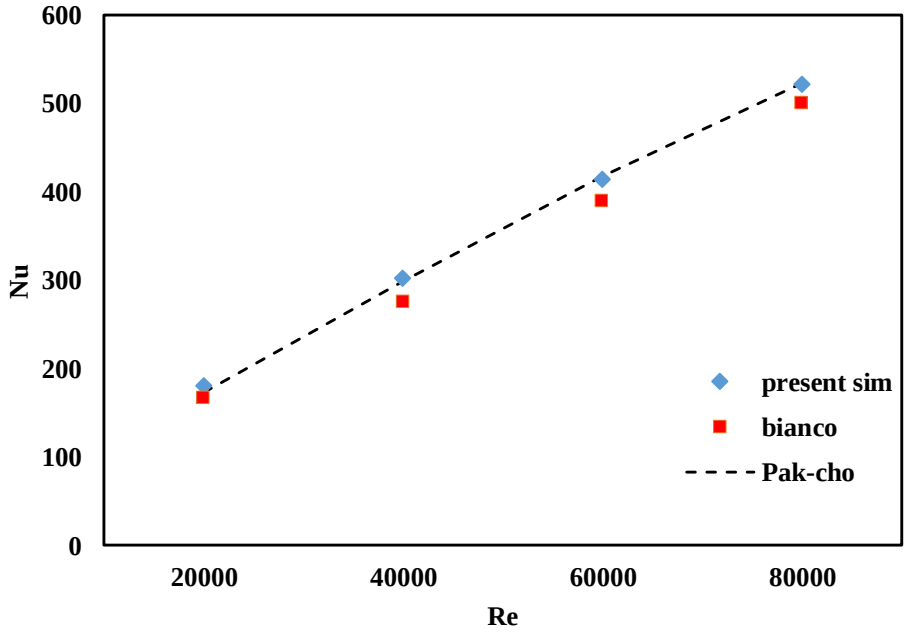


Fig 4.9. Nusselt number as a function of Re for φ=4%

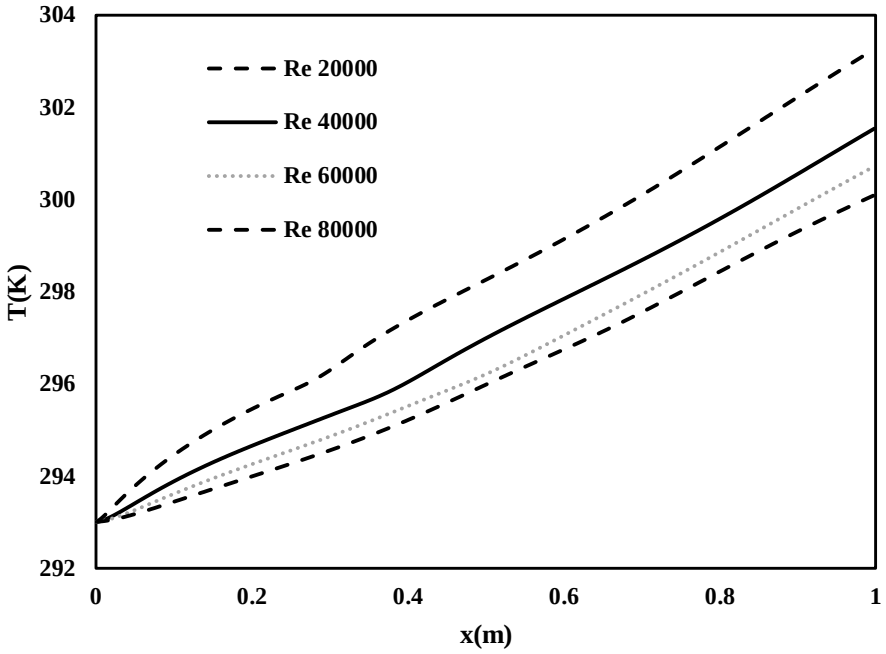


Fig 4.10 Profiles of bulk temperature along tube axis for volume concentrations 1%

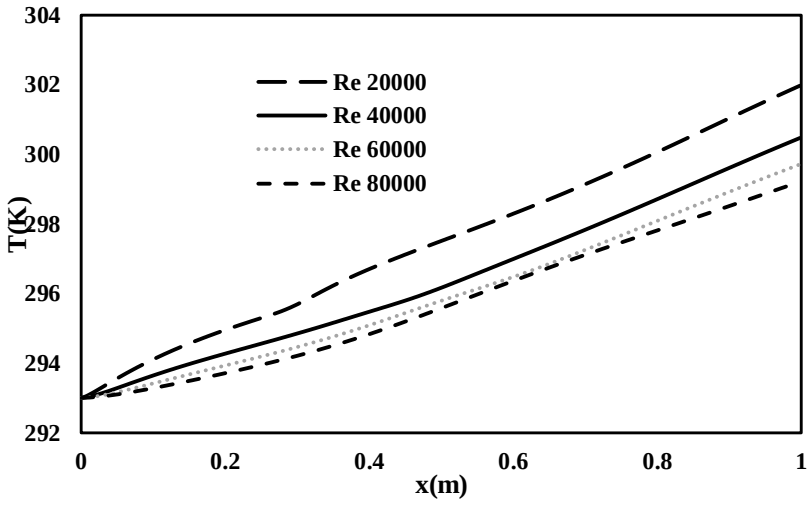


Fig 4.11 Profiles of bulk temperature along tube axis for volume concentrations 4%.

Figure 4.10 and 4.11 represent the bulk temperature along tube axis for several concentration and values of Reynolds number varied from 20000 to 80000. The bulk temperature of the nanofluid decreases as Reynolds number increases.

The effect of Reynolds number is strong passing from Re = 2.0×10^4 to Re = 4.0×10^4 and becomes weaker for higher values. Also it observed a decrease of the bulk temperature at the increase of the concentration of the nanoparticles. This might be explained with the fact that at the increase of the concentration corresponds an increase of the Nusselt number, as shown in Fig. 4.8 and fig 4.9. The increase of Re corresponds an increase of Nu, which in turn causes a further decrease of the bulk temperature.

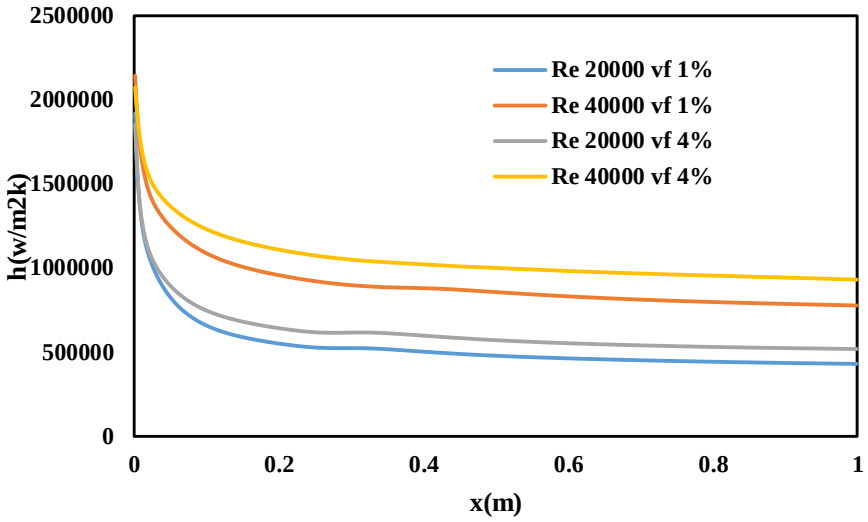


Figure 4.12 Heat flux for several concentration and Reynolds number.

Heat transfer on the wall of the tube is reported in Figure 4.12 for Re 20000 and Re 40000 and for all the concentrations. The heat transfer coefficient is found maximum value at the inlet and then start decreases along the tube axis, because the temperature on the wall is constant, whereas the bulk temperature increases, causing the decrease of the transferred heat flux.

Also it is detected that heat transfer is augmented at the increase of particles concentration. This effect is due to the increase of the thermal conductivity of nanofluids, which provokes an enhancement of the heat transfer. As expected, heat transfer at Re 40×10^4 is higher than the one at Re 20×10^4, but they show a similar trend.

4.5.2.2 Friction factor

Figure 4.7 shows the friction factor for nanofluid in tube versus Reynolds number and several volume concentration. As shown in this figure, the friction factor decreased with increasing of

Reynolds number and the nanoparticles volume concentrations have an insignificant effect on the enhancement of the friction factor.

It is possible to draw a conclusion, the slight increase of friction factor can lead to increase a little in pumping power. And for that the heat transfer can enhanced without loss in energy cost and be more effectiveness in practical applications.

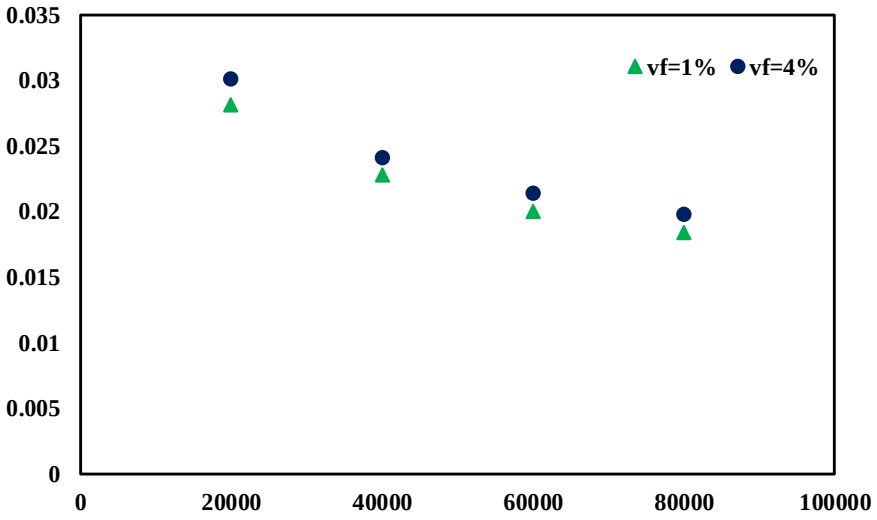


Fig 4.13 Simulation results for friction factor as function of Reynolds number.

4.6 Conclusion

In this chapter, a numerical investigations have been carried out to understand heat transfer and friction factor behaviour of Al_2O_3 nanofluids in a horizontal circular pipe under laminar and turbulent flow condition. The effects of Reynolds number and nanoparticles volume concentration on heat transfer are investigated. According to our findings, following conclusion can be made and summarised as follows:

a) The Numerical modelling based on the computational fluid dynamics method with the Single phase approach is employed for both laminar and turbulent flow. The CFD results showed a good agreement with available literature.
b) Heat transfer enhance by increasing the volume concentration of nanoparticles in nanofluid and Reynolds number.
c) The friction factor increased with decreasing the Reynolds number but raising the volume concentration has a slight effect on friction factor.

Simulation of Fe3O4 magnetic nanofluid with presence of magnetic field

5.1 Introduction

In this chapter, numerical investigations are carried out using single phase approach (SP) and mixture approach (MP) to analyze the thermal of the considered nanofluid (Fe3O4/water) with presence of magnetic field. Here, two-dimensional axi-symmetric model of a horizontal pipe with the length L of 1.7m and circular section with the diameter D equal to 0.014 m. The geometry is shown in Fig. 5.1.

The main objective of this research is to analyze the effects of different nanoparticles size and concentrations with and without the Brownian motion of nanoparticles on heat transfer under transition flow condition. Besides, the effect of turbulent flow nanofluid containing magnetic nanoparticle (Fe3O4) with average diameter (d=36 nm) in a horizontal tube is investigated by using CFD tools. The aim of our study is to examine the effect of flow rate and nanofluid concentration on the Nusselt number and friction factor in a system with the influence of magnetic field.

Finally, results are presented in terms of local and average Nusselt number, Darcy friction factor and pressure drop.

5.2 Choice of turbulence model

In this investigation three different turbulence models Realizable k-ε, Standard k-ε and RNG k-ε have been compared with each other are shown in Fig. 5.2. As we can see below, the error percentage for Standard k-ε, realizable k-ε and RNG k-ε is 8.93%, 14.44% and 9.72% respectively. Since the standard k-ε model with enhanced wall functions gave accurate results for the high Reynolds number then this model is selected for this work.

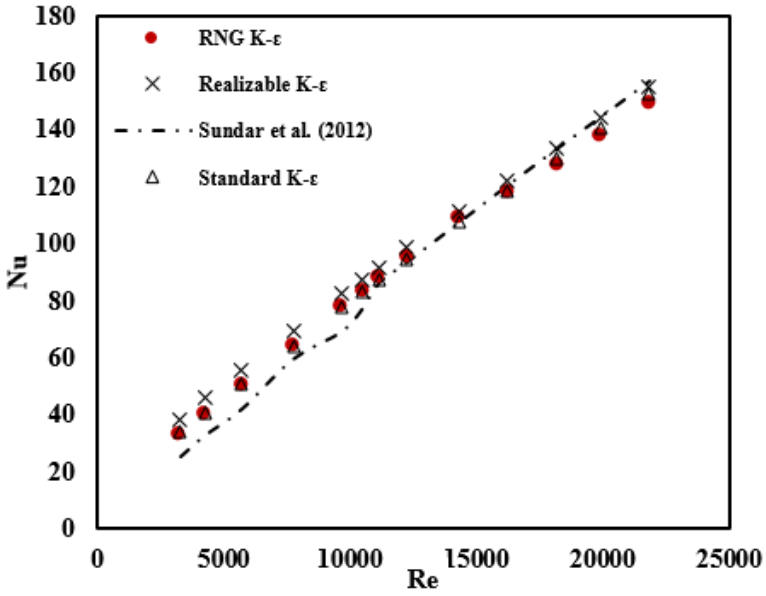


Fig. 5.2 tested of three turbulence models

5.3 Boundary Conditions

The following boundary conditions are used to solve the system of nonlinear partial differential equations which are given in chapter 3.

At the pipe inlet, a uniform velocity v as well as a uniform temperature ($T_{in} = 303K$) with a turbulent intensity (I = 4 to 6%) and hydraulic diameter (D = 0.014m) are stated. And, all the thermal properties used in this work are calculated at the inlet temperature T_{in} that also is considered to be the reference temperature.

At the pipe outlet, a static gauge pressure Pgauge = 0 is used. And On the pipe wall, a non-slip boundary and uniform heat flux boundary conditions have been implemented with a value of 1000 W. The enhanced wall treatment was chosen for near-wall treatment. Reynolds number varied from 3000 to 25000 at each step of iterations as input data. In the MHD module we used the add-on module that can be loaded by ANSYS fluent, and the insulation boundary condition used for the wall in both single and mixture phase approaches. The magnetic field B for electrical potential and magnetic induction are applied. Also an UDF was interpreted on FLUENT to define the electrical conductivity of the nanofluid.

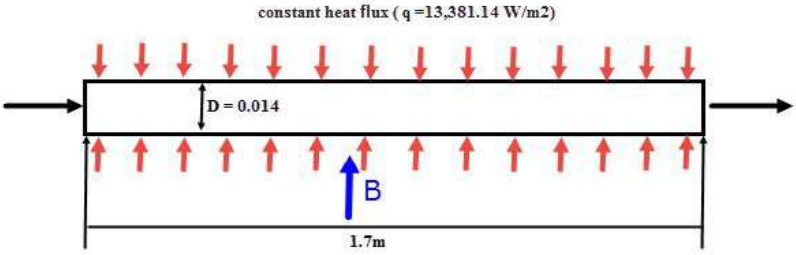


Fig. 5.1 Pipe schema

5.4 Grid Sensitivity Test

To obtain an accurate result a grid sensitivity analysis is done using the Standard k-ε. This is applicable to resolve both the velocity and the temperature fields inside the horizontal pipe. The grid sensitivity test is done by varying the total number of grid distributions in both the axial *(Nx)* and the radial *(Nr)* directions. Here, two different grid combinations such as 14×340 and 28×680 are used.

It is observed that the grids 14 × 340 and 28 × 680 generate the most reasonable results because the differences found among the results are quite insignificant. In order to save the computing time and to avoid any inconsistencies in the numerical results, particular grid for the present calculations is selected to be consisted of 14 and 340 nodes along the axial and the radial directions respectively. Fig. 5.3 represent Nu number simulation data of water for two meshes, the results are very close to the experimental (Sunder) [51] and proposed correlation by Notter Rouse [66]. 28×680 grid has percentage error around 7.63%, and for 14×340 grid has percentage error 8.93%.

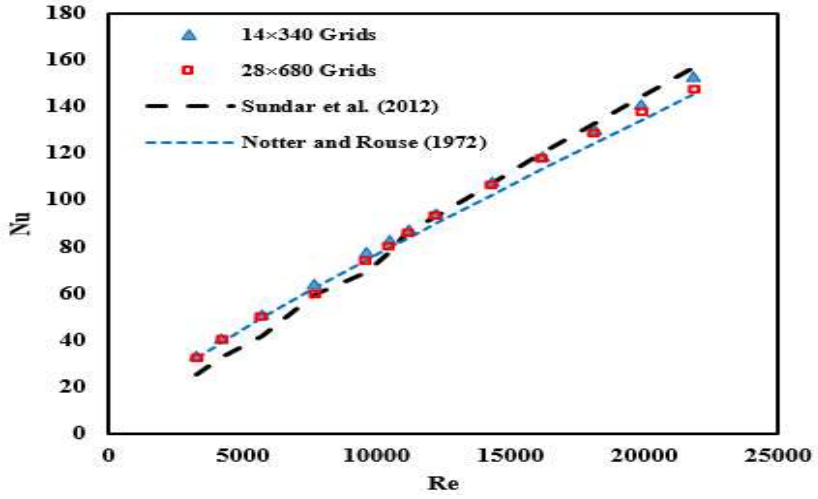


Fig. 5.3 grid test with experimental (tested with water)

In order to save the computing time and to avoid any conflicts in the numerical results, particular grid for the present calculations is selected to be consisted of 340 and 14 nodes along the axial and the radial directions respectively Fig 5.4 represent the selected mesh.

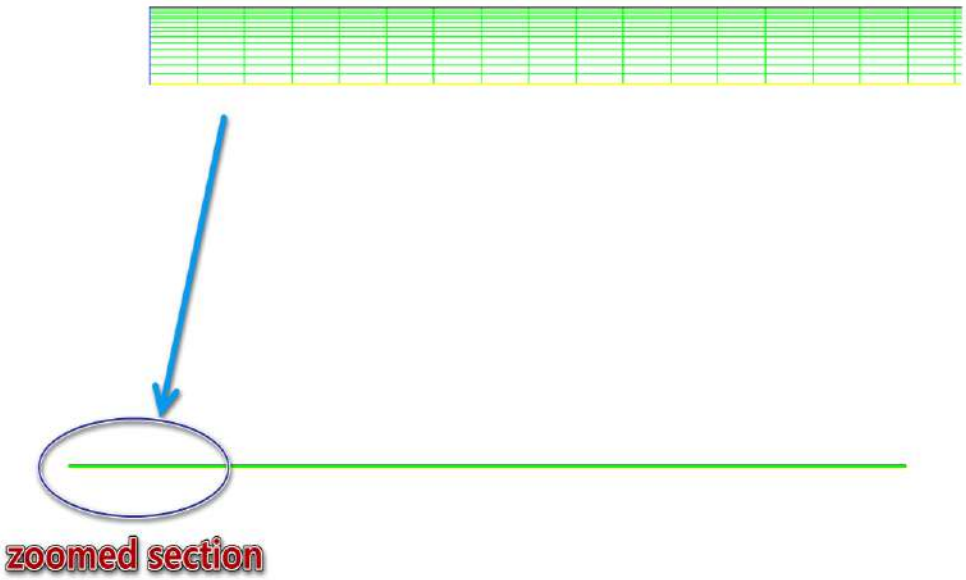


Fig. 5.4 grid 14×340

5.5 Validation

In order to demonstrate the validity and also the precision of numerical results for nanofluid and water a comparisons with the previously published experimental results has been done.

Firstly, in the following, numerical results of Darcy friction factor are presented and compared with different correlations as well as numerical results for different Reynolds number. Details are given below:

Fig. 5.5 displays comparison of the friction factor between present work and the literature for water. The Reynolds number varied from 10^4– 4.10^4, and it is observed from the results that the simulation and literature from Ahsan [67] and Moody [68]) are in very good agreement with minimum error 0.036 % and maximum error 2.01%.

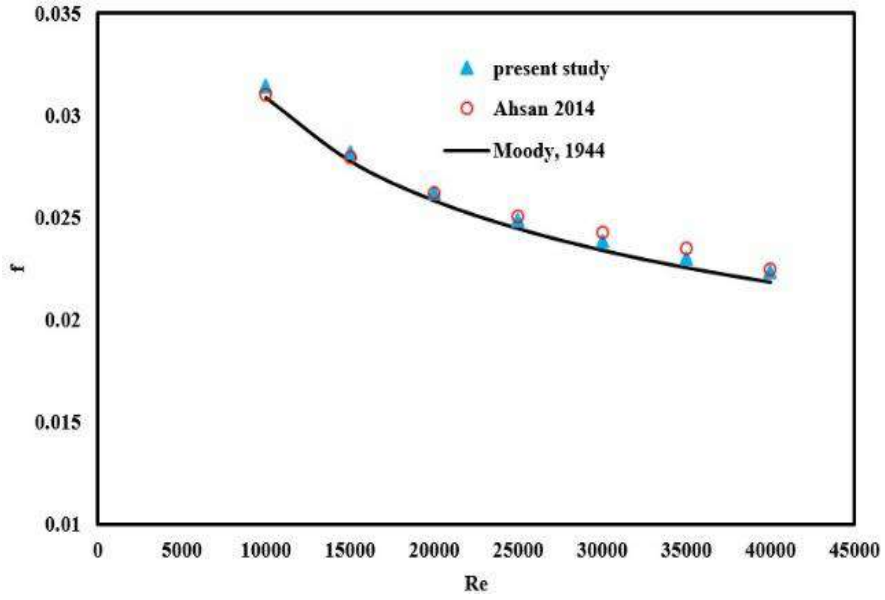


Fig. 5.5 Comparison of friction factor with literature (Ahsan [67] , Moody [68]) and computed values for water.

Secondly, numerical results of the Nusselt number and friction factor are compared with the experimental data by Sunder [51] for a Fe3O4 – water nanofluid, using the two approaches (SP) and (MP).

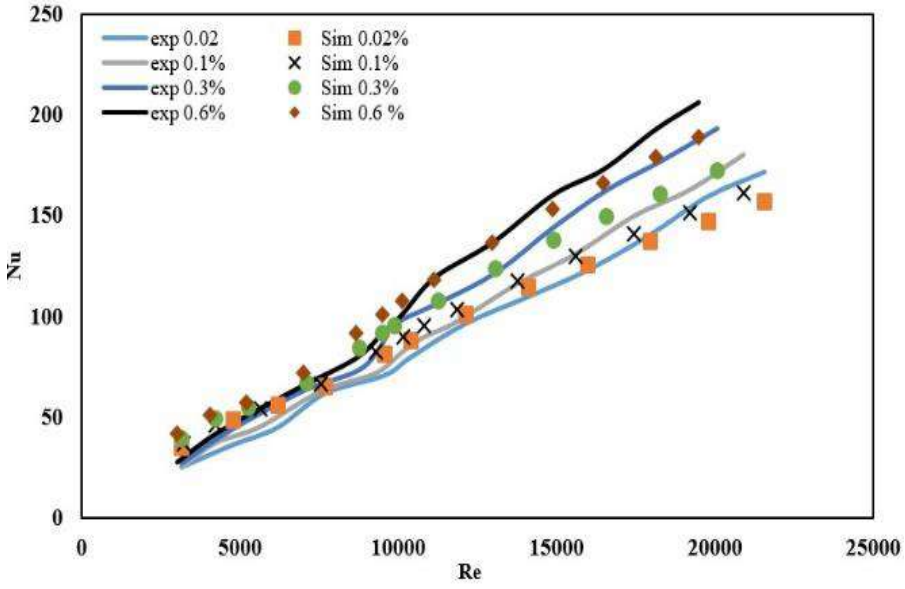


Fig. 5.6 Comparison of the average Nusselt using single phase approach with the experimental data of Sunder [51]

Fig. 5.6 represent a comparison between the present result and that of Sunder [51] is shown graphically for the nanofluid (Fe_3O_4–H_2O) volume fraction φ= 0.02, 0.1, 0.3 and 0.6% and Reynolds number Re 3000 to 22000. It is observed the increasing of Re number and volume concentration led to increase the value of Nusselt number.

The average percentage error for single phase approach 0.02, 0.1, 0.3 and 0.6% are 13.4%, 11.8%, 11.3% and 12.1% respectively.

In Fig. 5.7 Comparison of mixture approach with the same experimental data, the maximum average percentage error is 12.80% in volume fraction 0.02%.

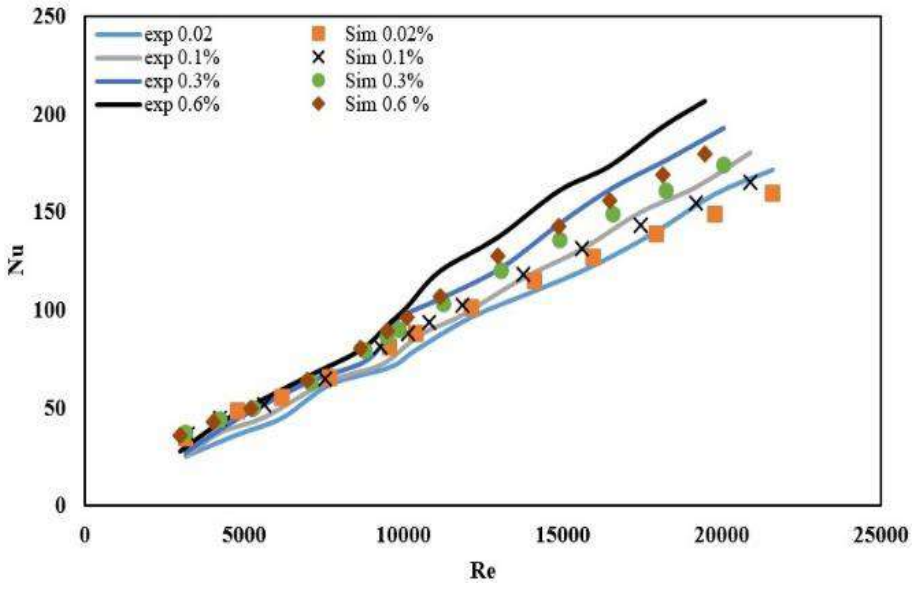


Fig. 5.7 Comparison of the average Nusselt using mixture approach with the experimental data of Sunder [51].

Fig. 5.8 and Fig. 5.9 show a comparison of friction factor using the two approaches. It can be observed friction factor decreased with increasing the Reynolds number. The average percentage error for single phase approach 0.02, 0.1, 0.3 and 0.6% are 5.20%, 6.9%, 3.8% and 10.5% respectively. And for the mixture approach 0.02, 0.1, 0.3 and 0.6% are 4.5%, 6.2%, 4.2% and 10.5% respectively.

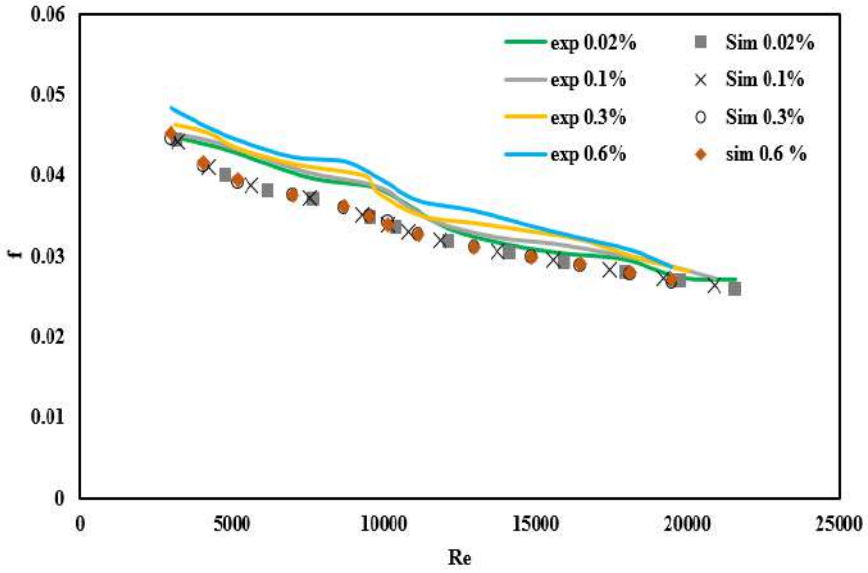


Fig. 5.8 Comparison of friction factor using single phase approach with the experimental data of Sunder [51].

It is shown that the present numerical results are in good agreement with experimental data of heat transfer and friction factor especially in high Reynolds number.

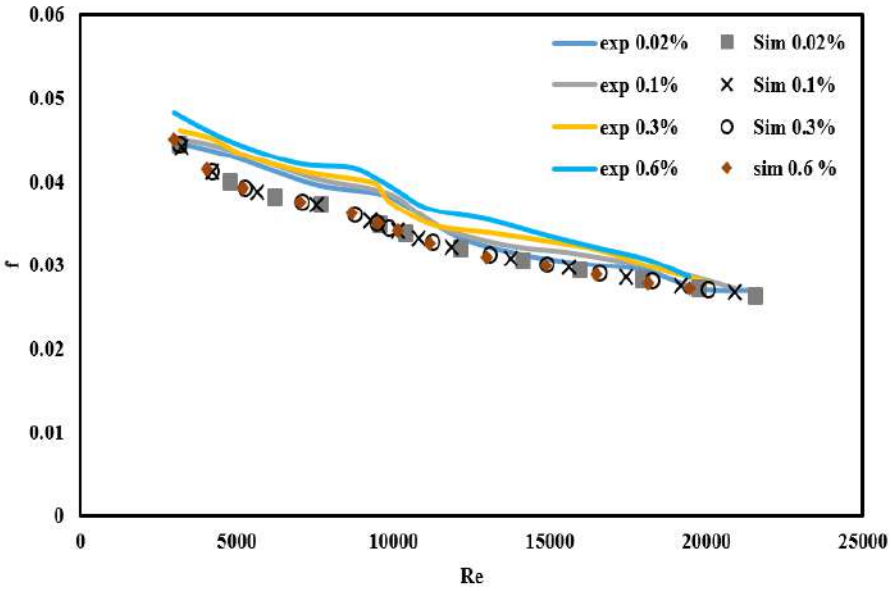


Fig.5.9 Comparison of friction factor using mixture approach with the experimental data of Sunder [51].

Average error of friction factor and Nusselt number for the two approaches are summarized in table 5.1, as we can see the mixture approach show less error.

φ	0.02%		0.1%		0.3%		0.6%	
	SP	MP	SP	MP	SP	MP	SP	MP
Nu	13.4	12.8	11.8	9.5	11.3	8	12.1	8.8
f	5.2	4.5	6.9	6.2	3.8	4.2	10.5	10.5

Table 5.1 Average error (%) of friction factor and Nusselt number for the two approaches

5.6 Results and Discussion

Extensive numerical simulations are performed using the single phase and mixture approaches for Fe3o4 water nanofluids with Re= 7000, 9500 and volume concentrations φ = 0.3, 0.6 %. The effect of magnetic field B (2, 5, 7.5, 10 T) on velocity, local Nusselt number, friction factor and pressure drop are discussed in the following sections.

5.6.1 Effect of magnetic field on velocity

Fig. 5.10 represents fully developed turbulent flow velocity profile at the outlet for Re=7000 and volume fraction φ= 0.6% for the two approaches.

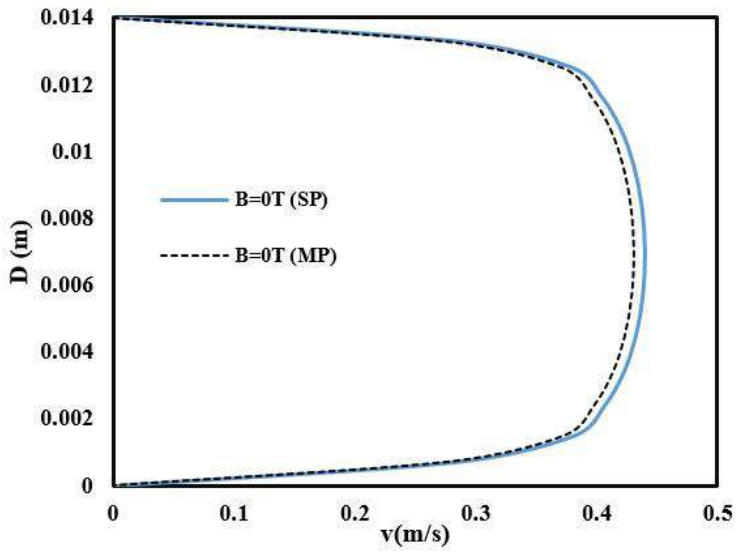


Fig.5.10 fully developed velocity profile at outlet for turbulent flow (Re=7000, Ø=0.6%)

Fig. 5.11 represents the velocity at the center of the pipe (Re = 7000 and ∅= 0.6%) under the effect of magnetic field (B) values as B=0 T, B= 5 T, B= 7.5 T, B= 10 T were compared at 1.7 m thermal fully developed region of the pipe length.

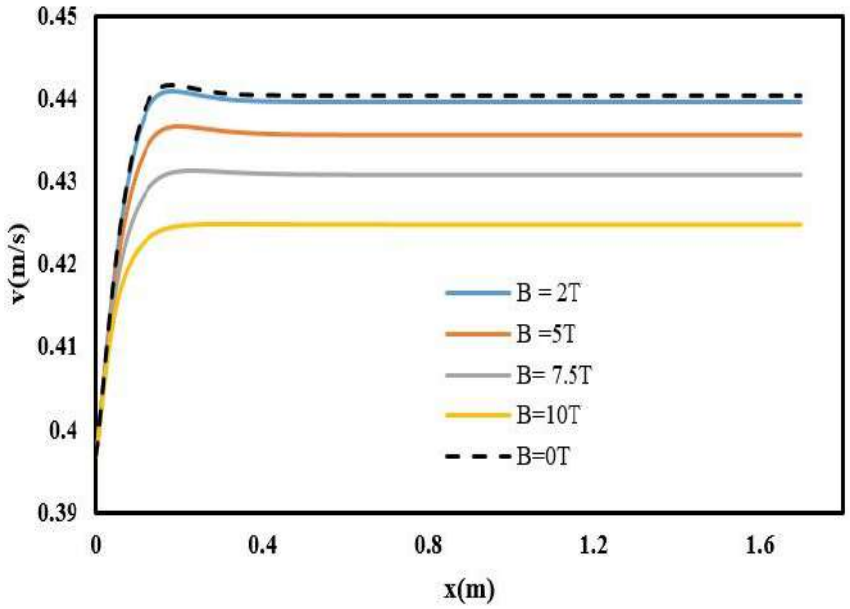


Fig. 5.11 Effect of magnetic field on the velocity at the center of the pipe, Re =7000 and 0.6% (SP).

The Results clarified that if the magnetic field is increased the velocity profile is decreased. B= 0 T was accepted as a reference state and achieved a statistical analysis to identify the decrease of local velocity values. For B=2T almost there is small decrease 0.19%, this is can be explained by the low volume fraction and the big domain of calculation, but when applying a stronger magnetic field the reduction of velocity can be observed. Decreasing of local velocity values specified for the B= 5 T was approximately about 1.08%, for B = 7.5 T was 2.23% and for B = 10 T was 3.64%.

Fig. 5.12 represents the influence of magnetic field that obtained from electrical potential and shows approximately the same decrease that represented by magnetic induction previously. So the increase in the magnetic field reduces the velocity profiles due to the opposite Force 'Lorentz force' that applied in the inverse direction of the flow.

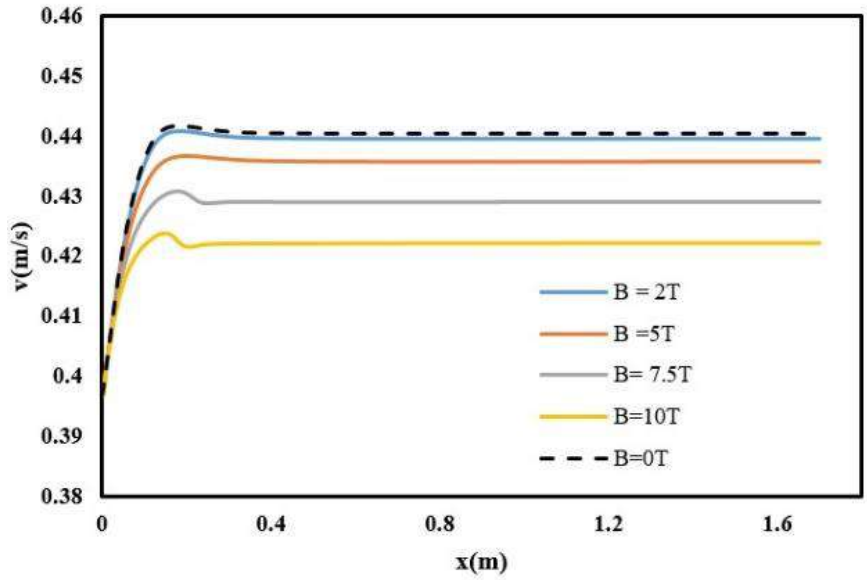


Fig. 5.12 Effect of magnetic field (electrical potential) on the velocity at the center of the pipe Re 7000 and 0.6% (SP)

Fig. 5.13 shows the effect of magnetic field on the velocity at the center of the pipe using the mixture approach, as a comparison with data that obtained from single phase approach it can be observed more decrease of the velocity for the B= 2 T was about 0.72%, for B = 5 T was 6.28%, for B=7.5T was 8.17% and for B = 10 T was 9.79%.

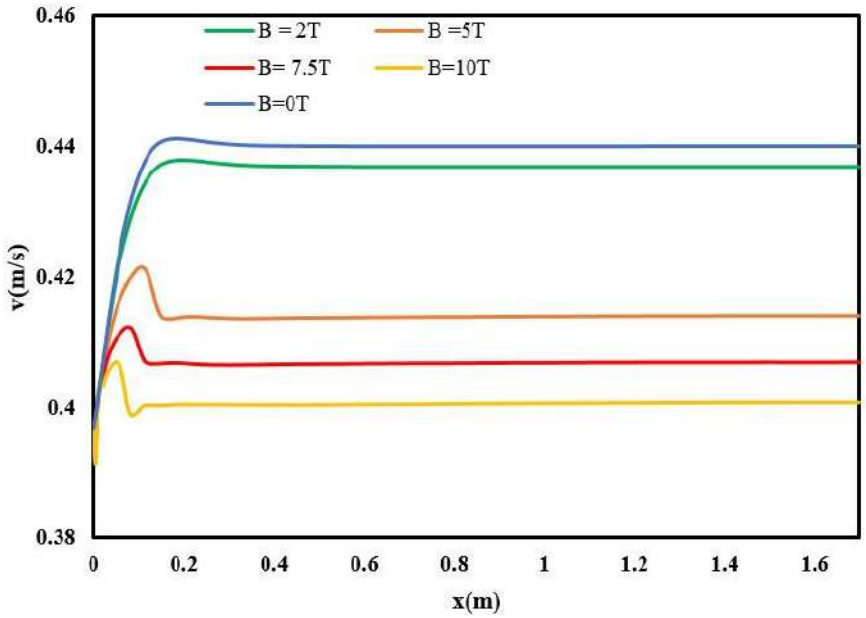


Fig. 5.13 Effect of magnetic field (electrical potential) on the velocity at the center of the pipe Re 7000 and 0.6% (MP).

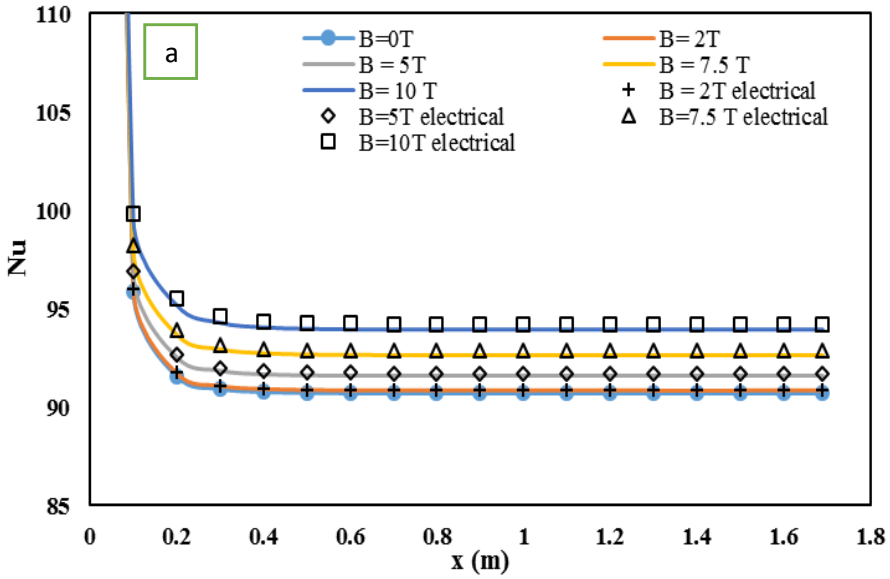
5.6.2 Effect of magnetic field on Nusselt number

Fig. 5.14, Fig 5.15 and Fig 5.16 represent the influence of magnetic field on Nusselt and Reynolds number for different volume fraction 0.3% and 0.6%. When the magnetic field is applied to fluid flow, Nu number has largely increased compared to Nu without magnetic field. This heat transfer becomes large with increasing of magnetic field.

For 0.3% and Re 9800 in Fig. 5.14 a slight enhanced of Nu can be seen at B=10T, the value was 3.6% in the single phase and 9% in the mixture.

In Fig.5.15 the increase of Nu at B=2T is not remarkable in both single phase and mixture approach, the value was 0.45% and 1.72% respectively, but when we augmented the magnetic field we observed that there is enhancement of heat transfer. In the single phase (electrical and magnetic) B=5T, 7.5T and 10T, the value was 2.5%, 5.04% and 7.68% respectively. For the mixture B=5T, 7.5T and 10T, the value was 8.72%, 10.85% and 13.89% respectively.

In Fig. 5.16 the maximum increasing at B=10T was 6.54% in single phase and 11.54% in mixture for volume fraction 0.6% and Re 9500.



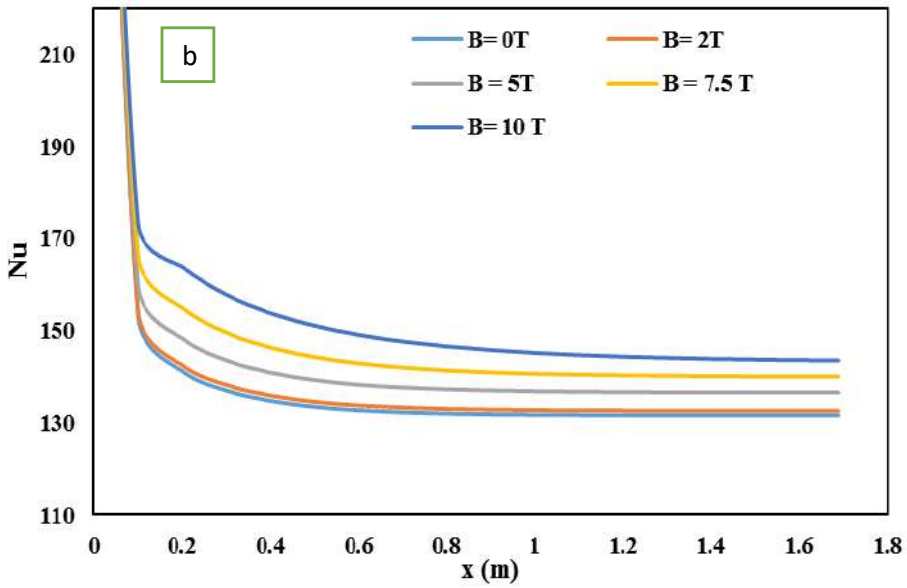
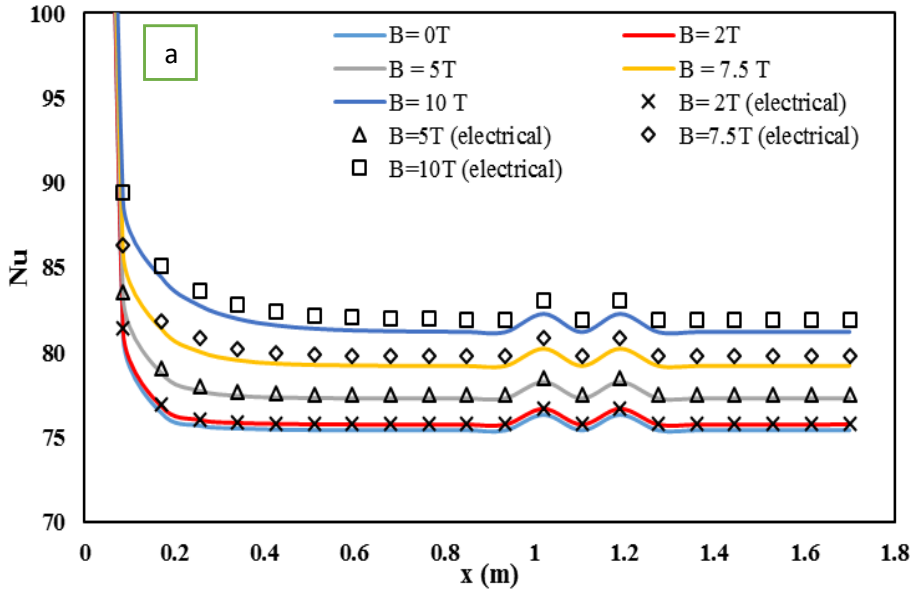


Fig. 5.14 Effect of magnetic field on Nusselt number Re9800 and 0.3% (a-SP, b-MP)



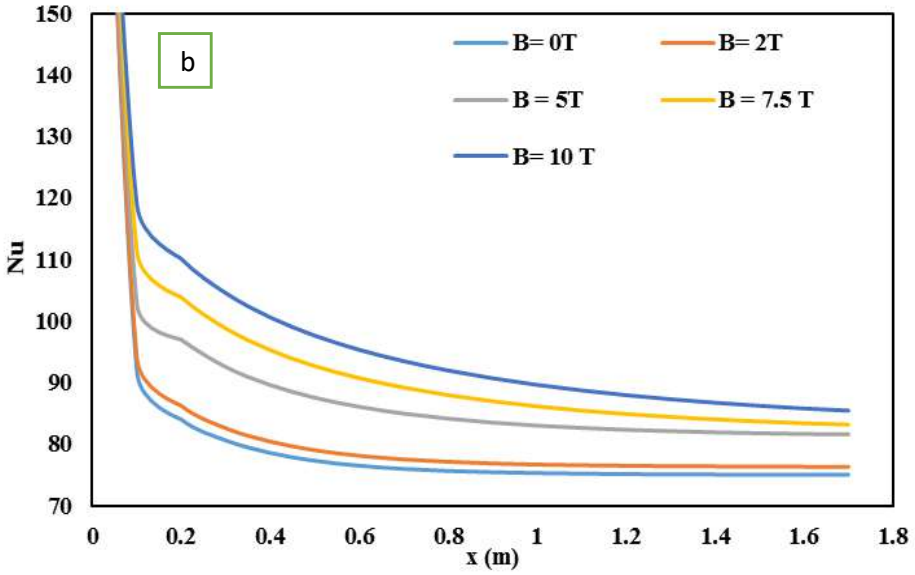
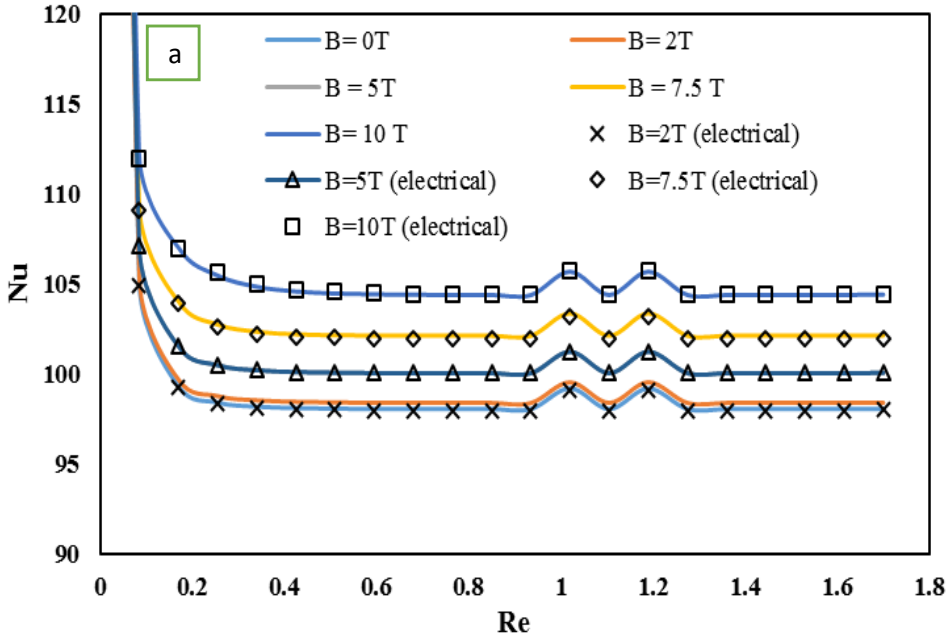


Fig. 5.15 Effect of magnetic field on Nusselt number Re 7000 and 0.6% (a-SP, b-MP)



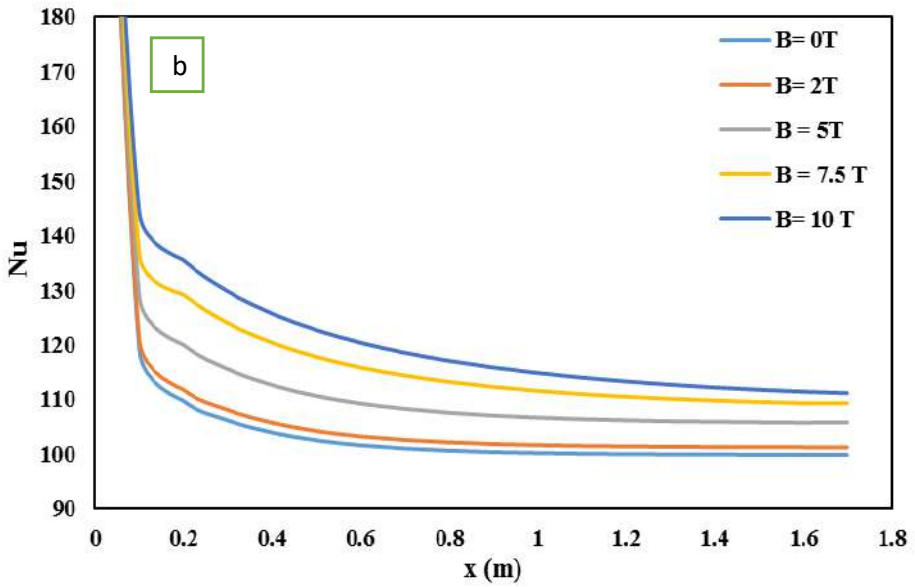
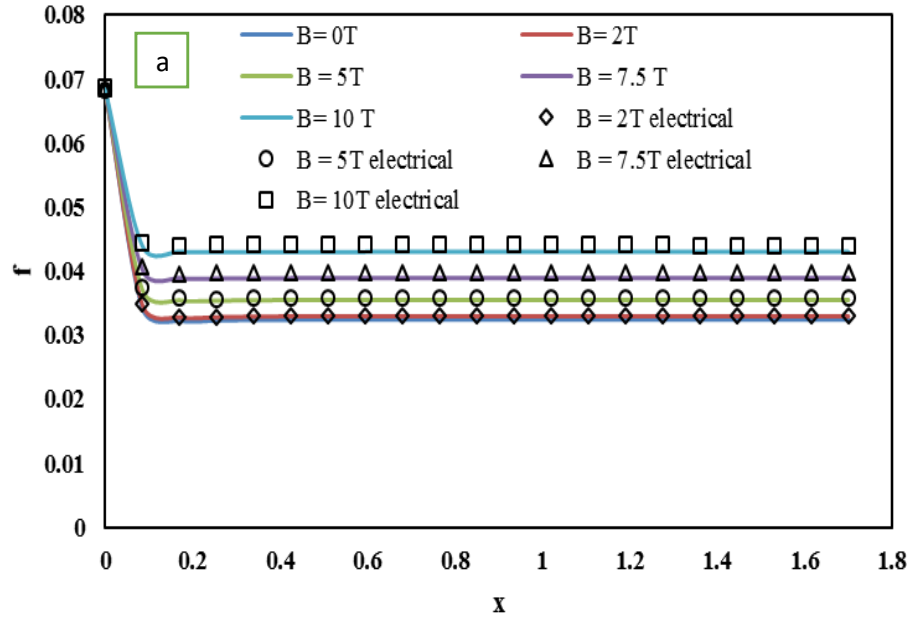


Fig. 5.16 Effect of magnetic field on Nusselt number, Re = 9500 and 0.6% (a-SP, b-MP).

5.6.3 Effect of magnetic field on friction factor



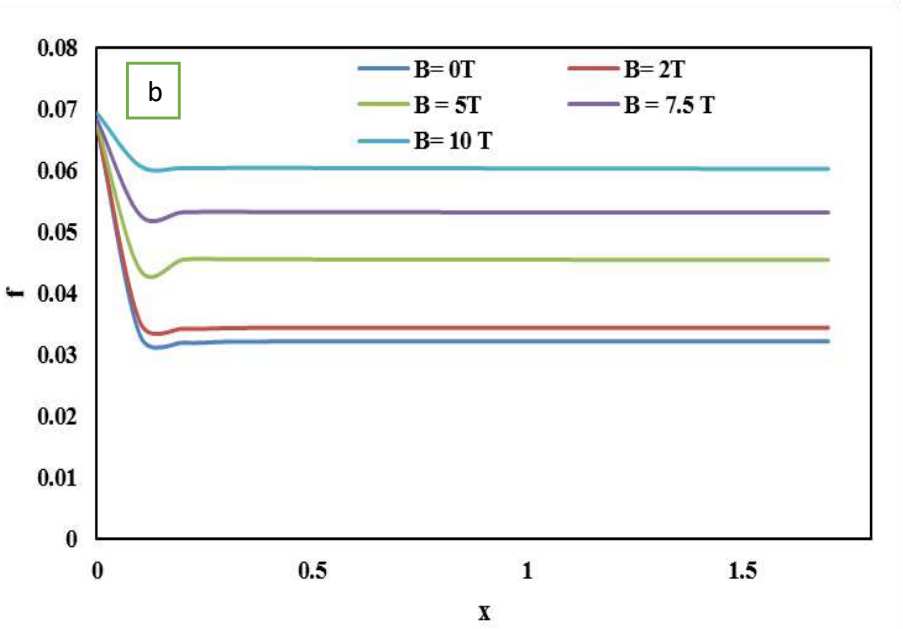


Fig.5.17 Effect of magnetic field on friction factor Re 9800 and 0.3% (a-SP, b-MP)

Fig. 17, Fig. 18 and Fig. 19 shows the effect of magnetic field on the friction factor in tube for different Reynolds number and volume fraction (0.3% and 0.6%). As shown in these figures, friction factor is found enhanced by increasing the magnetic field. Also, in the same Reynolds number the friction factor of nanofluid enhanced when the nanoparticle concentration increased. In fig. 17 friction factor enhanced about 12.1% in single phase and 42.9% in mixture at B=10T.

Fig. 18 shows the maximum increasing of friction factor in single phase and in mixture, the value is 32.6% and 78.4% respectively. As shown in fig. 19 the increasing of friction factor at B=2T, 5T, 7.5T and 10T the value is 4.6%, 23.4%, 45.1% and 61.24% respectively. For single phase at B=2T, 5T, 7.5T and 10T, the value is 1.23%, 7.23%, 15.34% and 25.17% respectively.

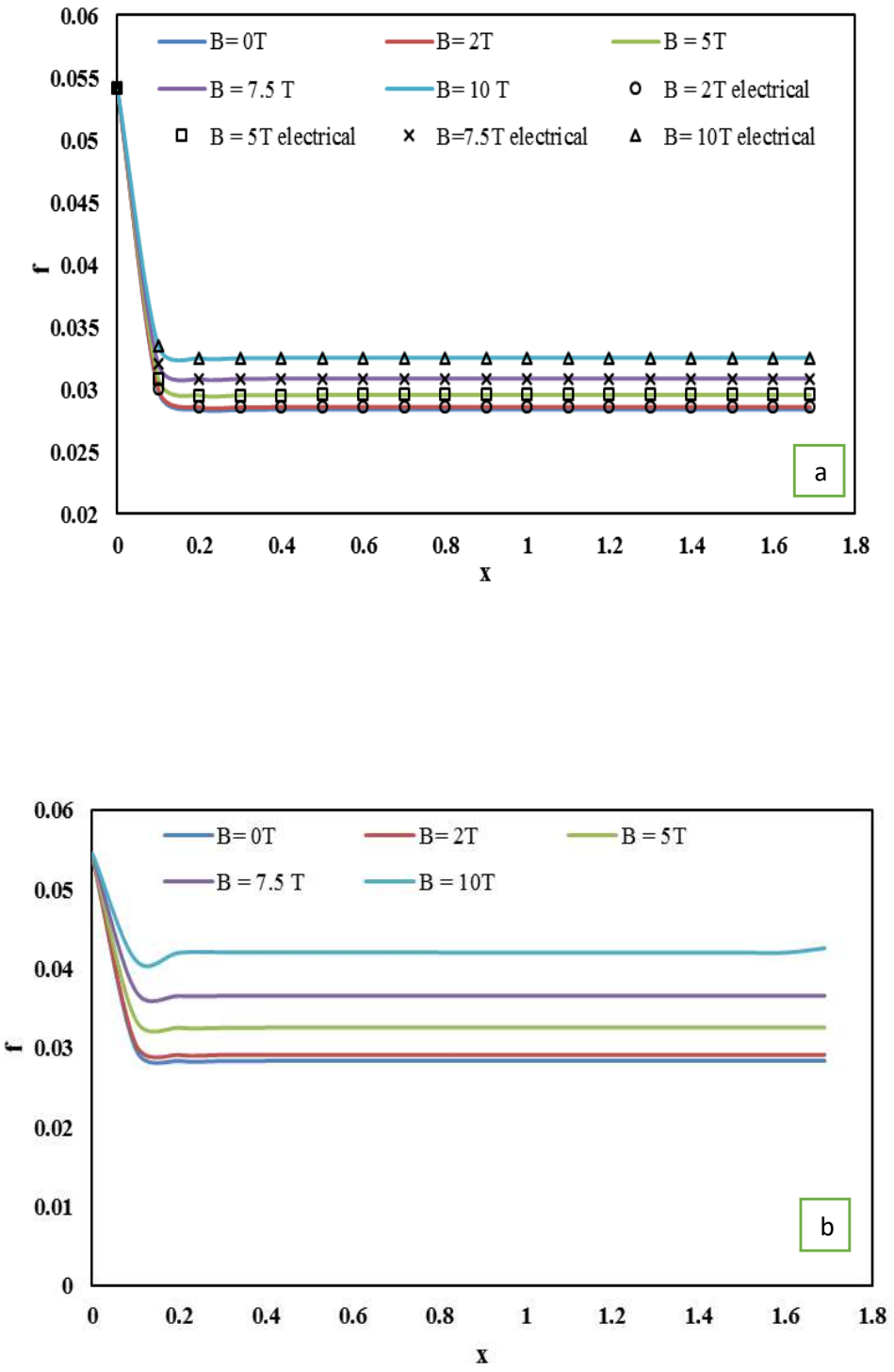


Fig. 5.18 Effect of magnetic field on friction factor Re7000 and 0.6% (a-SP, b-MP)

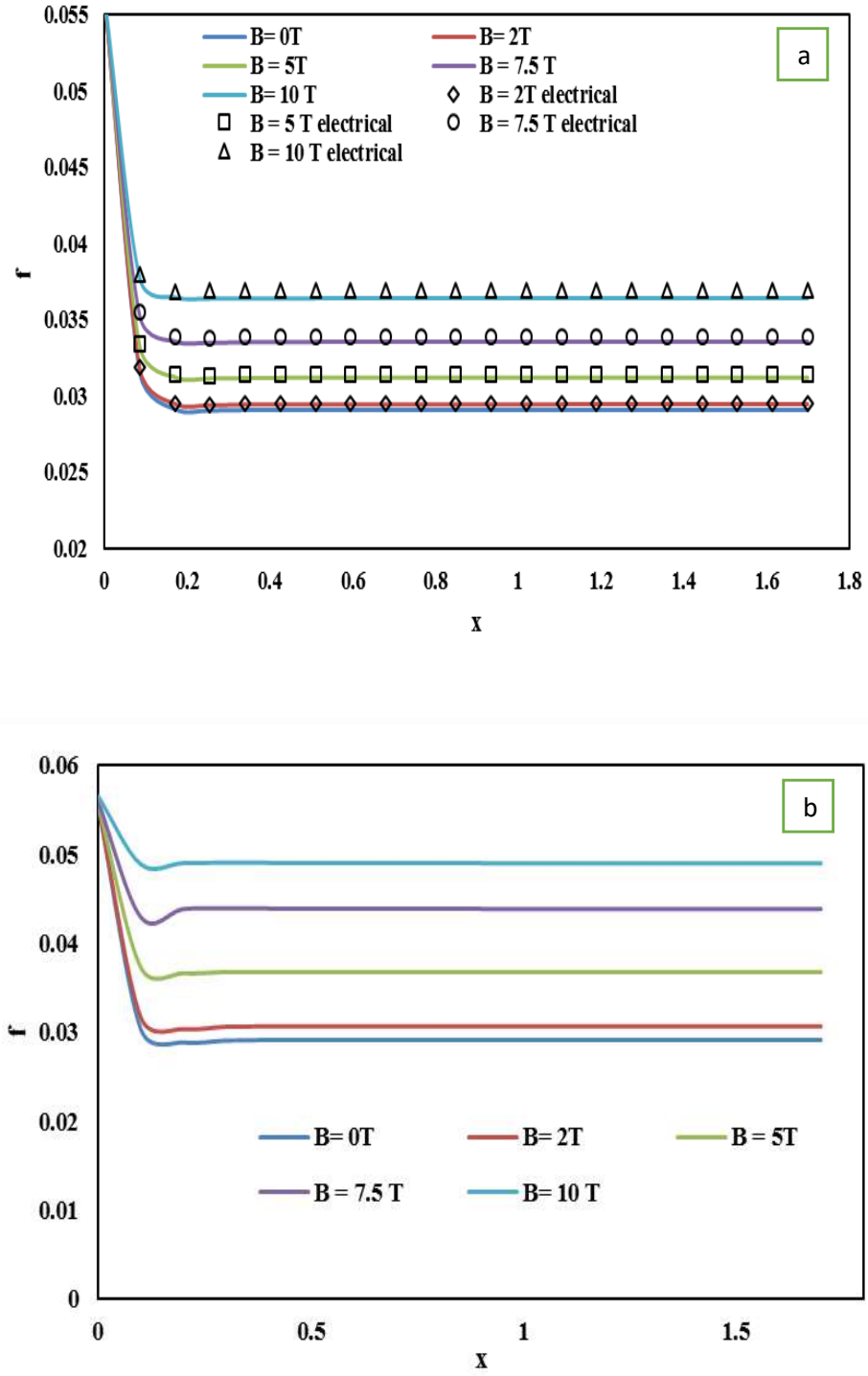


Fig. 5.19 Effect of magnetic field on friction factor Re9500 and 0.6% (a-SP, b-MP)

Motozawa, Chang [69], investigates experimentally the effect of magnetic field on ferrofluid. He find when the temperature gradient is vertical to the magnetic field, the chain-like cluster will be formed along the direction of the magnetic field. Therefore, as the shear rate in the temperature gradient direction increases, the velocity boundary layer and the thermal

boundary layer near wall becomes thinner than without magnetic field. The results indicate that the heat transfer enhanced with presence of a magnetic field.

From fig. 5.20 it can be seen that by increasing intensity of the magnetic field Nusselt number ratio for ferrofluid increases. Also when we set the value of magnetic field and increase the volume fraction of ferrofluid still the Nu ratio increase up to 20% at 0.1% , 29% at 0.2 % , 34% at 0.3% and 36% at 0.4% volume fraction.

Fig. 5.21 shows the effect of magnetic field and volume fraction on the friction factor ratio in Re=15000. It can be seen that by increasing the intensity of magnetic field and volume fraction the ratio of friction factor increases.

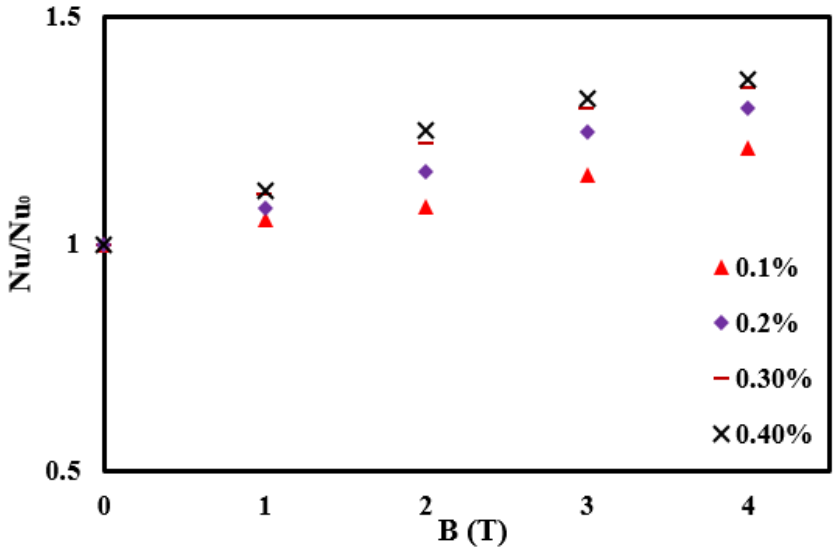


Fig.5.20 Investigation of Nusselt number ratio in different volume fraction and field intensities (SP) for ferrofluid

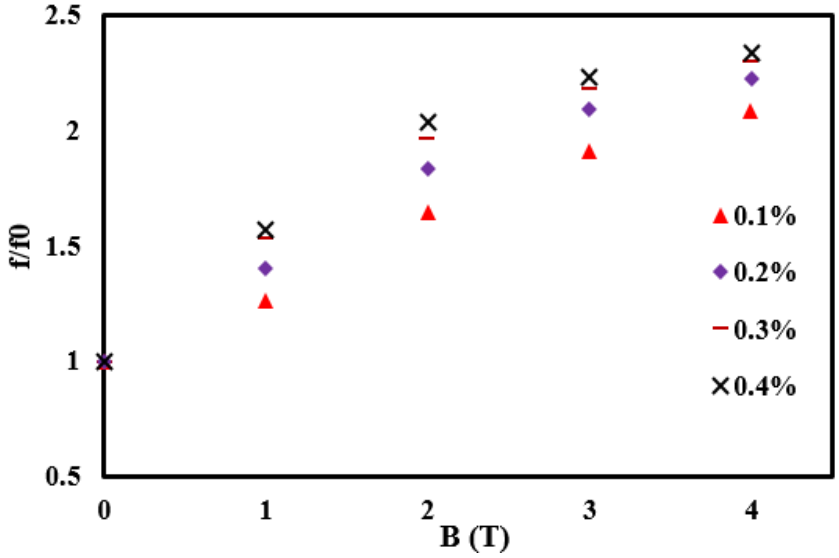


Fig. 5.21 Investigation of friction factor ratio in different volume fraction and field intensities (SP) for ferrofluid

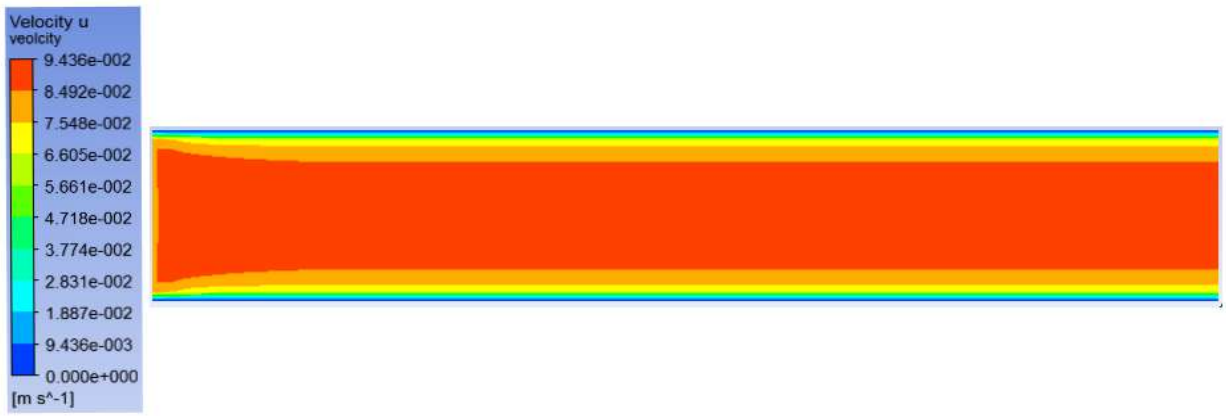


Fig. 5.22 velocity contour of ferrolfuid for volume fraction φ= 1% and B=0T (Re=15000)

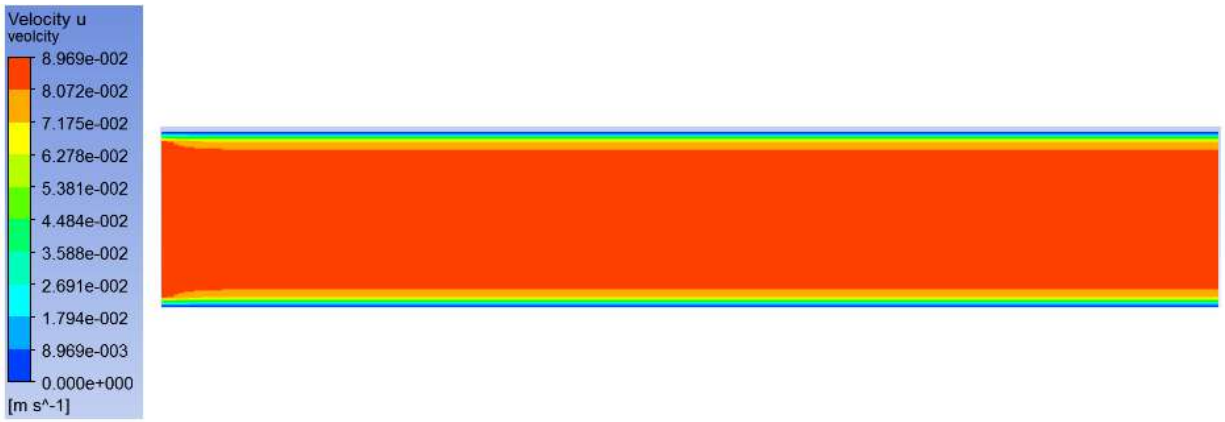


Fig. 5.23 velocity contour of ferrolfuid for volume fraction φ= 1% and B=1T (Re=15000)

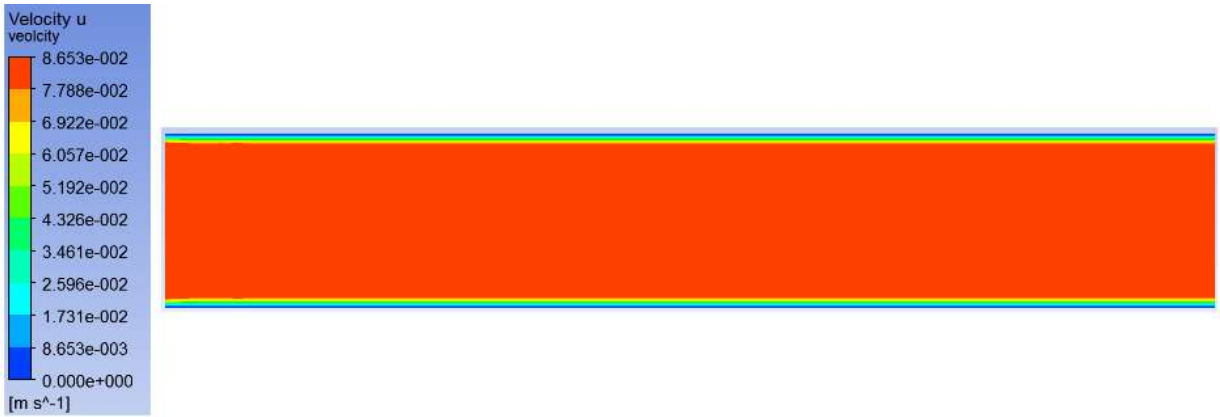


Fig. 5.24 velocity contour of ferrolfuid for volume fraction φ= 1% and B=2T (Re=15000)

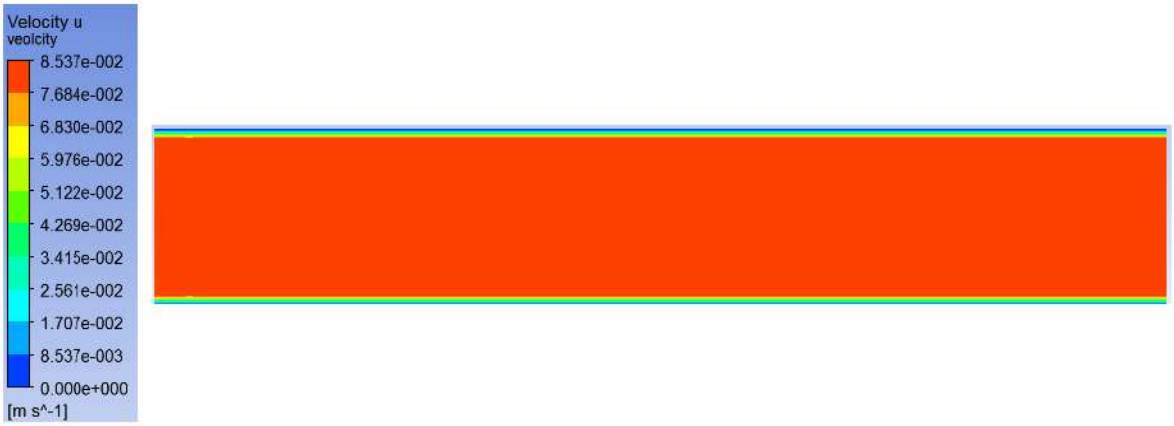


Fig. 5.25 velocity contour of ferrolfuid for volume fraction φ= 1% and B=3T (Re=15000)

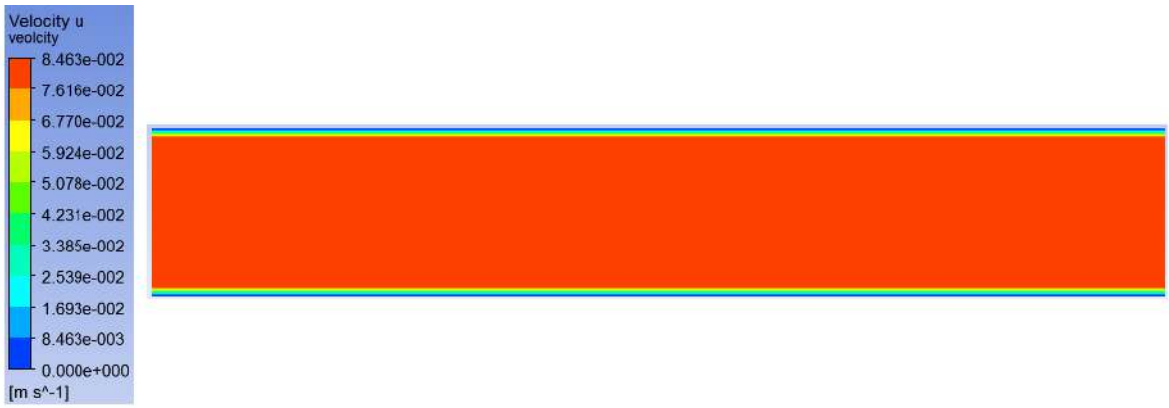


Fig. 5.26 velocity contour of nanofluid for volume fraction φ= 1% and B=4T (Re=15000)

Fig 5.22, 5.23, 5.24, 5.25 and 5.26 represent velocity contour of nanofluid for volume fraction φ= 1% and different magnetic field B=0, 1, 2, 3, 4 T respectively.

Existence of magnetic field leads to the generation of the Lorentz force in the opposite direction of X. Hence, more of magnetic field B corresponds to less maximum of velocity at horizontal centerline and higher fluid velocity adjacent to the walls. As a result, the fully developed velocity profile would change with magnetic field.

So that stronger magnetic field corresponds to thinner boundary layer along the walls. Moreover, the thickness growth of the boundary layer is low at higher values of B.

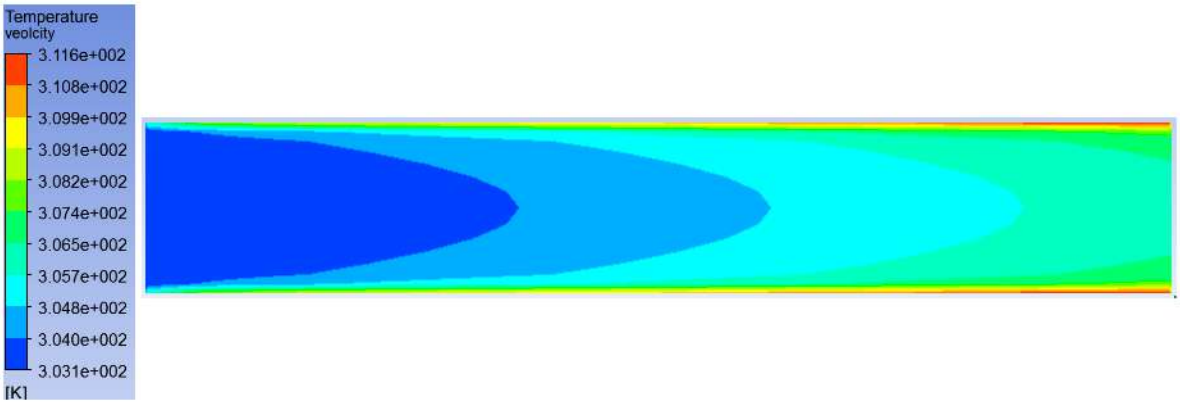


Fig. 5.27 temperature contour of nanofluid for volume fraction φ= 1% and B=0T (Re=15000)

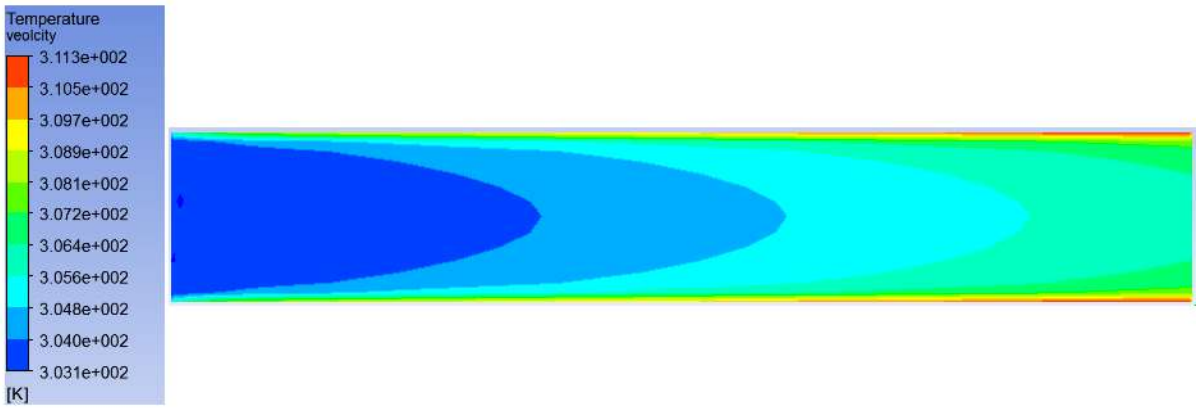


Fig. 5.28 temperature contour of nanofluid for volume fraction φ= 1% and B=1T (Re=15000)

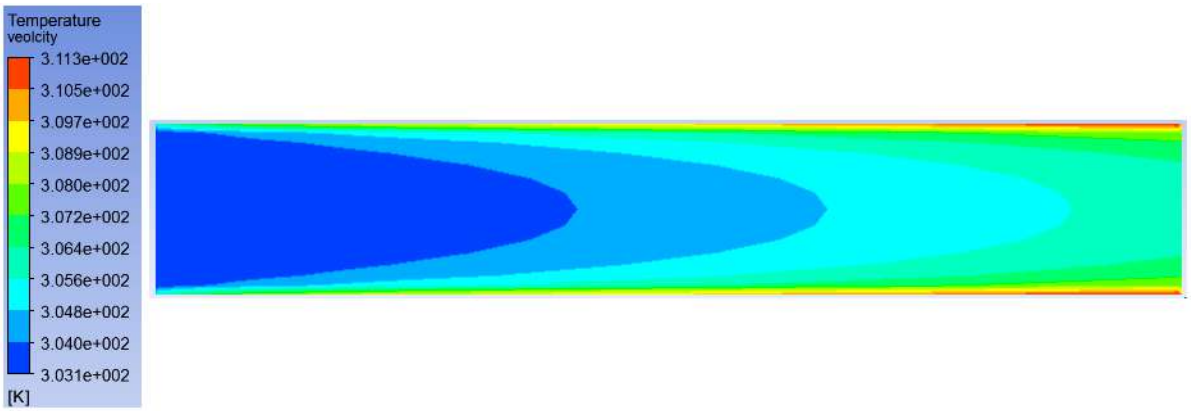


Fig. 5.29 temperature contour of nanofluid for volume fraction φ= 1% and B=2T (Re=15000)

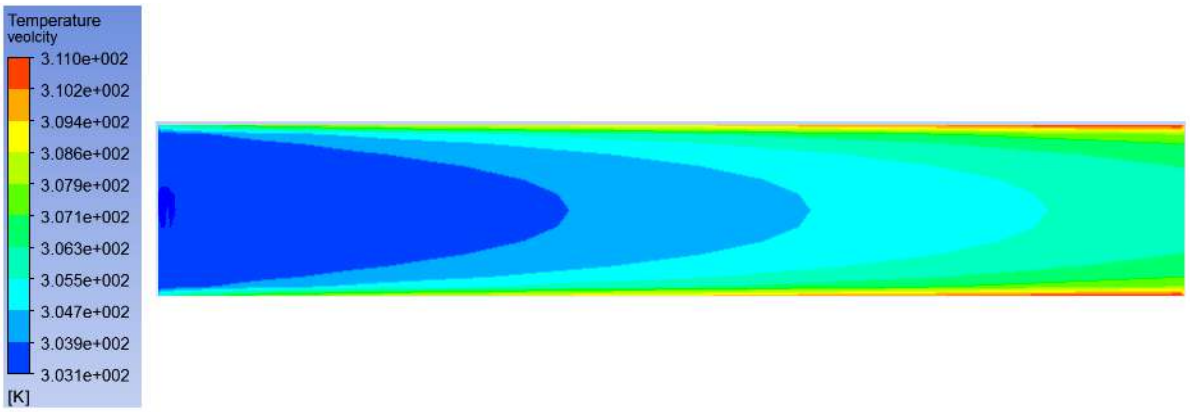


Fig. 5.30 temperature contour of nanofluid for volume fraction φ= 1% and B=3T (Re=15000)

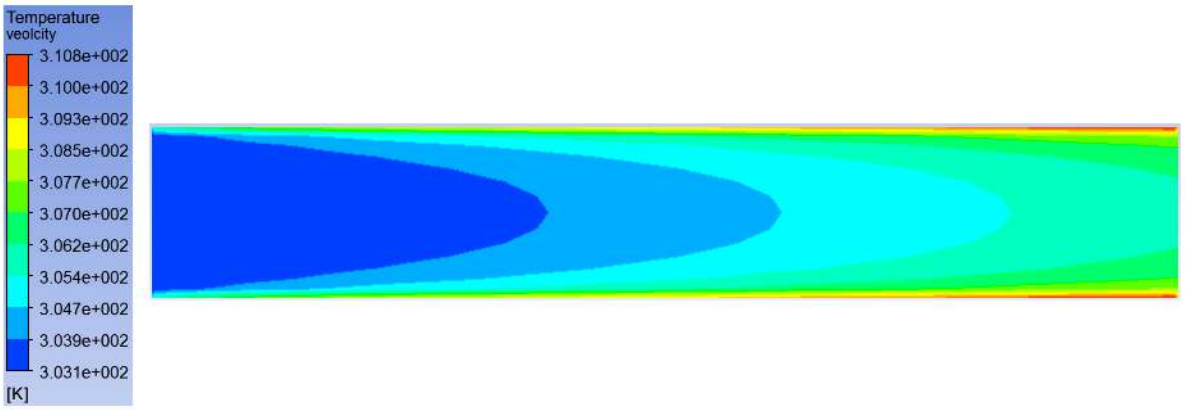


Fig. 5.31 temperature contour of nanofluid for volume fraction φ= 1% and B=4T (Re=15000)

Fig 5.27, 5.28, 5.29, 5.30 and 5.31 represent temperature contour of nanofluid for volume fraction φ= 1% and different magnetic field B=0, 1, 2, 3, 4 T respectively.

It is observed that the fluid temperature increases along the pipe and the wall temperature decrease. This fact implies more heat transfer existences due to more fluid velocity and the state of stronger magnetic field.

5.6.4 Effect of magnetic field on pressure drop

Fig. 5.32 showed the effect of magnetic field on nanofluid pressure drop for volume fraction at 0.6%, the pressure drop increased with Reynolds number and magnetic field. The pressure drop increased in the absence of magnetic field because the fluid viscosity increased due to addition of nanoparticles in the base fluid. In the presence of magnetic field, the nanoparticles

suspended in the carrier fluid tend to remain chained-alignment along with the direction of the external magnetic field and the nanofluid viscosity increased [70] . The magnetic field has an undesirable effect for the pressure drop, which need to increase the power pumping for getting high transfer rate.

For a pressure drop imposed, fixed B* and Re* from the fig. 5.32 are indicated two cases appeared:

- Nu desired with B* and Re we are satisfied
- Nu desired is not satisfied, the solution become a trade-off based on economic sense. If it is selected than using powered pump will lead to small extra cost, while changing the entire pipe with bigger diameter will lead to very expensive solution.

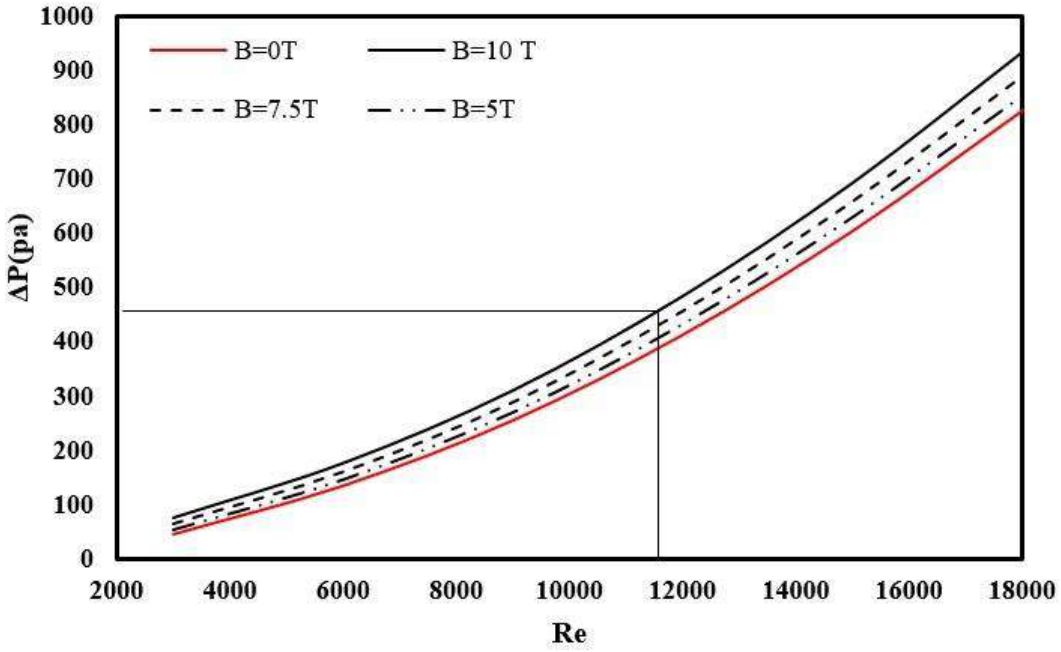


Fig. 5.32 The effect of magnetic field of nanolfuid (0.6%) pressure drop

5.7 Conclusion

In this chapter, the behaviours of the velocity, Nusselt number, friction factor and pressure drop with magnetic field for a nanofluid (Fe3o4-water) in horizontal have been presented.

The two-phase mixture and single phase approach were employed to simulate the nanofluid convection. The validation of friction factor and Nusselt number are compared with experimental results of L. Sunder, which shows good convergence. The obtained results indicate that the friction factor and Nu number have increased with increasing of magnetic field

using induction and electrical potential. Also the effect of magnetic field leads to decrease of velocity due the Lorentz force. For the ratio of average Nu and friction factor are enhanced by increasing the volume fraction of nanoparticles and magnetic field. It concludes that the heat transfer and friction factor depend on the increment of magnetic field, electrical conductivity and volume fraction.

Simulation of nanofluids (Cu-H_2O) Flow in an Inclined Heated Pipe

6.1 Introduction

Almost all of the flows are turbulent in practical situation, and many of these experience extremely high Reynolds numbers e.g. flows in aircraft wings, cars, ships, submarines, turbine blades and large pipe. It is important to understand the phenomena of high Reynolds number turbulence in order to develop models for energy efficient applications. Therefore, the present investigation.

In this chapter, a numerical study has been carried out to understand the heat transfer behaviour of Cu-H_2O nanofluids flow (100 nm diameter) an inclined pipe 0 and 30 ° using the single phase approach, two-dimensional model are considered to describe the turbulent flow under uniform heat flux boundary condition. Computational geometry consists of a pipe with length *L* of 800 mm and a circular section with diameter D = 10 mm as shown in Fig. 5.1.

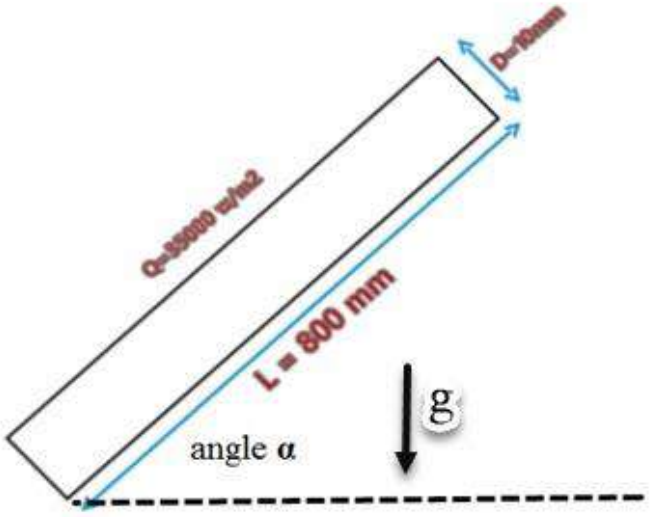


Fig 6.1 Schematic diagram of the geometry under consideration

6.2 Boundary condition

At the pipe inlet, uniform velocity *v* as well as uniform temperature T=295 k turbulent and hydraulic diameter D_h= 10 mm have been stated. . All the thermal properties calculation is taken at T_{in} which is also considered as a reference temperature.

At the pipe outlet, a static gauge pressure P_{gauge} = 0 is specified. On the pipe wall, a no-slip boundary condition is introduced and uniform heat flux (Q=35000 w/m2) boundary condition is implemented. The Boussinesq approximation is introduced in the momentum equation for mixed convection nanofluids flow in the inclined pipe as shown in Eq. (3.23) of Chapter 3.

Enhanced wall treatment is a near-wall modelling method that combines a two-layer model with enhanced wall functions. If the near-wall mesh is fine enough to be able to resolve the laminar sublayer, then the enhanced wall treatment will be identical to the traditional two-layer model. However, the restriction that the near-wall meshes must be sufficiently fine everywhere which might impose to large computational requirement. So, ideally one would like to have a near-wall formulation that can be used with coarse meshes as well as fine meshes. In addition, excessive error should neither be incurred for intermediate meshes that are too fine for the near-wall cell centroid to lie in the fully turbulent region, nor too coarse to properly resolve the sublayer (Fluent [57]). That is why; enhanced wall treatment is used in the present analysis.

6.3 Selected Grid

In order to ensure the accuracy as well as the consistency of the numerical results. Extensive computations have been performed to identify the number of grid points that produce a suitable arrangement result which will be applicable to determine the turbulent flow and thermal field inside the pipe with single phase model. We tested a grid for 80 × 800 with experimental data (Xuan [53]) and we have obtained a good results. The figure 6.2 show the selected grid 80×800 with aspect ratio 1.064 in Nr direction it is finer near the tube entrance and the tube wall.



Fig 6.2 grid 80×800

6.4 Properties of nanofluid

the constitutive relations that used to determine the thermophysical properties are given in chapter 3. For density (equation 3.28), specific heat (equation3.29), thermal conductivity (equation 3.30) a model proposed by wasp and for viscosity (equation 3.31) we used a brinkman model.

For the thermal expansion of nanofluid is defined as:

$$\beta_{nf} = (1-\varphi)\beta_f + \varphi\beta_p$$

With:

β_{nf} : Thermal expansion of nanofluid

β_f : Thermal expansion of base fluid $\beta_f = 21\times10^{-5}(1/k)$

β_p : Thermal expansion of nanoparticle $\beta_p = 1.67\times10^{-5}(1/k)$

6.5 Validation

In order to verify the accuracy of the numerical procedure, we have compared our results with experimental data that were reported by Xuan [53]. Validation is done for nanofluids flowing under turbulent regime through a horizontal circular channel with a constant heat flux. The Cu nanoparticles with diameters of 100 nm and water as a base-fluid were used in these simulation. Fig. 6.3 compares the obtained results of Nusselt

number with the experimental data. The comparison are presented for the fully developed region Re =10000 to 20000 and for two volume fraction φ=0.012 and φ=0.016.

It shows that single phase model simulation results are in good agreement with the experimental data for the average Nusselt number with average percentage error for volume fractions 1.2% and 1.5% are 1.85 % and 1.90 % respectively. Also It indicated that the convective heat transfer coefficient of the nanofluid increases with the increase of Reynolds number and volume concentration of nanofluid.

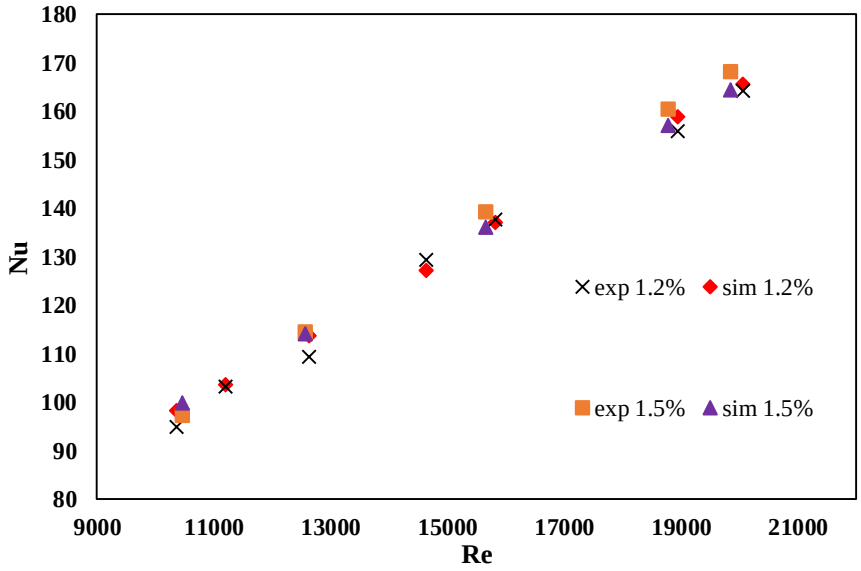


Fig. 6.3 Comparison of Nusselt number with literature Xuan [53]

6.6 Results and Discussions

Here, Numerical investigations have been carried out using the Cu-H_2O nanofluids with the following parameters: Reynolds number Re = 10000 and 12000 (turbulent regime), nanoparticles concentration, φ = 1.2%, diameter of nanoparticles, d_p =100 nm and pipe inclination angles from θ = 0° and 30°. In order to understand the flow behaviour we have plotted contour of axial velocity.

Later on, variation of the wall temperature and local Nusselt number as well as the Darcy friction factor and average Nusselt number with inclination angles α=30° using the single phase approaches (SP) are also presented and discussed.

6.6.1 Velocity Contours

In this section, 2D contour plots of velocity have been generated by placing a horizontal plane along the pipe and also at different axial positions in order to understand the flow field behaviour for inclination angle φ = 30° as shown in Fig.6.4, it observed the velocity profile at the outlet with angle $\theta = 0°$ it's fully developed turbulent and the variations of the velocity profile at the outlet with inclination angle $\theta = 30°$ the higher velocity region tends to move towards the lower wall zone and forms a large size of lower velocity region at the upper wall zone.

Only Cu-H_2O nanofluid with single phase model and volume fraction 1.2% has been selected, Reynolds number has been fixed for Re = 10000 and 12000.

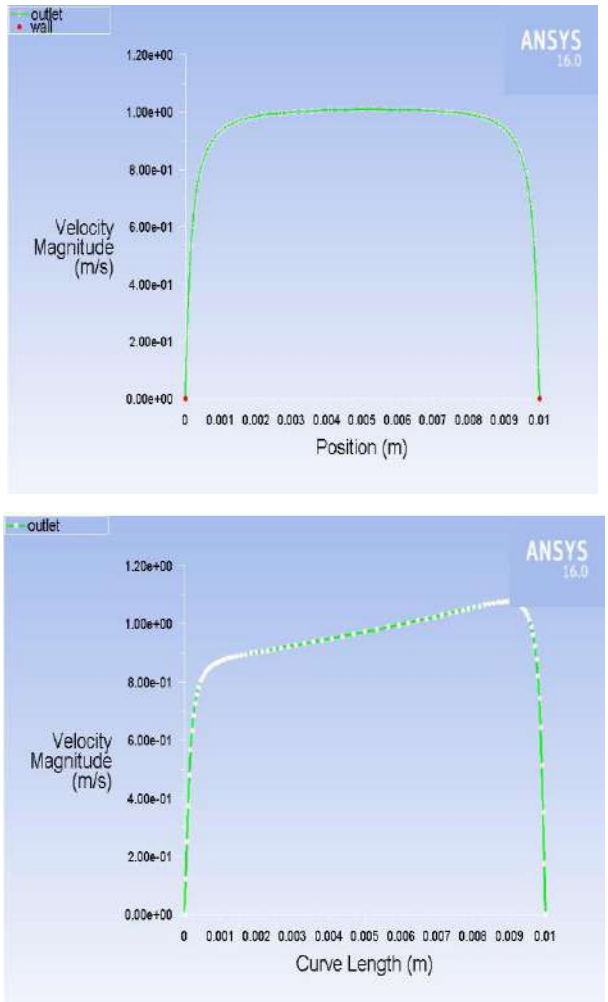


Fig 6.4 velocity profile at the outlet of pipe for two angle 0° (a) ; 30° (b) and Re=10000

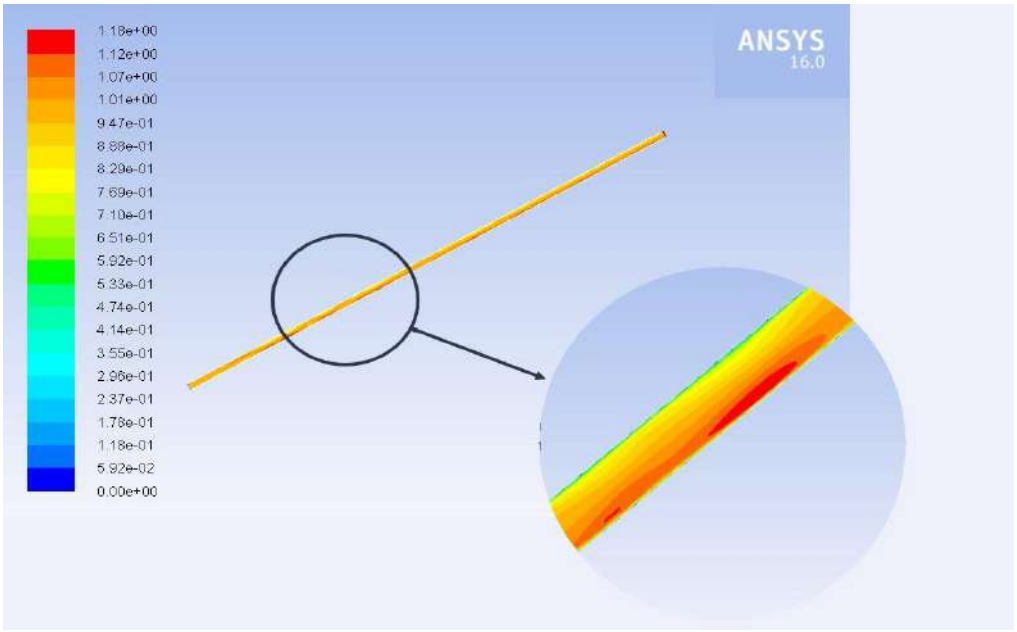


Fig 6.5 velocity contour of pipe for angle 30° and Re=10000

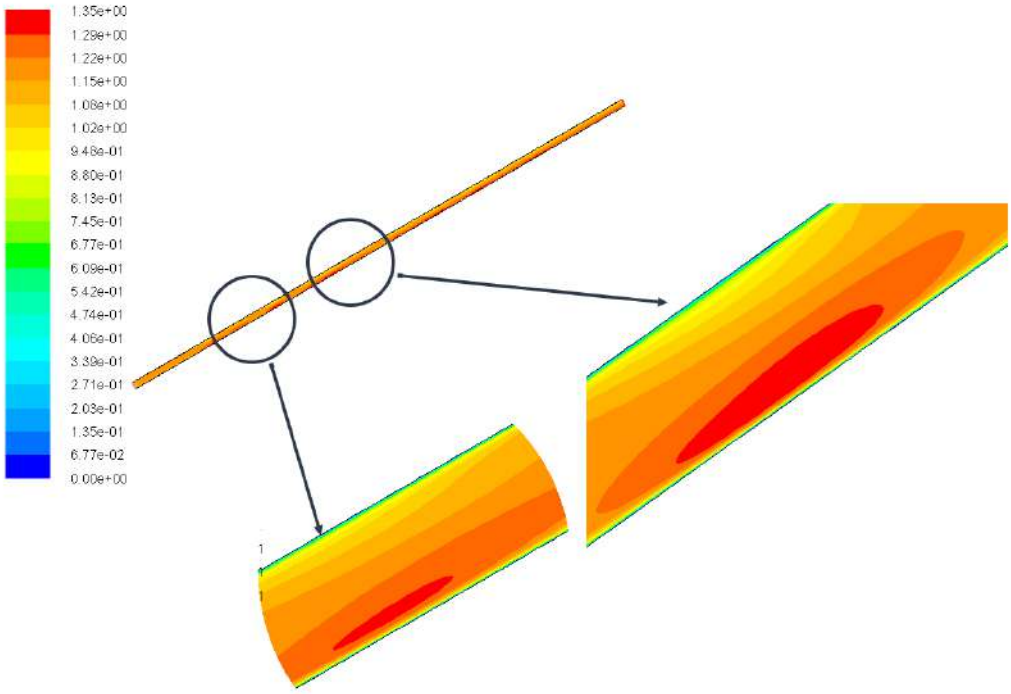


Fig 6.6 velocity contour of pipe for angle 30° and Re=12000

Fig. 6.5, 6.6 shows the variations of the velocity contours at different Reynolds number (Re=10000 and 12000) with inclination angle of 30°. For Re =10000 and x = 0.25 m, a rapid increase of higher velocity region at the lower wall region is observed. And a rapid development of lower velocity region is observed for upper wall zone. For Re =12000 and x =

0.25, 0.4 m, it is observed that the higher velocity cell moves towards the lower wall region and forms an oval profile while other regions are covered with the lower velocity of the nanofluid.

6.6.2 Temperature Contours

In this section, contour of the temperature along the pipe for different inclination angles has been presented in Figs. 6.7 and 6.8.

For $\theta = 0°$, it is found that most of the region of the pipe is covered with the blue and light blue colour that refers to the change of temperature gradually. On the other hand, higher temperature is observed near the wall region. Also, the maximum temperature difference between the higher and lower temperature region is found to be approximately 8K. Moreover, the growth of thermal boundary layer seems to be changed when X > 0.32m.

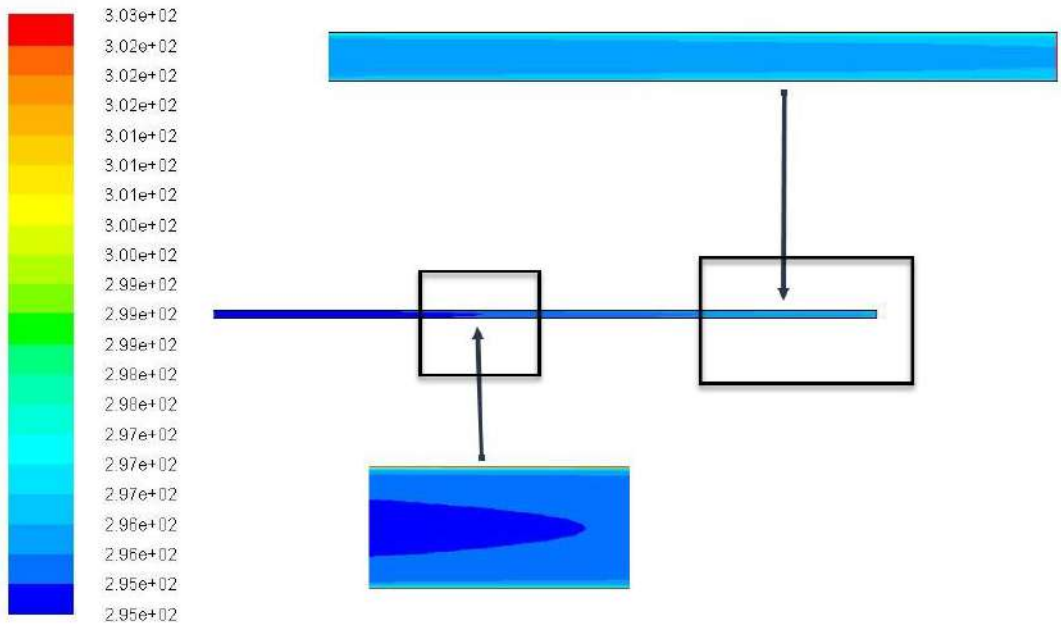


Fig 6.7 temperature contour of pipe for angle 0° and Re=10000

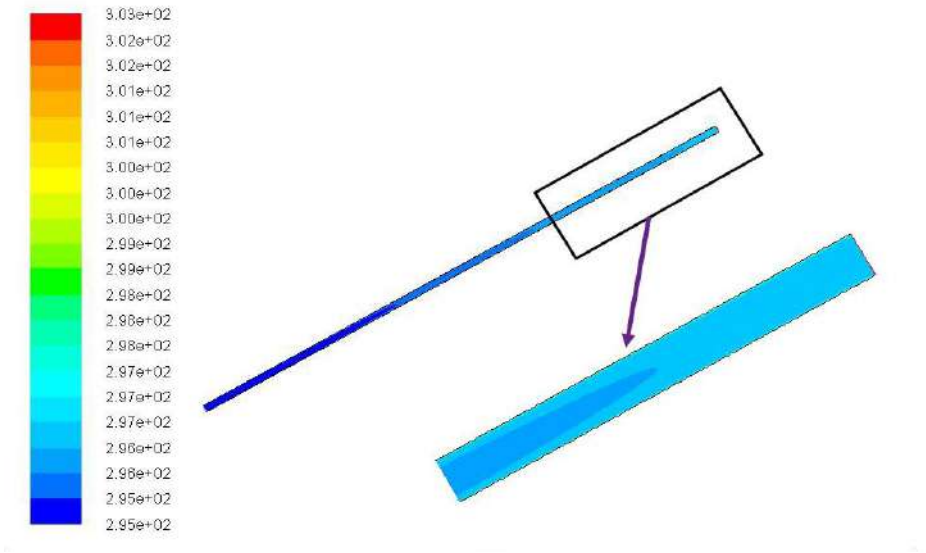


Fig 6.8 temperature contour of pipe for angle 30° and Re=10000

For θ = 30°, a change in the growth of thermal boundary layer is observed near the outlet region when X>0.6m. This behaviour indicates the effect of the Buoyancy force when the Boussinesq approximation is considered. The development of boundary layer seems to be higher when the increase of inclination angles.

6.6.3 Local Nusselt Number

Figure 6.9 and 6.10 shows the variations of local Nusselt number with different inclination angles for Cu-H_2O nanofluids using single model and Reynolds number (Re 10000, 12000). It observed the local Nusselt number has always been found to be maximum at the beginning of the pipe although it starts to decrease rapidly afterwards.

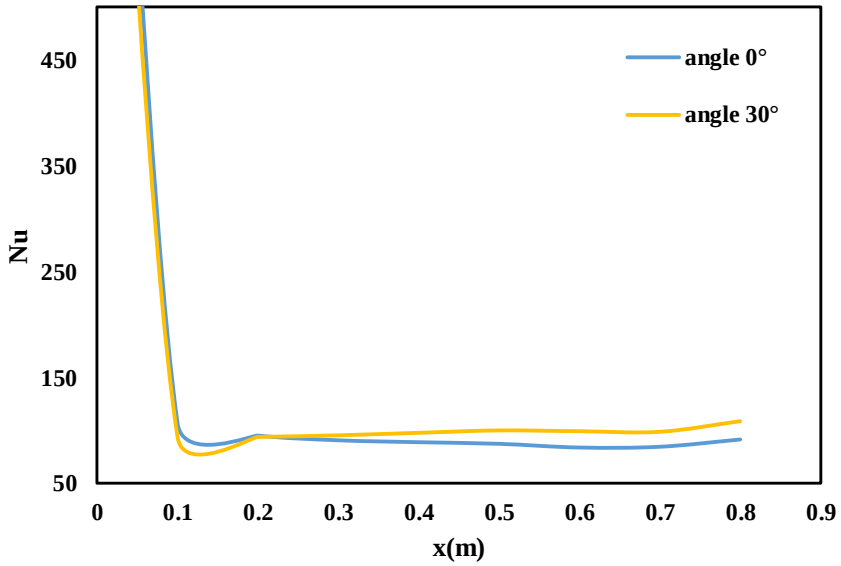


Fig 6.9 local Nusselt number with different inclination and Re=10000

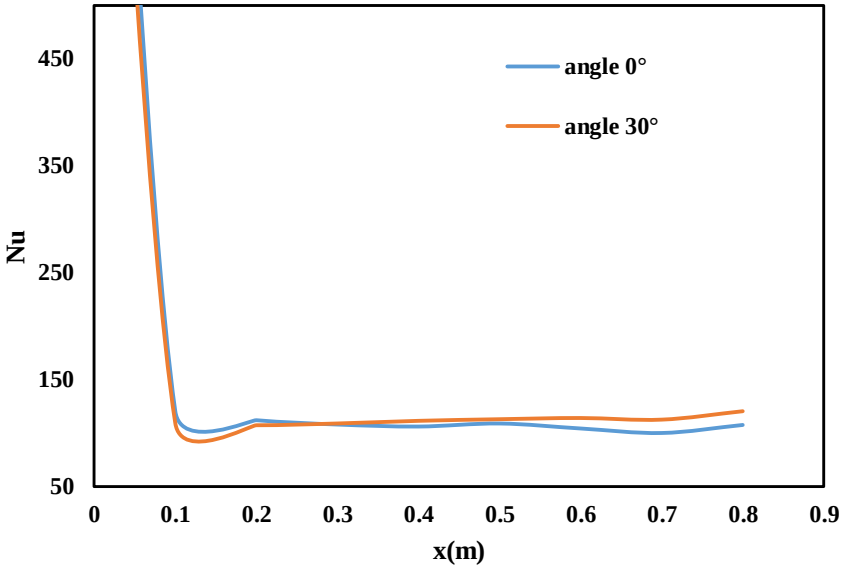


Fig 6.10 local Nusselt number with different inclination and Re=12000

The local Nusselt number has always been found to be maximum at the beginning of the pipe after that it starts to decrease rapidly afterwards. Further, the local Nusselt number tends to become constant and steady as the flow tends to become fully developed.

The local Nu is observed to increase with the rise of inclination angles from θ = 0 to 30°, for Re =10000 increased percentage was 7.49 % and for Re=12000 increased percentage was 3.63%.

6.6.4 Darcy Friction Factor

Darcy friction factor results are presented in Fig. 6.8 and 6.9 with a view to understand the pressure drop behaviour affected by the Buoyancy force inside the inclined pipe. To do this, the variations of Darcy friction factor with inclination angles and the Reynolds numbers for Cu-H_2O nanofluids (φ=1.2%) have been presented here.

The Darcy friction factor increases with the increase of inclination angle from θ = 0° to 30° in the inclined pipe. Also, a higher Darcy friction factor is observed in the mixed convection case for Re=10000. It is the additional buoyant force which compels to enhance the pressure drop inside the pipe. The average percentages of the variations of Darcy friction factor are 12.22% for Re=10000 and 5.95% for Re=12000.

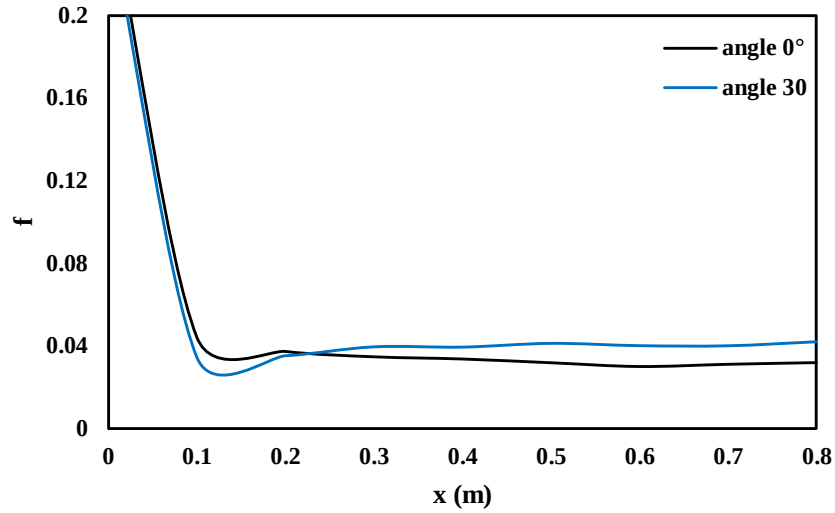


Fig 6.11 local Darcy friction factor with different inclination and Re=10000

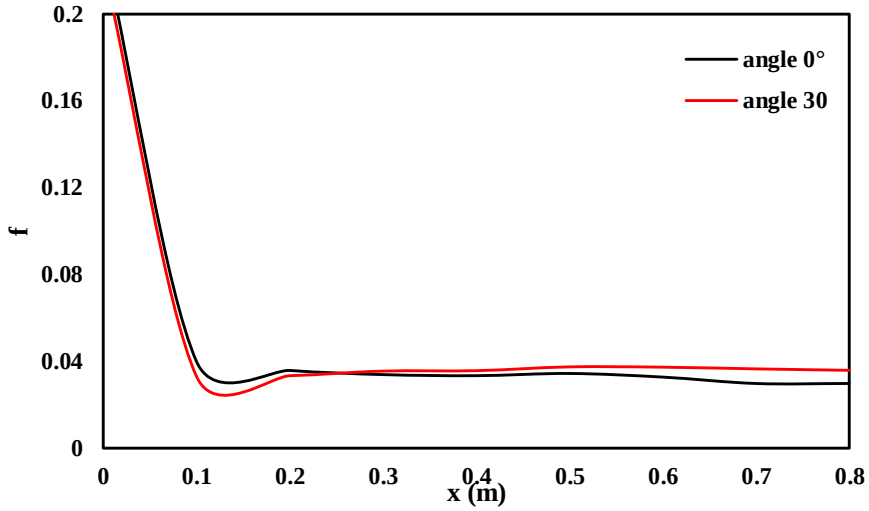


Figure 6.12 local Darcy friction factor with different inclination and Re=12000.

6.7 Conclusion

As it is stated at the beginning, numerical investigation has been performed in order to understand the heat transfer behaviour of mixed convection in inclined pipe for this chapter. And, a nanofluids of Cu–water have been considered as working fluid, a single phase approach have been used throughout this investigation. Results are presented in terms of velocity temperature, local Nusselt number and Darcy friction factor. So, the following conclusions can be drawn from the outcomes:

- The contours of flow field to be deformed near the downstream region along with the increase of inclination angles due to Buoyancy force.

- The temperature is observed to increase along the pipe near the outlet with the increase of angle.
- The local Nusselt number is increased with the increase of inclination angles.
- A significant enhancement of Darcy friction factor in the mixed convection case has been observed than that found in the forced convection case for Reynolds number Re=10000 and 12000. So the Darcy friction factor is increased with the increase of inclination angles, and, this enhancement is found to be liable for the higher penalty in pumping power.

Conclusion

Numerical investigations of forced convection flow have been studied in a horizontal pipe with and without magnetic field under turbulent flow regimes. Particular investigation has been done in order to show the effect of nanoparticules volume concentration, Reynolds number and magnetic field on the heat transfer and the flow considered turbulent. Finally, the effect of inclination angle in mixed convection flow in an inclined pipe is presented. From the above studies, the following conclusions are drawn:

The friction factor results for Al_2O_3 nanofluid rise with decreasing of Reynolds number but when the volume concentration increase the friction factor also increase slightly. This is can be seen for both regime flow laminar and turbulent.

When we apply a magnetic field to the ferrofluid flow (Fe_3O_4-H_2O) the velocity decreased along the pipe due to the opposite Force 'Lorentz force' that react in the inverse direction of the fluid flow.

The results show the friction factor increase with rise of stronger magnetic field. As we know for a high friction factor it indicate we need a higher in pumping power. So the magnetic field has an undesirable effect for the friction factor and pressure drop, which need to increase the power pumping for getting high transfer rate.

Heat transfer enhance by increasing the volume concentration of nanoparticles in nanofluid and Reynolds number for different nanoparticules Al_2O_3 and Fe_3O_4. Also we can see enhancement of heat transfer when we apply a magnetic field to the ferrofluid turbulent flow (Fe_3O_4-H_2O).

It is observed that the friction factor is increased along with the increase of inclination angles from 0 to 30°. Also, local Nusselt number is increased with the increase of inclination angles. This indicates that the heat transfer rate is higher in the mixed convection than that in the forced convection.

Overall, heat transfer enhancement and the decrease of friction factor are observed while using both the single and mixture models in forced convection of ferrofluid with magnetic field. It is seen that there are small difference between the results obtained using SP and MP. Such findings help us to conclude that single phase model can still be applied in the practical

applications considering the limitations that there is no interaction between the fluid particles and nanoparticles.

Future Work:

The present research shows the impact of different nanoparticules, volume concentration, Reynolds number and magnetic field on nanofluids and heat transfer under turbulent flow regimes. In the following section, some recommendations for future research work are presented to extend the present work potentially:

The study of heat transfer behaviour in forced convection of nanofluids flow in micro sized pipe is very limited. More attention is necessary to investigate such behaviour which will help to understand the use of nanofluids flow in micro pipe under laminar to turbulent flow regimes.

It is important to understand the behaviour of fluid-nanoparticles mixture. Very limited information is available in the literature about the performance of Brownian force and Thermophoretic force of nanoparticles on heat transfer enhancement under laminar to turbulent flow regimes.

In order to acquire knowledge on heat transfer enhancement, more experimental investigations are necessary to show the effect of magnetic field on ferrolfuid flow in turbulent regime. Also, the performance of magnetic nanofluid flow through porous zone with MHD effect.

References

[1] Godley, M., B.P.S. Tomar, and A. Tripathi, Investigation of Automobile Radiator Using Nanofluid-CuO/Water Mixture as Coolant. International Journal of Advanced Research in Science, Engineering and Technology, 2015. 2(12): p. 1136-1145.

[2] Peyghambarzadeh, S., et al., Experimental study of heat transfer enhancement using water/ethylene glycol based nanofluids as a new coolant for car radiators. International Communications in Heat and Mass Transfer, 2011. 38(9): p. 1283-1290.

[3] Özerinç, S., A.G. Yazıcıoğlu, and S. Kakaç. Convective Heat Transfer Enhancement With Nanofluids: The Effect of Temperature-Variable Thermal Conductivity. in ASME 2010 10th Biennial Conference on Engineering Systems Design and Analysis. 2010. American Society of Mechanical Engineers.

[4] Yu, W. and H. Xie, A review on nanofluids: preparation, stability mechanisms, and applications. Journal of Nanomaterials, 2012. 2012: p. 1.

[5] Yu, W., et al., Review and comparison of nanofluid thermal conductivity and heat transfer enhancements. Heat Transfer Engineering, 2008. 29(5): p. 432-460.

[6]Yatsuya, S., et al., Preparation of extremely fine particles by vacuum evaporation onto a running oil substrate. Journal of Crystal Growth, 1978. 45: p. 490-494.

[7] Wagener, M. and B. Günther, Sputtering on liquids–a versatile process for the production of magnetic suspensions? Journal of Magnetism and Magnetic Materials, 1999. 201(1): p. 41-44.

[8] Li, Y., et al., A review on development of nanofluid preparation and characterization. Powder Technology, 2009. 196(2): p. 89-101.

[9] Zhu, H.T., et al., Novel synthesis and thermal conductivity of CuO nanofluid. The Journal of Physical Chemistry C, 2007. 111(4): p. 1646-1650.

[10] Witharana, S., et al., Stability of glycol nanofluids—the theory and experiment. Powder technology, 2013. 239: p. 72-77.

[11] Solangi, K., et al., A comprehensive review of thermo-physical properties and convective heat transfer to nanofluids. Energy, 2015. 89: p. 1065-1086.

[12] Das, S.K., et al., Nanofluids: science and technology. 2007: John Wiley & Sons.

[13] Tzeng, S.-C., C.-W. Lin, and K. Huang, Heat transfer enhancement of nanofluids in rotary blade coupling of four-wheel-drive vehicles. Acta Mechanica, 2005. 179(1-2): p. 11-23.

[14] Yu, W., S. Choi, and J. Drobnik. Temperature and concentration dependence of effective thermal conductivities of alumina oil based nanofluids. in conference of Nanofluids: Fundamentals and Applications, Cooper Mountain, Colorado. 2007.

[15] Xuan, Y. and Q. Li, Heat transfer enhancement of nanofluids. International Journal of heat and fluid flow, 2000. 21(1): p. 58-64.

[16] Kulkarni, D.P., D.K. Das, and R.S. Vajjha, Application of nanofluids in heating buildings and reducing pollution. Applied Energy, 2009. 86(12): p. 2566-2573.

[17] Donzelli, G., R. Cerbino, and A. Vailati, Bistable heat transfer in a nanofluid. Physical review letters, 2009. 102(10): p. 104503.

[18] Kim, S., et al., Study of pool boiling and critical heat flux enhancement in nanofluids. 2007.

[19] Kim, S.J., et al., Surface wettability change during pool boiling of nanofluids and its effect on critical heat flux. International Journal of Heat and Mass Transfer, 2007. 50(19): p. 4105-4116.

[20] Otanicar, T.P., et al., Nanofluid-based direct absorption solar collector. Journal of renewable and sustainable energy, 2010. 2(3): p. 033102.

[21] Jordan, A., et al., Magnetic fluid hyperthermia (MFH): Cancer treatment with AC magnetic field induced excitation of biocompatible superparamagnetic nanoparticles. Journal of Magnetism and Magnetic Materials, 1999. 201(1): p. 413-419.

[22] Hiergeist, R., et al., Application of magnetite ferrofluids for hyperthermia. Journal of Magnetism and Magnetic Materials, 1999. 201(1): p. 420-422.

[23] Wen, D. and Y. Ding, Experimental investigation into convective heat transfer of nanofluids at the entrance region under laminar flow conditions. International journal of heat and mass transfer, 2004. 47(24): p. 5181-5188.

[24] Jung, J.-Y., H.-S. Oh, and H.-Y. Kwak, Forced convective heat transfer of nanofluids in microchannels. International Journal of Heat and Mass Transfer, 2009. 52(1): p. 466-472.

[25] Wu, X., H. Wu, and P. Cheng, Pressure drop and heat transfer of Al2O3-H2O nanofluids through silicon microchannels. Journal of Micromechanics and Microengineering, 2009. 19(10): p. 105020.

[26] Yang, Y., et al., Heat transfer properties of nanoparticle-in-fluid dispersions (nanofluids) in laminar flow. International Journal of Heat and Mass Transfer, 2005. 48(6): p. 1107-1116.

[27] Heris, S.Z., S.G. Etemad, and M.N. Esfahany, Experimental investigation of oxide nanofluids laminar flow convective heat transfer. International Communications in Heat and Mass Transfer, 2006. 33(4): p. 529-535.

[28] Heris, S.Z., M.N. Esfahany, and S.G. Etemad, Experimental investigation of convective heat transfer of Al 2 O 3/water nanofluid in circular tube. International Journal of Heat and Fluid Flow, 2007. 28(2): p. 203-210.

[29] Maiga, S.E.B., et al., Heat transfer enhancement by using nanofluids in forced convection flows. International journal of heat and fluid flow, 2005. 26(4): p. 530-546.

[30] Ebrahimnia-Bajestan, E., et al., Numerical investigation of effective parameters in convective heat transfer of nanofluids flowing under a laminar flow regime. International journal of heat and mass transfer, 2011. 54(19): p. 4376-4388.

[31] Bayat, J. and A.H. Nikseresht, Investigation of the different base fluid effects on the nanofluids heat transfer and pressure drop. Heat and mass transfer, 2011. 47(9): p. 1089-1099.

[32] Moraveji, M.K. and E. Esmaeili, Comparison between single-phase and two-phases CFD modeling of laminar forced convection flow of nanofluids in a circular tube under constant heat flux. International Communications in Heat and Mass Transfer, 2012. 39(8): p. 1297-1302.

[33] Bianco, V., et al., Numerical investigation of nanofluids forced convection in circular tubes. Applied Thermal Engineering, 2009. 29(17): p. 3632-3642.

[34] Akbarinia, A. and A. Behzadmehr, Numerical study of laminar mixed convection of a nanofluid in horizontal curved tubes. Applied Thermal Engineering, 2007. 27(8): p. 1327-1337.

[35] Fard, M.H., M.N. Esfahany, and M. Talaie, Numerical study of convective heat transfer of nanofluids in a circular tube two-phase model versus single-phase model. International Communications in Heat and Mass Transfer, 2010. 37(1): p. 91-97.

[36] Lotfi, R., Y. Saboohi, and A. Rashidi, Numerical study of forced convective heat transfer of nanofluids: comparison of different approaches. International Communications in Heat and Mass Transfer, 2010. 37(1): p. 74-78.

[37] Kalteh, M., et al., Experimental and numerical investigation of nanofluid forced convection inside a wide microchannel heat sink. Applied Thermal Engineering, 2012. 36: p. 260-268.

[38] Lajvardi, M., et al., Experimental investigation for enhanced ferrofluid heat transfer under magnetic field effect. Journal of Magnetism and Magnetic Materials, 2010. 322(21): p. 3508-3513.

[39] Azizian, R., et al., Effect of magnetic field on laminar convective heat transfer of magnetite nanofluids. International Journal of Heat and Mass Transfer, 2014. 68: p. 94-109.

[40] Goharkhah, M., M. Ashjaee, and M. Shahabadi, Experimental investigation on convective heat transfer and hydrodynamic characteristics of magnetite nanofluid under the influence of an alternating magnetic field. International Journal of Thermal Sciences, 2016. 99: p. 113-124.

[41] Pak, B.C. and Y.I. Cho, Hydrodynamic and heat transfer study of dispersed fluids with submicron metallic oxide particles. Experimental Heat Transfer an International Journal, 1998. 11(2): p. 151-170.

[42] Behzadmehr, A., M. Saffar-Avval, and N. Galanis, Prediction of turbulent forced convection of a nanofluid in a tube with uniform heat flux using a two phase approach. International Journal of Heat and Fluid Flow, 2007. 28(2): p. 211-219.

[43] Bianco, V., O. Manca, and S. Nardini, Numerical investigation on nanofluids turbulent convection heat transfer inside a circular tube. International Journal of Thermal Sciences, 2011. 50(3): p. 341-349.

[44] Azmi, W., et al., Experimental determination of turbulent forced convection heat transfer and friction factor with SiO 2 nanofluid. Experimental Thermal and Fluid Science, 2013. 51: p. 103-111.

[45] Chen, Y.-j., Y.-y. Li, and Z.-h. Liu, Numerical simulations of forced convection heat transfer and flow characteristics of nanofluids in small tubes using two-phase models. International Journal of Heat and Mass Transfer, 2014. 78: p. 993-1003.

[46] Fotukian, S. and M.N. Esfahany, Experimental investigation of turbulent convective heat transfer of dilute γ-Al 2 O 3/water nanofluid inside a circular tube. International Journal of Heat and Fluid Flow, 2010. 31(4): p. 606-612.

[47] Namburu, P.K., et al., Numerical study of turbulent flow and heat transfer characteristics of nanofluids considering variable properties. International Journal of Thermal Sciences, 2009. 48(2): p. 290-302.

[48] Azmi, W., et al., Heat transfer and friction factor of water based TiO 2 and SiO 2 nanofluids under turbulent flow in a tube. International Communications in Heat and Mass Transfer, 2014. 59: p. 30-38.

[49] Hanafizadeh, P., et al., The comparative study of single and two-phase models for magnetite nanofluid forced convection in a tube. International Communications in Heat and Mass Transfer, 2015. 65: p. 58-70.

[50] Hejazian, M., M.K. Moraveji, and A. Beheshti, Comparative study of Euler and mixture models for turbulent flow of Al 2 O 3 nanofluid inside a horizontal tube. International Communications in Heat and Mass Transfer, 2014. 52: p. 152-158.

[51] Hussein, A.M., et al. Simulation study of turbulent convective heat transfer enhancement in heated tube flow using TiO2-water nanofluid. in IOP Conference Series: Materials Science and Engineering. 2013. IOP Publishing.

[52] Sundar, L.S., et al., Experimental investigation of forced convection heat transfer and friction factor in a tube with Fe 3 O 4 magnetic nanofluid. Experimental Thermal and Fluid Science, 2012. 37: p. 65-71.

[53] Moraveji, M.K. and M. Hejazian, Modeling of turbulent forced convective heat transfer and friction factor in a tube for Fe 3 O 4 magnetic nanofluid with computational fluid dynamics. International Communications in Heat and Mass Transfer, 2012. 39(8): p. 1293-1296.

[54] Li, Q., Y. Xuan, and J. Wang, Investigation on convective heat transfer and flow features of nanofluids. Journal of Heat transfer, 2003. 125(2003): p. 151-155.

[55] Davarnejad, R. and M. Jamshidzadeh, CFD modeling of heat transfer performance of MgO-water nanofluid under turbulent flow. Engineering Science and Technology, an International Journal, 2015. 18(4): p. 536-542.

[56] Manninen, M., V. Taivassalo, and S. Kallio, On the mixture model for multiphase flow. 1996, Technical Research Centre of Finland Finland.

[57] Schiller, L. and Z. Naumann, A drag coefficient correlation. Vdi Zeitung, 1935. 77(318): p. 51.

[58] Manual, F., Version 6.2. 16, 2005, Fluent. Inc.

[59] Launder, B. and D. Spalding, Lectures in mathematical models of turbulence. 1972.

[60] Wasp, E.J., J.P. Kenny, and R.L. Gandhi, Solid--liquid flow: slurry pipeline transportation.[Pumps, valves, mechanical equipment, economics]. Ser. Bulk Mater. Handl.;(United States), 1977. 1(4).

[61] Maiga, S.E.B., et al., Heat transfer enhancement by using nanofluids in forced convection flows. International journal of heat and fluid flow, 2005. 26(4): p. 530-546.

[62] Brinkman, H., The viscosity of concentrated suspensions and solutions. The Journal of Chemical Physics, 1952. 20(4): p. 571-571.

[63] Shen, L., et al., Solvothermal synthesis and electrical conductivity model for the zinc oxide-insulated oil nanofluid. Physics Letters A, 2012. 376(10): p. 1053-1057.

[64] Bagheli, S., et al., Synthesis and experimental investigation of the electrical conductivity of water based magnetite nanofluids. Powder Technology, 2015. 274: p. 426-430.

[65] Sundar, L.S., et al., Effect of full length twisted tape inserts on heat transfer and friction factor enhancement with Fe 3 O 4 magnetic nanofluid inside a plain tube: an experimental study. International Journal of Heat and Mass Transfer, 2012. 55(11): p. 2761-2768.

[66] Notter, R. and C. Sleicher, A solution to the turbulent Graetz problem—III Fully developed and entry region heat transfer rates. Chemical Engineering Science, 1972. 27(11): p. 2073-2093.

[67] Ahsan, M., Numerical analysis of friction factor for a fully developed turbulent flow using k–ε turbulence model with enhanced wall treatment. Beni-Suef University Journal of Basic and Applied Sciences, 2014. 3(4): p. 269-277.

[68] Moody, L.F., Friction factors for pipe flow. Trans. Asme, 1944. 66(8): p. 671-684.

[69] Motozawa, M., et al., Effect of magnetic field on heat transfer in rectangular duct flow of a magnetic fluid. Physics Procedia, 2010. 9: p. 190-193.

[70] Li, Q., Y. Xuan, and J. Wang, Experimental investigations on transport properties of magnetic fluids. Experimental Thermal and Fluid Science, 2005. 30(2): p. 109-116.

ANNEX

UDF to define the electrical conductivity

```
#include "udf.h"
/***UDF for electrical conductivity of Water and Fe3O4 nano-particles****/
#define FI 0.01 /***volume fraction of the nanofluid ***/
#define r 18e-9 /****radius of the nanoparticule ***/
#define U0 -40 /*** nanoparticule Zeta potential ****/
#define E_0 8.854e-12 /***relatively dielectric of vacuum***/
#define E_f 80 /*** relatively dielectric of base fluid***/
#define U_f 0.000081727 /***viscosity of the nanofluid***/
#define R 8.31 /*** thermodynamic constant***/
#define A 6.023e23 /***Avogadro constant***/
#define S_0 0.05 /***electrical conductivity of Water ***/

DEFINE_PROPERTY (Shen_electrical_conductivty, c, t)
{
real S_nf, S_m, S_e, S_b, Con, C, T = C_T(c,t);
/***Maxwell model***/
S_m = (1+(3*FI))* S_0;
/*** electrophoresis conductivity ***/
S_e =  (2*FI* pow(E_0,2) * pow(E_f,2) * pow(U0,2))/(U_f * pow(r,2));
/*** Brownian motion of nano particles ***/
Con = (R * T) / ( A * 3 * 3.14 * U_f);
C = pow(Con,(0.5));
S_b = (3*FI * E_0 * E_f * U0)/pow(r,(3/2)) * C;
S_nf = S_m + S_e + S_b;
return S_nf;
}
```

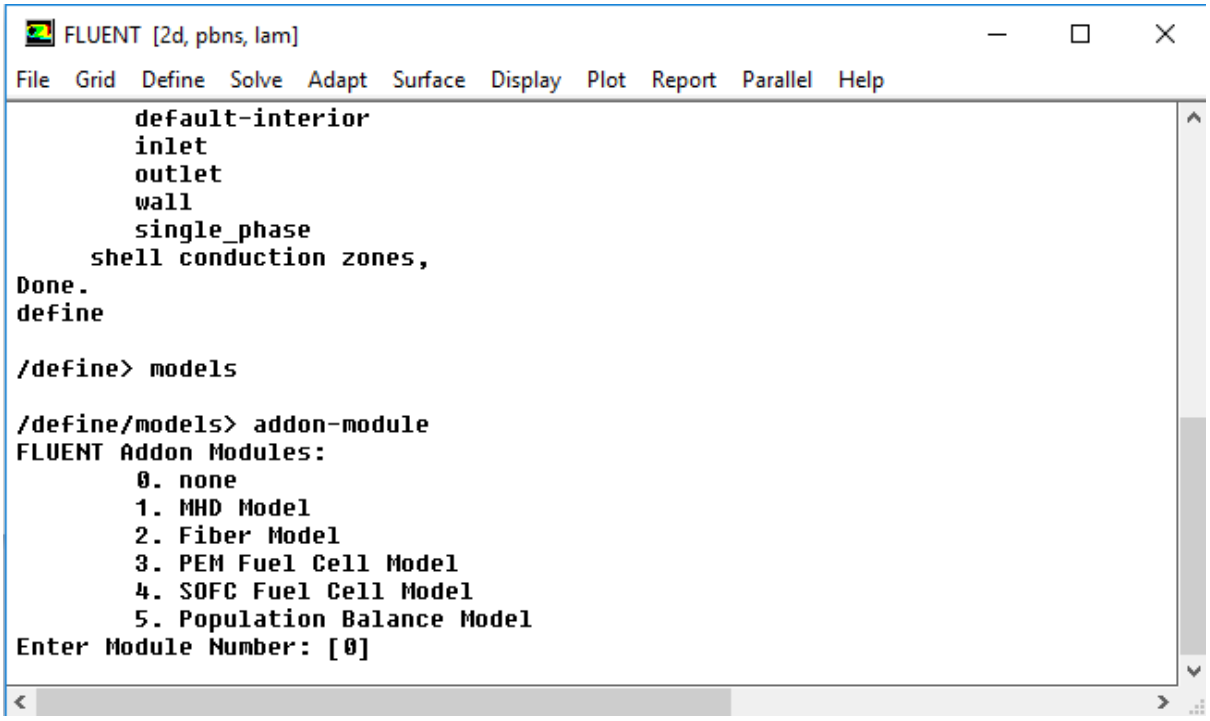
```
#include "udf.h"
/***UDF for electrical conductivity of Water and Fe3O4 nano-particles****/
#define FI 0.006 /***volume fraction of the nanofluid ***/
#define r 18e-9 /****radius of the nanoparticule ***/
#define U0 -40 /*** nanoparticule Zeta potential ****/
#define E_0 8.854e-12 /***relatively dielectric of vacuum***/
#define E_f 80 /*** relatively dielectric of base fluid***/
#define U_f 0.00080958 /***viscosity of the nanofluid***/
#define R 8.31 /*** thermodynamic constant***/
#define A 6.023e23 /***Avogadro constant***/
#define S_0 0.05 /***electrical conductivity of Water ***/

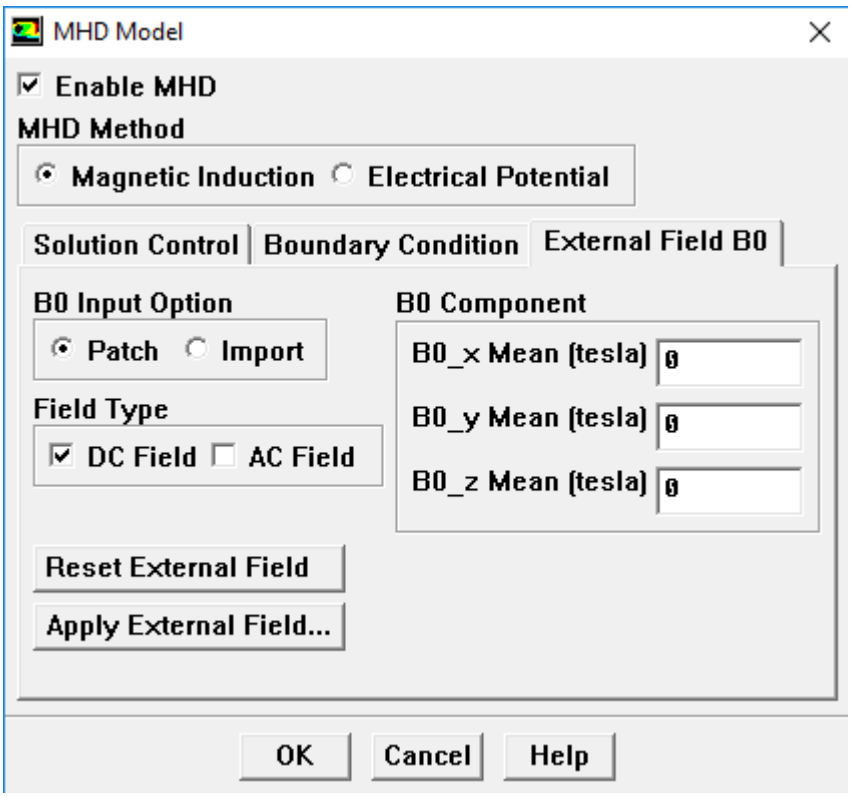
DEFINE_PROPERTY (Shen_electrical_conductivty, c, t)
{
real S_nf, S_m, S_e, S_b, Con, C, T = C_T(c,t);
/***Maxwell model***/
S_m = (1+(3*FI))* S_0;
/*** electrophoresis conductivity ***/
S_e =  (2*FI* pow(E_0,2) * pow(E_f,2) * pow(U0,2))/(U_f * pow(r,2));
/*** Brownian motion of nano particles ***/
Con = (R * T) / ( A * 3 * 3.14 * U_f);
C = pow(Con,(0.5));
S_b = (3*FI * E_0 * E_f * U0)/pow(r,(3/2)) * C;

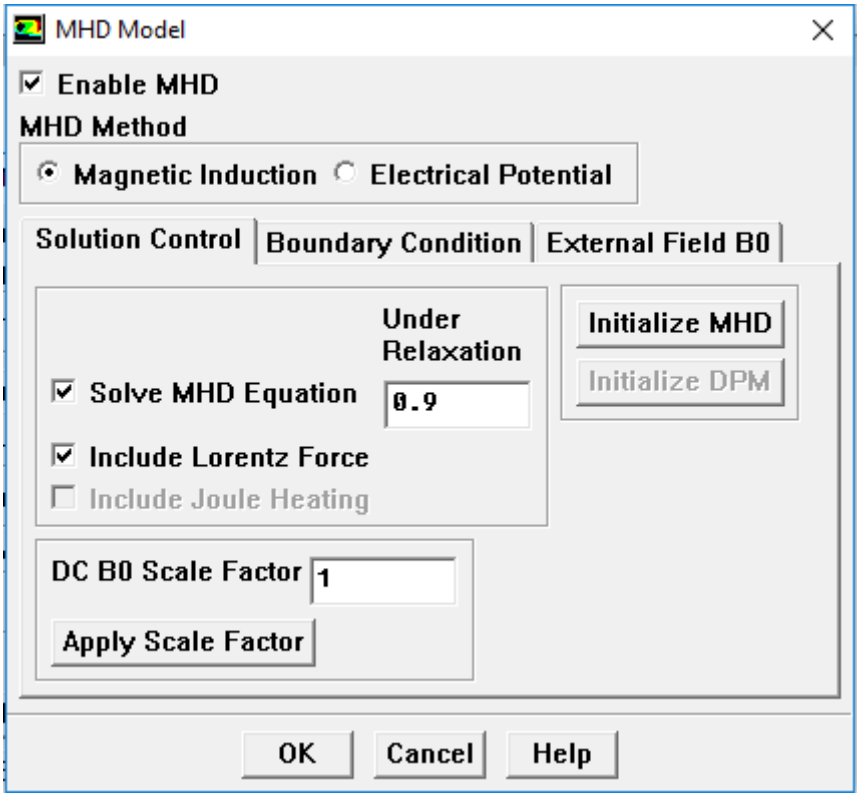
S_nf = S_m + S_e + S_b;
return S_nf;
}
```

Console command to load MHD module into FLUENT

Write in the console "/define/models> addon-module" and select the MHD Model (1)






MHD Model
Enable MHD
MHD Method
Magnetic Induction
Electrical Potential
Solution Control
Boundary Condition
External Field B0
Under Relaxation
Solve MHD Equation
0.9
Include Lorentz Force
Include Joule Heating
Initialize MHD
Initialize DPM
DC B0 Scale Factor
1
Apply Scale Factor
OK
Cancel
Help